Stimuli responsive photonic polymers

Document status and date:
Published: 16/05/2018

Document Version:
Publisher's PDF, also known as Version of Record (includes final page, issue and volume numbers)

Please check the document version of this publication:

• A submitted manuscript is the version of the article upon submission and before peer-review. There can be important differences between the submitted version and the official published version of record. People interested in the research are advised to contact the author for the final version of the publication, or visit the DOI to the publisher's website.
• The final author version and the galley proof are versions of the publication after peer review.
• The final published version features the final layout of the paper including the volume, issue and page numbers.

Link to publication

Download date: 04. Oct. 2023

Stimuli Responsive Photonic Polymers

PROEFSCHRIFT

ter verkrijging van de graad van doctor

aan de Technische Universiteit Eindhoven

op gezag van de rector magnificus prof.dr.ir. F.P.T. Baaijens

voor een commissie aangewezen door het College voor Promoties

in het openbaar te verdedigen

op woensdag 16 mei 2018 om 16:00 uur

door

Monali Moirangthem

geboren te Thangmeiband, Manipur, India

Dit proefschrift is goedgekeurd door de promotoren en de samenstelling van de promotiecommissie is als volgt:

Voorzitter : prof. dr. ir. Kitty Nijmeijer

1e promotor : prof. dr. Albert P. H. J. Schenning

2e promotor : prof. dr. Dirk J. Broer

Leden : prof. dr. Peng Jiang (University of Florida)

prof. dr. Nathalie Katsonis (Universiteit Twente)

prof. dr. Rint P. Sijbesma

dr. ing. Cees W. M. Bastiaansen

adviseur : dr. ir. Tom A. P. Engels

To

Mama, Baba, Che, Ibungo, Angang

Table of Contents

Summary

In the past decade, cholesteric liquid crystalline polymers which are one dimensional photonic materials have emerged as attractive materials for development of stimuli-responsive systems. They exhibit selective reflection of only one-handed circularly polarized light due to the presence of helical molecular organization, and the wavelength of light reflected is directly proportional to length of the helical pitch. As the number of helical pitches is fixed in the polymer, change in optical response can be brought about by changing the helical pitch length by a swelling or a shrinking agent. Therefore, these photonic polymers can be developed to give an optical response to changing external environment like temperature, pressure, humidity, pH or presence of chemical analytes like alcohol, amino acids, amines and metal ions. This thesis focusses on the photonic polymers that are responsive to temperature, liquid water, humidity, and metal ions.

First, an orange reflecting photonic polymer coating which could be patterned easily by evaporating the non-reactive chiral dopant at specific locations with a hot pen or a laser beam was fabricated. Removal of chiral dopant led to a decrease in the helical pitch at the heat treated areas leading to a change in color from orange to green revealing a high contrast pattern. The photonic patterns created are irreversible and stable at ambient conditions making them interesting as writable photonic papers.

For purposes like notice boards and signage which need to be changed frequently, rewritable photonic paper are more appealing. Therefore, a blue color photonic coating was developed on which a liquid crystal ink could be printed to

create patterns by inducing local swelling of the pitch. The color of the patterns ranging from violet to orange, covering almost the entire visible spectrum, could be obtained by simply controlling the amount of the ink. The printed patterns are durable and could also be erased readily giving back the original coating which could be re-patterned. Such rewritable, durable and printable full color photonic paper could be an alternative to cellulose-based paper.

By using photonic polymers containing benzoic acid metal binding sites, an optical calcium sensor was also fabricated. The polymer coating was sensitive to Ca^{2+} ions within the physiologically relevant concentration range of 0.1 and 1 mM. And the optical responses to normal serum and samples mimicking hypocalcemia and hypercalcemia could be clearly distinguished, providing a cheap, battery–free, and easy-to-use alternative for calcium determination in clinical diagnostics.

The principle behind the calcium sensor was further extended to develop a full color camouflage pattern in a photonic polymer coating using aqueous calcium nitrate solution as ink. The pattern in the coating was hidden in the blue color dry state and appeared upon exposure to water or by exhaling breath onto it due to different degrees of swelling of the polymer network. The degree of swelling depends on the printed amount of calcium which acts as a cross-linker. The printed full color pattern could also be hidden simply by using a circular polarizer. The responsive full color camouflage polymers are interesting for various applications ranging from responsive house and automobile decors to anti-counterfeit labels and data encryption.

Ultimately, cholesteric liquid crystalline polymer was combined with a soft polymer – poly(benzyl acrylate) to develop a shape memory photonic semi-interpenetrating polymer network which displayed stable multiple colors covering

almost the entire visible spectrum from blue to orange. The multiple structural colors were generated when the mechanically embossed photonic film recovers on heating through the broad thermal transition from 0 to 55 °C. Such photonic shape memory polymers with stable multiple colors are attractive for various applications ranging from optical sensors to reconfigurable optical materials and devices.

Our findings emphasized the versatility of cholesteric liquid crystalline polymers in developing stimuli-responsive photonic materials for various applications in search of alternative solutions to many of our societal challenges.

Chapter 1

Stimuli-responsive Photonic Polymers

1.1 Introduction

Structural colors that arise due to periodic alteration of refractive indices are abundantly found in nature – living and non-living.[1] An example of non-living being which exhibit structural colors is the opal stone, a hydrated amorphous form of silica. Other examples with naturally observed structural colors are the exoskeleton of beetles like *Entimus imperialis*, tail feather of male peacocks, wings of *Morpho* butterflies, skin of chameleons and cephalopods, petals of flowers like *H. trionum*. Adaptive structural colors perform various functions such as blocking harmful UV radiation, signaling to communicate with other members of same species, mimicry to warn predators, camouflaging to hide from predators and thermoregulation to control body temperature and have continued to inspire researchers, over the years, to develop responsive photonic materials.[2]

Photonic materials which exhibit structural colors generally consist of colloidal crystals, block copolymers or cholesteric liquid crystals (CLC) and depending on the periodicity of the photonic structure, they are classified as one-dimensional, two-dimensional, and three dimensional. The CLC or chiral nematic polymers, which are one-dimensional photonic materials, have emerged as attractive materials for development of stimuli responsive systems in the past decade as the color and response can be programmed in a modular way.[3–6] Due to the presence of helical molecular organization, CLC polymers reflect circularly polarized light of same handedness. The reflection of light is governed by Bragg's law:

$$\lambda_b = \bar{n}Pcos\theta$$

where λ_b is the wavelength of Bragg reflection, $\bar{n}$ is the average refractive index, P is the length of the helical pitch, and θ represents the angle of incidence of light.

The pitch of a CLC is defined as the length traversed by the molecular director $\hat{n}$ on 360° rotation (Scheme 1.1a). It is inversely proportional to the concentration *[C]* as well as the helical twisting power β of the chiral dopant added to the nematic liquid crystal to obtain a chiral nematic phase. The optical anisotropy of the material gives rise to birefringence Δn which renders the selective reflection band (SRB) with an optical bandwidth $\Delta\lambda$, given by:

$$\Delta\lambda = \Delta nP$$

A change in the length of pitch P translates into a change in the position of the reflection band. When the pitch is in the regime of visible wavelength, such a shift in the wavelength of light reflected is visible to the naked eye. As the color seen of the material is purely structural and it does not involve any electronic excitation, it is photostable.[7] These attributes place CLC polymers as one of the favorites for development of responsive photonic materials as for example, optical sensors.
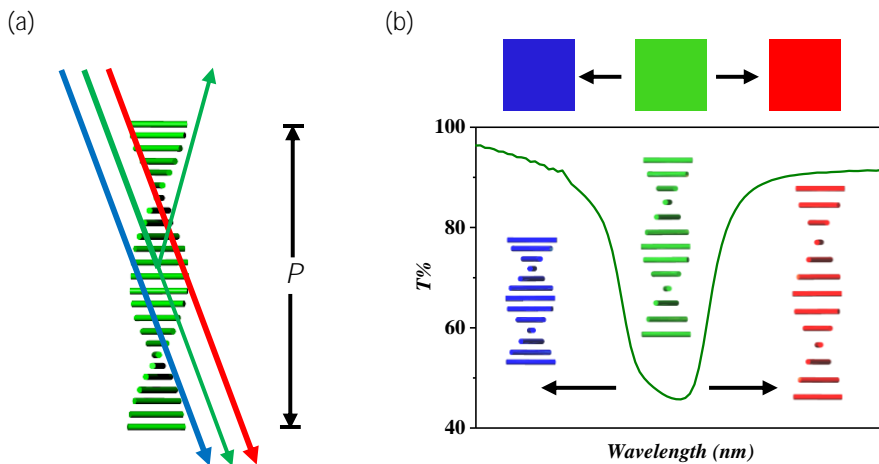
Scheme 1.1. (a) Schematic of a chiral nematic liquid crystal that reflects circularly polarized light of same handedness as its helicity while transmitting the one with opposite handedness (b) Swelling of chiral nematic polymer network leads to increase in pitch length thereby red shifting the reflection band whereas shrinking decreases the pitch length resulting to blue shift of the reflection band.

Optical sensors are great tools for fast and easy qualitative analysis. For instance, low-cost and easy-to-use optical test strips are attractive in the field of health care[8] for medical diagnostics as they can be used by common man without specific training and in areas with limited resources. They are also appealing for real-time[9] or time-integrating monitoring of environment, for example, to detect toxins in water or hazardous chemicals in the surrounding environment. Moreover, they are interesting for controlling quality and authentication of consumer products such as food, beverages, drugs, fuel, cosmetics *etc.*

Although various optical sensors have been designed by using non-reactive liquid crystalline materials,[5] this chapter focuses solely on polymer based optical sensors which have been fabricated by polymerizing functionalized-reactive mesogens to form photonic organic films. Polymerization of reactive mesogens in the CLC phase freezes the helical structure in a polymeric form and provides mechanical strength and thus facilitates fabrication of optical sensors as polymer strips or coatings with ease. Moreover, copolymerization of different reactive mesogens with varying number of end-reactive groups (monoacrylate and diacrylate) enables tailoring of the desired properties of the material.[10] These photonic films can be constructed to respond to a changing external environment like temperature, pressure, humidity, pH or in the presence of a chemical analyte like alcohol, amino acids, amines and metal ions. As the number of cholesteric pitches is fixed due to polymerization, the optical response arises due to a change in the helical pitch length large enough to cause an alteration in color of the photonic film, perceivable by the naked eye (Scheme 1.1b). The response may also be in the form of loss of molecular order leading to disappearance of reflection band.

In this chapter, the aspect of CLC polymer photonic films as stimuli-responsive

materials will be discussed with main focus on optical sensor applications as they form the crux of this thesis.[5] For sensor applications, polymers which consist of hydrogen bonds (H-bonds) have been largely explored for the development of different kinds of optical sensors in which the observed optical response is due to rupture of H-bonds. Optical sensors whose working principle is based on absorption and release of water molecules leading to change in pitch will be detailed. Besides, other non-H-bonded optical sensors will also be elaborated in the following section.

1.2 Responsive CLC polymers as Optical Sensors

1.2.1   pH-responsive CLC polymers
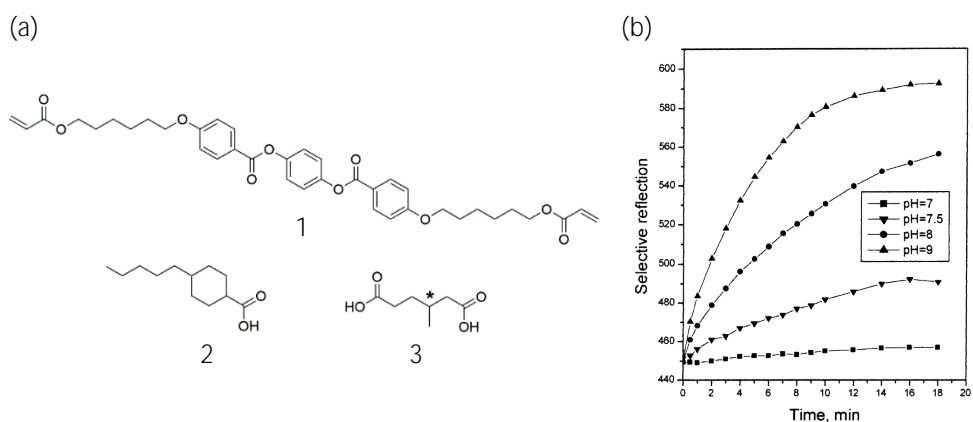
Figure 1.1. (a) Chemical structure of the components of the polymer composite (b) Changes in the position of reflection band on exposing the polymer film to different pH conditions. (Reproduced with permission from Ref. [11])

A pH sensor based on hydrogen-bonded cholesteric polymer composite was first reported by P. V. Shibaev *et. al.*[11]   The composite consisted of 1,4-di-(4-(6-acryloxyhexyloxy)benzoyloxy)benzene (DIAB), 1, as a diacylate cross-linker and 3-methyladipic acid (MAA), 3, as the chiral dopant. It also contained a polymerizable mesogen, (6-hexaneoxy-4-benzoic acid) acrylate (HBA), and a non-polymerizable

(a)

4

5

6   7   8

9   10

(b)
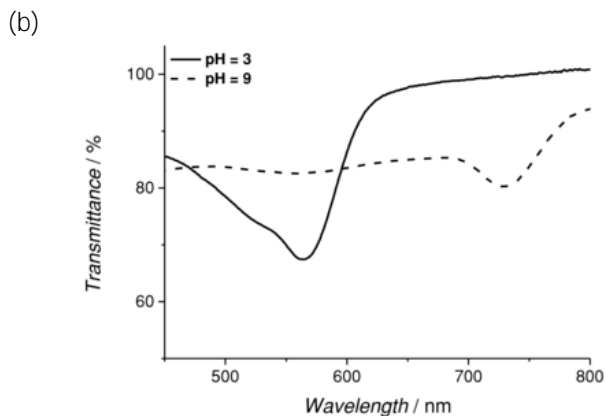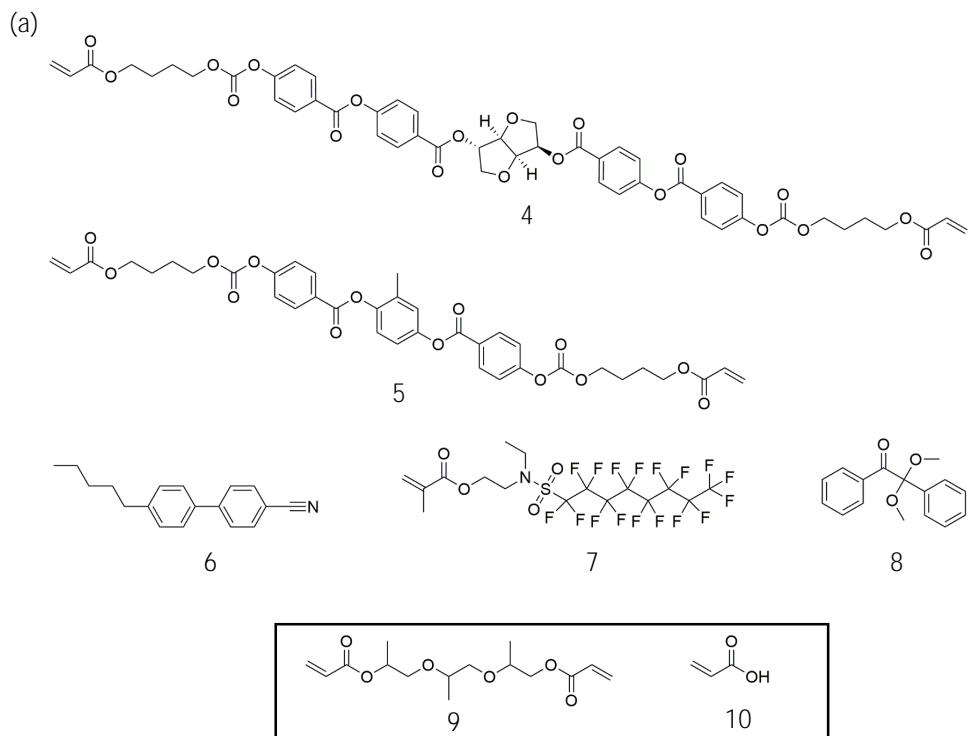
Figure 1.2. (a) Chemical structure of the components and (b) UV-Vis transmission Spectrum of the interpenetrating network of cholesteric polymer and poly(acrylic acid) at pH = 3 and 9. (Reproduced with permission from Ref. [13])

mesogen, pentylcyclohexanoic acid (PCA), 2, with benzoic acid and carboxylic acid functional groups respectively (Figure 1.1a). On exposing to pH above 7, the

reflection band red shifted with as high as 100 nm change in wavelength when pH = 9 (Figure 1.1b). The observed effect was attributed to disruption of hydrogen bonds due to neutralization of acid groups which might have triggered the phase separation of the chiral dopant MAA with consequent decrease in its helical twisting power. Another probable reason suggested was the mechanical stress imposed on the polymer matrix due to volumetric changes accompanying the neutralization of acid groups. Treatment of these films with acidic solutions did not help in restoration of the initial color.

In 2015, Stumpel *et. al.* made a novel pH sensor from an interpenetrating network (IPN) of a CLC polymer and a poly(acrylic acid) hydrogel (Figure 1.2a).[13] At pH 9, deprotonation of poly(acrylic acid) occurs and a polymer hydrogel salt, which swells in water, is formed. Absorption of water led to increase in helical pitch resulting to a remarkable red shift of the reflection band by 170 nm (Figure 1.2b). On further treating with a pH 3 buffer, poly(acrylic acid) was formed again and the color reverted back to its original position.

1.2.2   Amino acid –responsive CLC polymers

The concept behind the development of basic amino acid sensor is similar to those of pH sensors. Like the pH sensors, amino acid sensor also employs H-bonded CLC polymer and is based on the neutralization of the acid group to form salt. An amino acid sensor was first developed by P. V. Shibaev *et. al.*[14] based on a H-bonded CLC polymer comprising of monomers 1, 11 and 12, and MAA as the chiral dopant. When the CLC polymer was exposed to the naturally occurring basic L-arginine solution, deprotonation of the benzoic acid took place which increased the hydrophilicity of the polymer film. As a result, the film swelled, causing a huge red

shift of the reflection band by 170 nm (Figure 1.3). Drying of the film did not bring back the reflection band to its original position suggesting presence of the amino acid residues in the polymer matrix. It was also established that the concentration of 12 and MAA both having carboxylic acid groups plays a role in the response, with higher concentrations leading to faster responses.

(a)

11

12   13
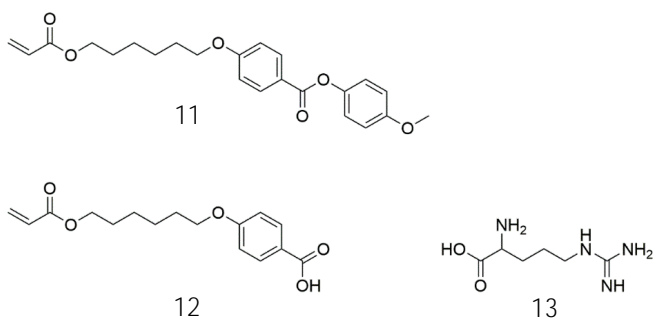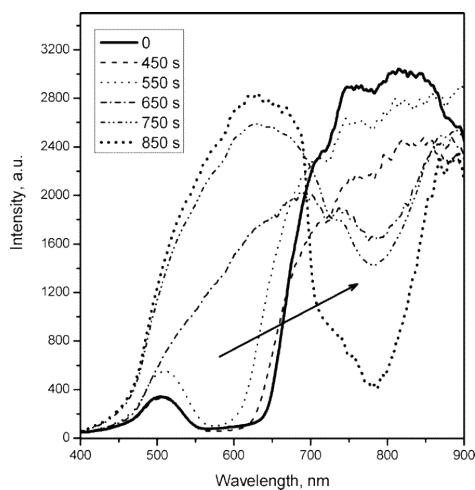
(b)   (c)
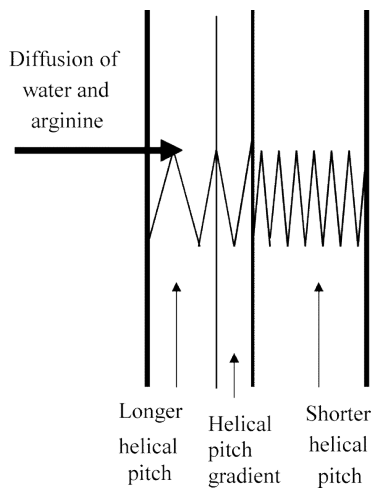
Figure 1.3. (a) Chemical structure of the components used. (b) UV-Vis transmission spectra with left-handed circularly polarized light of H-bonded polymer film when exposed to a solution of L-arginine. (c) Formation of a pitch gradient when arginine solution diffuses through the polymer matrix. (Reproduced with permission from Ref. [14])

1.2.3   Amine-responsive CLC polymers

(a)

14   15

(b)   (c)

(d)   (e)
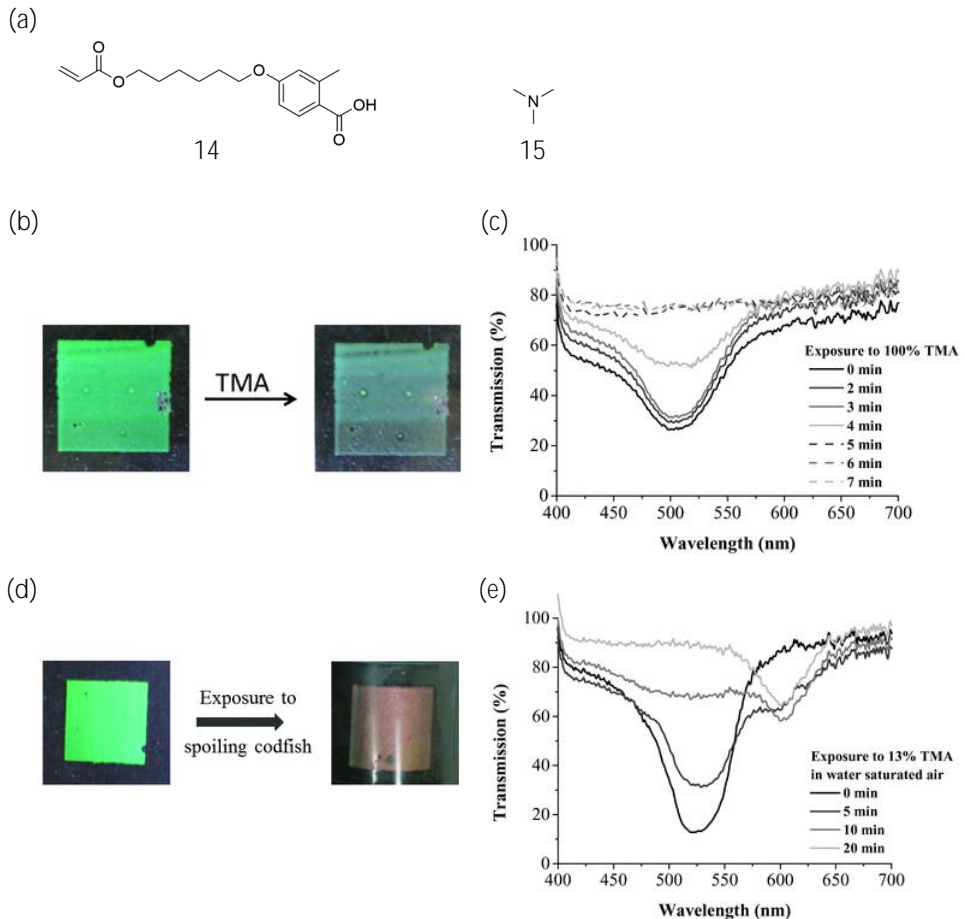
Figure 1.4. (a) Structure of monomer 14 used to make amine sensor in combination with the components of amino acid sensor[14]. Structure of trimethylamine (TMA) is shown as 15 (b) Film images and (c) UV-Vis transmission spectra of the cholesteric polymer film on exposure to pure TMA over time. (d) Image of the cholesteric film after 5 days of exposing to a fish which decayed. (e) Response of the cholesteric film on exposure to 13 % TMA in water saturated nitrogen gas over time. (Reproduced with permission from Ref. [15])

With H-bonded CLC polymer film similar to the one used by P. V. Shibaev *et. al.*,[14] an amine sensor can also be made. Stumpel *et. al.*[15] fabricated a sensor for trimethylamine (TMA), 15 (Figure 1.4a), which is produced by decaying fish. Interaction of 100 % pure TMA with the benzoic acid groups in the polymer film led

to complete loss of cholesteric order and hence disappearance of the reflection band occurred and the polymer film became colorless (Figure 1.4b, c). The response behavior was found to follow an S-shaped as TMA requires time to diffuse into the polymer film in a non-Fickian manner. On using 13 % TMA in water saturated nitrogen gas as the carrier, a new red-shifted band appeared with reduced intensity (Figure 1.4e). It has been explained that interaction with TMA caused formation of carboxylate salts, like in pH and amino acid sensors (*vide supra*), causing absorption of water by the hygroscopic polymer salt film. Moreover, as a proof of principle, the inkjet-printed polymer film was investigated for its ability to sense the vaporous amine compounds emanated from a decaying fish in a humid environment and indeed, the film kept exposed to a freshly caught codfish showed a clear color change, similar to the TMA in water saturated nitrogen gas, from green to red after 5 days (Figure 1.4d).

1.2.4   Humidity-responsive CLC polymers

So far we have seen that H-bonded CLC network can be developed into pH, amino acid or amine optical sensors based on the neutralization of the acid group resulting to change in helical pitch. N. Herzer *et. al.* explored the possibility of hygroscopic carboxylic salt cholesteric polymer film of similar components as was employed by P. V. Shibaev *et. al.*[14] for using as humidity sensor.[16] The carboxylic acid salt was obtained by treating the pristine H-bonded CLC film with KOH solution. The hygroscopic film on exposing to a gas-flow chamber with a relative humidity (RH) of 83 %, the reflection band red shifted by 30 nm due to swelling of the polymer film (Figure 1.5a). The polymer salt film responded to a wide range of RH levels and was sensitive to RH as low as 3 % (Figure 1.5b). The blue shift of the

(a)

(b)
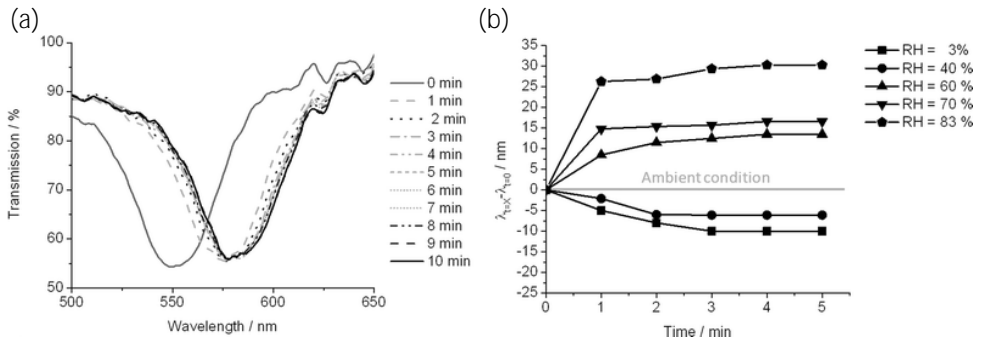
Figure 1.5. (a) UV-Vis transmission spectra of the polymer salt film on exposure to 83 % RH. (b) Change in the wavelength position of the reflection band of the polymer salt film on exposure to different RH levels. The reflection band position of the film at ambient condition conditions was considered the reference. (Reproduced with permission from Ref. [16])

reflection band observed for lower value of RH is due to lower content of water as compared to the ambient conditions under which the reference reflection band position was taken. The response to humidity is fast and reversible and successive exposure of the film to different RH levels gave different optical responses.
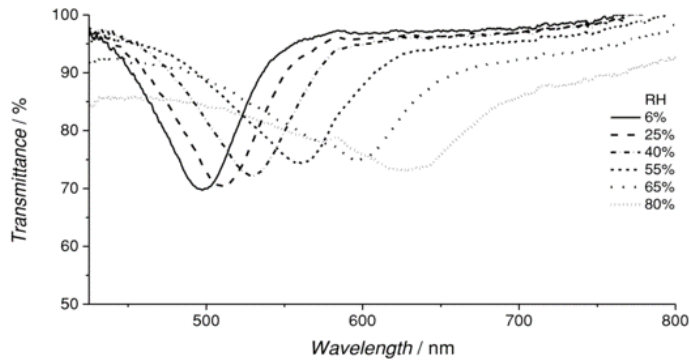
Figure 1.6. Optical response of the IPN to different relative humidity (RH) levels. (Reproduced with permission from Ref. [13])

The pH sensor which Stumpel *et. al.* had developed from an interpenetrating network (IPN) of cholesteric polymer and hydrogel poly(acrylic acid) can also be

applied as a humidity sensor.[13] Deprotonation of poly(acrylic acid) occurred on treatment with KOH solution leading to formation of potassium hydrogel salt which is highly hygroscopic. Such a polymer film was found to respond to different RH levels and the optical response as large as 120 nm was observed when going from RH = 6 % to RH = 80 % (Figure 1.6).

1.2.5 Alcohol-responsive CLC polymers

(a)

(b)

(c)
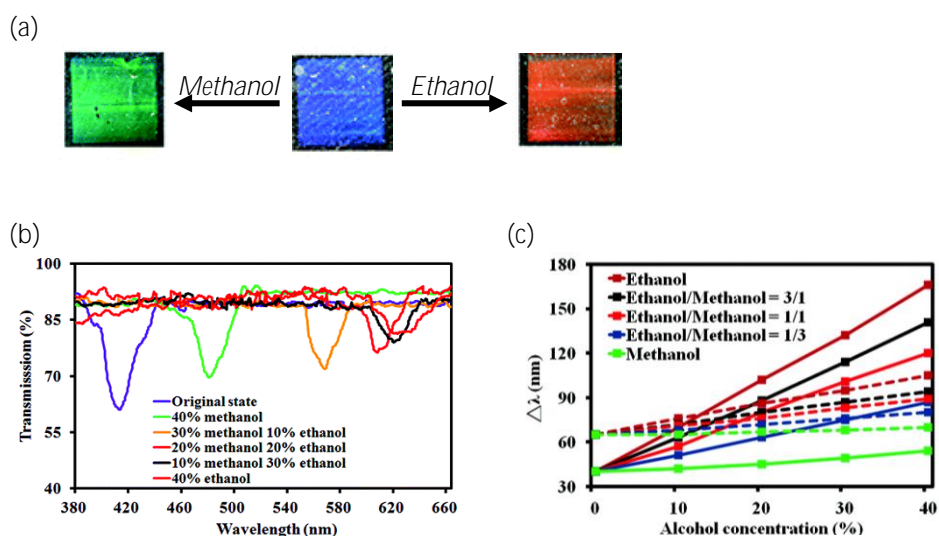
Figure 1.7. (a) Images of the carboxylate salt film on exposure to methanol and ethanol. (b) UV-Vis transmission spectra of the carboxylate salt film exposed to varying ratio of ethanol and methanol keeping total alcohol content 40 % and water 60%. (c) Optical response of polymer salt film with (solid) and without (dashed) porogen for different concentration of alcohol with varying ratios of ethanol to methanol in water. (Reproduced with permission from Ref. [17])

Carboxylate salt cholesteric films, besides water, may also attract other polar solvents like alcohol. Based on H-bonded CLC mixture consisting of mesogens 5, 6, 11, 12 and 14 with 4 as the chiral dopant, C. K. Chang *et. al.* fabricated a polymer film that can detect alcohol as well as distinguish between ethanol and methanol.[17,18] Such sensors are interesting to detect, for example, methanol in wine. Cyano

biphenyl mesogen 6 is non-polymerizable and acts as porogen. Removal of 6 by heating the film caused generation of porosity in the polymer film and that enhances the sensitivity of the film. The polymer film was activated by treating with alkaline solution to form the carboxylate salt which then interacts with polar alcohol molecules. The Hildebrand solubility parameter of ethanol (26.5 √MPa) is closer to that of benzoic acid (21.8 √MPa) compared to methanol (29.6 √MPa). As a result, exposure of the blue colored carboxylate salt film to 40 % ethanol – 60 % water led to a large degree of swelling leading to a red color whereas in the case of exposure to 40 % methanol – 60 % water, the film color changed to green (Figure 1.7a).

The response of the polymer film was also studied on exposure to varying ratio of ethanol and methanol keeping the total alcohol content at 40 % and water 60 % (Figure 1.7b). It was found that as the ratio of ethanol increases, the reflection band shifted more and more towards longer wavelength. The red shift was more pronounced at lower ratio of ethanol while at higher ratio, the intensity of the reflection is markedly less due to reduced order triggered by absorption of a large amount of ethanol in the system. The selectivity between ethanol and methanol was found to increase with increase in the amount of carboxylic salt sites in the polymer film. The importance of having a porogen in enhancing the sensitivity and selectivity of the film was also established. As can be seen in Figure 1.7c, the polymer film which had contained a porogen gave a more pronounced different optical response for different ratios of ethanol to methanol for a specific alcohol content in water.

1.2.6   Metal ion-responsive CLC polymers

Crown ethers are well known for their ability to form host guest complexes. Crown ethers act as host and cations act as guest and depending on the size of the cavity and the ionic radius, they show selectivity towards certain cations that fit well

in the cavity. V. Stroganov *et. al.* exploited this novel property of crown ethers by developing a metal ion sensor from a cholesteric polymer comprising of mesogens 5 (cross-linker), 16 (Nematic liquid crystal E48, Merck), 17 (chiral dopant) and 18 (monoacrylate) functionalized with 18-crown-6 moiety (Figure 1.8).[19] On exposing these films to solutions of Ba^{2+}, and K^+ ions, a blue shift of the reflection band was observed. The response was much higher for Ba^{2+} ions although both K^+ (1.33 Å) and Ba^{2+} (1.34 Å) have similar ionic radii. This result has been attributed to the charge of Ba^{2+} ions which is twice of that of K^+ ions. The observed blue shift might be due to microphase separation of the crown ether-metal complex and the non-reactive chiral

(a)

16   17

18

(b)   (c)

PSCLC with crown-ether moieties

M^{n+} in H_2O

Crown-ether

Complex

λ_{max} ~510 nm λ_{max} ~442 nm

Ba^{2+}
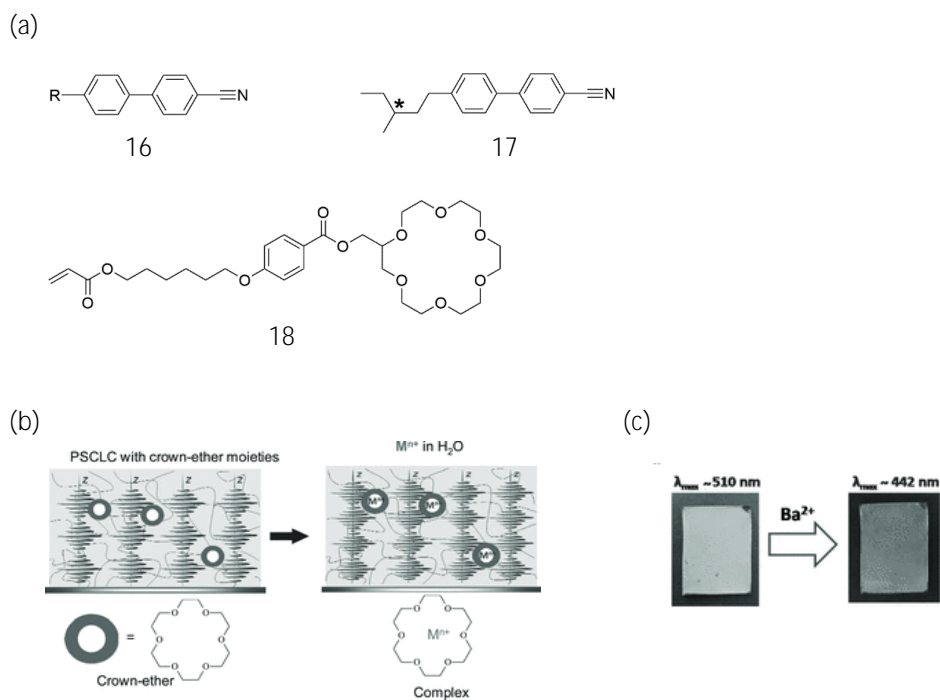
Figure 1.8. (a) Structure of the mesogens used to make metal ion sensor (b) Schematic illustration of the working principle of CLC polymer film with crown ether moiety for metal ion sensing. (c) Image of the polymer before and after treatment with Ba^{2+} ions. (Reproduced with permission from Ref. [19])

dopant causing further twisting of the helical structure. Another possible reason is a slight collapse of the polymer structure due to ionic interaction between the positively charged crown ether-metal complex and the counter ions.

1.2.7 Temperature-responsive CLC polymers

(a)
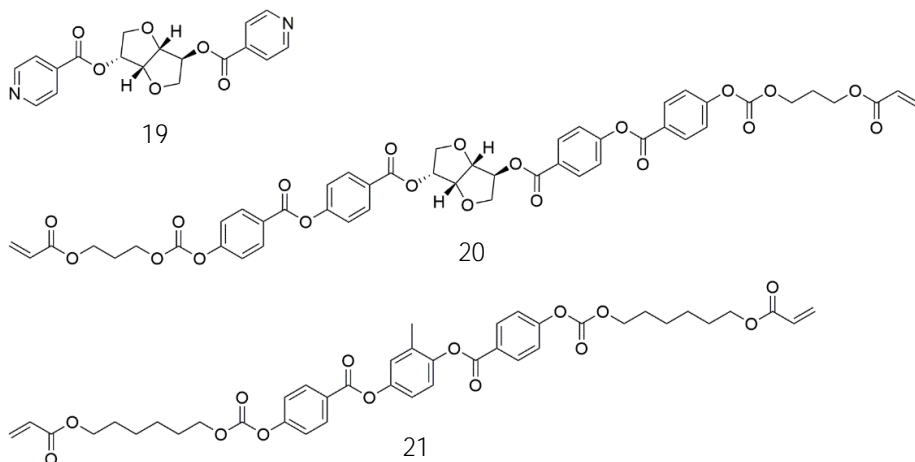
(b)
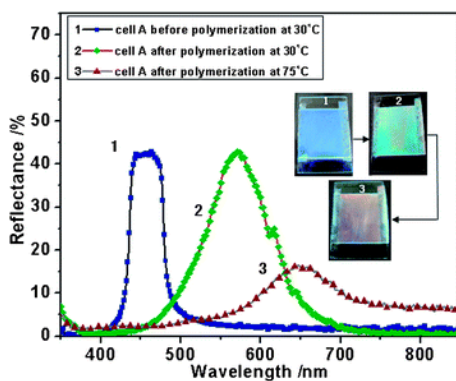
Figure 1.9. (a) Structure of the chiral dopants and diacrylate mesogens used to make the thermoresponsive polymer. (b) UV-Vis spectrum of the cholesteric mixture at 30 °C (curve 1), cholesteric polymer film at 30 °C (curve 2) and at 75 °C (curve 3). The insets shows the photographs of the respective cells. (Reproduced with permission from Ref. [20])

Chen *et. al.* developed a thermal responsive cholesteric polymer containing two

different chiral dopants, one of which is a non-polymerizable chiral pyridine derivative, 19, which can form hydrogen bonds by accepting protons from mesogen with benzoic acid moieties, 12, and a polymerizable chiral molecule, 20.[21] Diacrylate mesogen, 21, was also employed to act as cross-linker. The HTP of the chiral dopant 19 decreases with increasing temperature. At 30 °C, the reflection band of the polymer film was centered at 560 nm (Figure 1.9). However, on heating to 75 °C, the reflection band red shifted to 660 nm. Although the authors claimed reduction in HTP due to weakening of hydrogen-bonds as the possible reason, it is unlikely as the number of pitches is fixed in a polymer network. A plausible explanation could be partial loss in CLC order due to weakening hydrogen bonds as the refection intensity also decreased markedly.
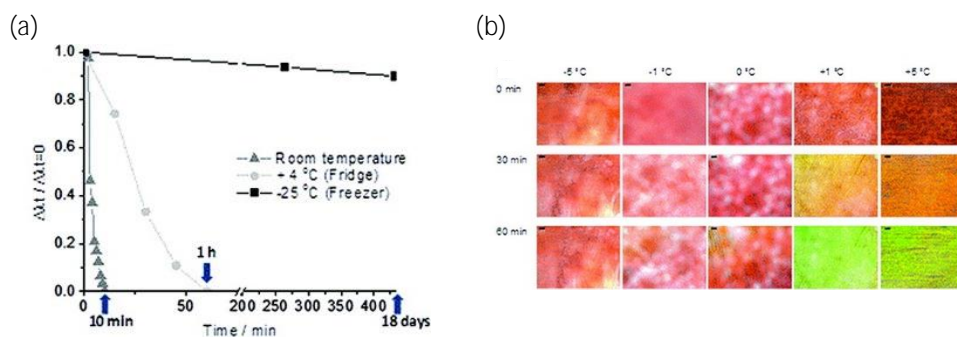
Figure 1.10. (a) Change in the wavelength of the reflection of the water saturated films kept at room temperature, +4 °C and -25 °C with reference to the ambient condition as a function of time. (b) Microscopy images of the films at -5 °C, -1 °C, 0 °C, +1 °C, +5 °C captured in reflection mode without cross-polarizers after 0, 30 and 60 min. (Reproduced with permission from Ref. [16])

N. Herzer *et. al.* studied the possibility of using a water saturated CLC polymer film (described earlier) as a temperature sensor.[16] The reflection band of the water saturated polymer film was monitored at three different temperatures – room temperature (20 °C), in a refrigerator maintained at 4 °C, and in a freezer kept at -25

^{o}C and it was found that the reflection band of the film at 20 ^{o}C was the first to return to its original position taking just 10 minutes (Figure 1.10a); the film kept at 4 ^{o}C took an hour while only a small blue shift could be seen in case of the film kept at -25 ^{o}C which might be attributed to the fact that the reflection band was measured at room temperature which must have led to evaporation of a small amount of water. Inspired by these results, the optical response of the film was monitored in the temperature window of -5 ^{o}C to +5 ^{o}C for a time interval of an hour (Figure 1.10b). The films kept at +1 ^{o}C and +5 ^{o}C were found to return to the original green color in an hour in agreement with the result obtained earlier and showed time-temperature integrating behavior. Moreover, the CLC mixture could also be inkjet printed on a triacetyl cellulose (TAC) foil and the printed film showed similar optical sensing properties which made them an interesting sensor for recording thermal history.

A temperature sensor can also be developed by using the shape memory behavior of CLC glassy polymers.[22] The CLC network was made by polymerization of a mixture consisting of a diacrylate, 5, a monoacrylate, 11, and monomers with benzoic acid moieties, 12 and 14, and 4 as the chiral dopant. Mechanical embossing of the polymer film with a spherical metal stamp above its glass transition temperature (T_g = 50 ^{o}C) at 60 ^{o}C, resulted to a spherical indentation of diameter 0.4 to 0.5 mm and compression of helical pitch that translated into a blue shift of the reflection band by ~30 nm (Figure 1.11). Re-heating the polymer film above its T_g caused the deformed area to recover its original shape accompanied by an irreversible red shift of the reflection band to its initial position. The temperature sensor was found to demonstrate time-temperature integrating behavior between 40 and 55 ^{o}C.

Similar approach was used by Benelli *et. al.* to develop a reversible temperature

sensor from a bright green cholesteric polymer containing azobenzene chromophores (Figure 1.12a, c).[23] The polymer exhibited bragg reflection at 477 nm (Figure 1.12b). Irradiating with UV light below T_g led to increase in population of cis-isomer of the azobenzene causing a decrease in LC order and hence the polymer became transparent (Figure 1.12d). Below the T_g, due to the confinement enforced, the azobenzene did not have enough mobility to isomerize back to the trans-form and the configuration stayed locked. It had to be heated above its T_g to regain the initial LC order (Figure 1.12e). The T_g of the polymers designed is notably very high ranging from 90 to 125 °C.
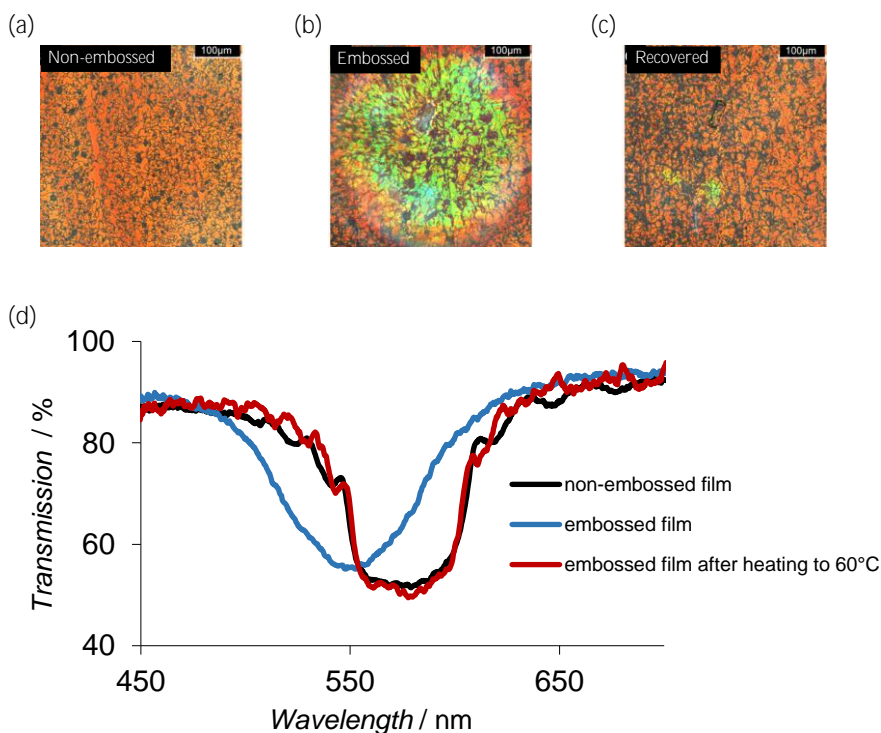
Figure 1.11. Microscopy images of (a) non-embossed film, (b) embossed film and (c) embossed film after heating to 60 °C. All the images were taken in the reflection mode. (d) Corresponding UV-Vis transmission spectra. (Reproduced with permission from Ref. [22])

(a)

(b)

(c) (d) (e)
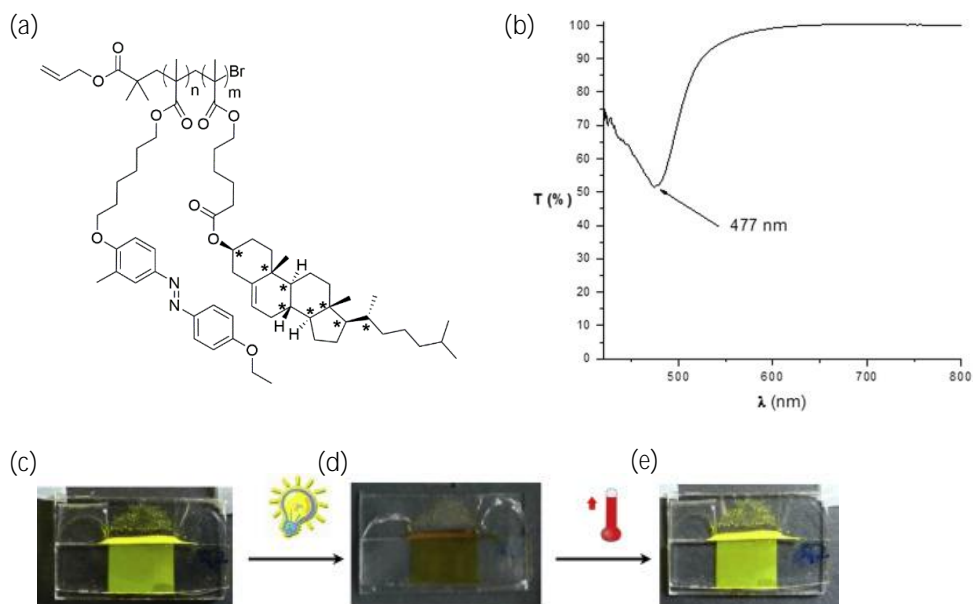
Figure 1.12. (a) Molecular structure (n:m = 52:48) and (c) film image of the Cholesteric polymer containing azobenzene chromophores. (b) UV-Vis spectra of the cholesteric polymer without azoaromatic co-units contribution. (d) UV irradiation leads to trans-cis isomerization. (e) cis-Isomer of azobenzene relaxes to the thermodynamically more stable trans-form on heating above the glass transition temperature. (Reproduced with permission from Ref. [23])

1.2.8   Strain-responsive CLC polymers

A real time optical strain sensor was developed by O. T. Picot *et. al.* for monitoring uniaxial deformations in oriented polymer films.[24] Cholesteric mixture was first spray coated on a uniaxially aligned polyamide 6 substrate and on photopolymerization, a cross-linked cholesteric polymer was obtained. When a uniaxial extension was applied on the substrate perpendicular to the direction of helical axis of the coated cholesteric polymer, the cholesteric polymer expanded in the xy plane with consequent shrinkage of pitch. A strain of 13 % resulted to blue shift of the reflection band by 40 nm and a color change from orange to green could be seen (Figure 1.13). On average, the sensitivity of the bilayer was approximately 3 nm / % strain. The close agreement of the mechanical response of the polymer

substrate to strain and the optical response of the cholesteric polymer coating illustrates the potential of the developed sensor for real time strain sensing.

(a)

(b)
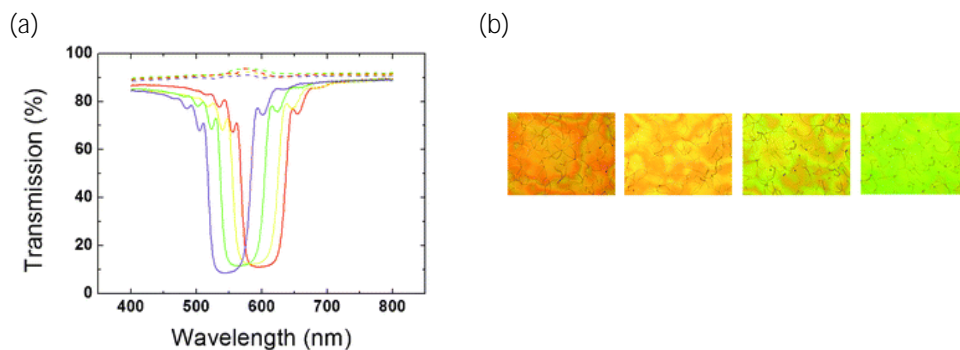
Figure 1.13. (a) UV-Vis transmission spectra and (b) corresponding microscopy images of the bilayer film on applying 0 % (red), 2.6 % (yellow), 7.7 % (green) and 13 % (violet) extensions. (Reproduced with permission from Ref. [24])

1.3 Aim and Outline of the Thesis

Although several optical sensors have been developed, as can be seen from the overview provided in the previous sections, for some of the applications such as detection of metal ions, fabrication of optical sensors that show high selectivity and sensitivity still remains a challenge. Moreover, sensors for physical parameters like temperature are not yet in the regime of actual relevance. Therefore, the work described in this thesis is aimed at developing responsive CLC polymers which are one-step closer to real-life applications. Furthermore, other applications of responsive CLC polymers such as (re)writable paper, anti-counterfeit labels and camouflage are explored.

Chapter 2 describes a polymer coating as photonic paper that can be patterned easily by evaporating a non-reactive chiral dopant at specific locations with a hot pen or a laser beam. Removal of chiral dopant leads to a decrease in the helical pitch at

the heat treated areas leading to a change in color revealing a high contrast pattern. The photonic patterns cannot be erased to get the original coating back.

Chapter 3 reports a blue color printable photonic coating which can be swollen with a non-reactive mesogen locally to create durable but erasable patterns. Patterns of color ranging from blue to red, covering the entire visible spectrum, can be inkjet-printed and simply controlled by the amount of the liquid crystal ink.

Chapter 4 details on the fabrication of an optical calcium sensor from a CLC polymer containing benzoic acid metal binding sites. The polymer coating is sensitive to Ca^{2+} ions within the physiologically relevant concentration range of 0.1 and 1 mM and the optical responses to normal serum and samples mimicking hypocalcemia and hypercalcemia can be clearly distinguished.

The principle behind the calcium sensor is extended to develop a full color camouflage pattern in a photonic polymer coating in Chapter 5. The pattern in the coating is hidden in the blue color dry state and appears on exposure to water or by exhaling breath onto it due to different degrees of swelling of the polymer network. The degree of swelling depends on the printed amount of calcium which acts as a crosslinker. The printed full color pattern can also be hidden simply by using a circular polarizer.

Chapter 6 presents a novel concept of combining CLC polymer with a softer polymer – poly(benzyl acrylate) to develop a shape memory photonic semi-interpenetrating polymer network with a broad glass transition temperature from 10 to 54 °C. The mechanically embossed photonic polymer displays stable multiple colors covering almost the entire visible spectrum from blue to orange, as it recovers to its original shape on heating.

Finally, Chapter 7 assesses the technological advancements of the responsive ph-

otonic polymers described in this thesis. It explores the potential applications of the photonic polymers which have been developed. It also touches upon the shortcomings of these polymers and provides an outlook for further improvement to achieve real-life applications.

1.4 References

[1]   J. Sun, B. Bhushan, J. Tong, *RSC Adv.* 2013, *3*, 14862.

[2]   J. Ge, Y. Yin, *Angew. Chem., Int. Ed.* 2011, *50*, 1492.

[3]   T. J. White, M. E. McConney, T. J. Bunning, *J. Mater. Chem.* 2010, *20*, 9832.

[4]   J. E. Stumpel, D. J. Broer, A. P. H. J. Schenning, *Chem. Commun.* 2014, *50*, 15839.

[5]   D.-J. Mulder, A. Schenning, C. Bastiaansen, *J. Mater. Chem. C* 2014, *2*, 6695.

[6]   C. Fenzl, T. Hirsch, O. S. Wolfbeis, *Angew. Chem., Int. Ed.* 2014, *53*, 3318.

[7]   **I. Burgess, M. Lončar, J. Aizenberg,** *J. Mater. Chem. C* **2013,** *1***, 6075-6086.**

[8]   S. J. Woltman, G. D. Jay, G. P. Crawford, *Nat. Mater.* 2007, *6*, 929.

[9]   D. Wang, S.-Y. Park, I.-K. Kang, *J. Mater. Chem. C* 2015, *3*, 9038.

[10]   T. J. White, D. J. Broer, *Nat. Mater.* 2015, *14*, 1087.

[11]   P. V. Shibaev, K. Schaumburg, V. Plaksin, *Chem. Mater.* 2002, *14*, 959.

[12]   P. V. Shibaev, J. Madsen, A. Z. Genack, *Chem. Mater.* 2004, *16*, 1397.

[13]   J. E. Stumpel, E. R. Gil, A. B. Spoelstra, C. W. M. Bastiaansen, D. J. Broer, A. P. H. J. Schenning, *Adv. Funct. Mater.* 2015, *25*, 3314.

[14]   P. V. Shibaev, D. Chiappetta, R. L. Sanford, P. Palffy-Muhoray, M. Moreira, W. Cao, M. M. Green, *Macromolecules* 2006, *39*, 3986.

[15]   J. E. Stumpel, C. Wouters, N. Herzer, J. Ziegler, D. J. Broer, C. W. M. Bastiaansen, A. P. H. J. Schenning, *Adv. Opt. Mater.* 2014, *2*, 459.

[16]   N. Herzer, H. Guneysu, D. J. D. Davies, D. Yildirim, A. R. Vaccaro, D. J. Broer, C. W. M. Bastiaansen, A. P. H. J. Schenning, *J. Am. Chem. Soc.* 2012, *134*, 7608.

[17]   C. K. Chang, C. W. M. Bastiaansen, D. J. Broer, H. L. Kuo, *Macromolecules* 2012, *45*, 4550.

[18]   C. K. Chang, C. M. W. Bastiaansen, D. J. Broer, H. L. Kuo, *Adv. Funct. Mater.*

2012, *22*, 2855.

[19]   V. Stroganov, A. Ryabchun, A. Bobrovsky, V. Shibaev, *Macromol. Rapid Commun.* 2012, *33*, 1875.

[20]   F. Chen, J. Guo, Z. Qu, J. Wei, *J. Mater. Chem.* 2011, *21*, 8574.

[21]   F. Chen, J. Guo, Z. Qu, J. Wei, *J. Mater. Chem.* 2011, *21*, 8574.

[22]   D. J. D. Davies, A. R. Vaccaro, S. M. Morris, N. Herzer, A. P. H. J. Schenning, C. W. M. Bastiaansen, *Adv. Funct. Mater.* 2013, *23*, 2723.

[23]   T. Benelli, L. Mazzocchetti, G. Mazzotti, F. Paris, E. Salatelli, L. Giorgini, *Dye. Pigment.* 2016, *126*, 8.

[24]   O. T. Picot, M. Dai, E. Billoti, D. J. Broer, T. Peijs, C. W. M. Bastiaansen, *RSC Adv.* 2013, *3*, 18794.

Chapter 2

Hot Pen and Laser Writable

Photonic Paper

Abstract: An orange-reflecting photonic polymer film has been fabricated based on a hydrogen-bonded cholesteric liquid crystalline (CLC) polymer consisting of non-reactive (R)-(+)-3-methyladipic acid as the chiral dopant. This polymer film can be patterned easily by evaporating the chiral dopant at specific locations with a hot pen or a laser beam. Removal of chiral dopant leads to a decrease in the helical pitch at the heat treated areas leading to a change in color from orange to green revealing a high contrast pattern. The photonic patterns are irreversible and stable at ambient conditions. This makes such a CLC polymer film interesting as writable photonic paper.

2.1 Introduction

Patterned photonic crystals[1] have garnered a lot of attention over the years due to their potential in several applications like battery-free optical sensors (see also Chapter 1), displays, photonic paper and anti-counterfeits.[2–4] The photonic patterns can be made either responsive or non-responsive, according to the desired applications. Photonic patterns that are permanent are interesting mainly as photonic papers.[5] Most of the work which have been reported explored use of mask for local chemical modification to create such patterns.[6–13] Use of mask, however, severely limits the possibility to produce diverse patterns.

CLC polymers owing to their ease of fabrication have emerged as attractive materials for making photonic patterns. CLC coatings with permanent patterns have been previously fabricated using a polymerizable chiral dopant with temperature dependent HTP.[7] Temperature has also been used to create patterns in CLC polymer film by employing as a trigger to break the hydrogen bonds present in a chiral dopant to give rise to two new chiral molecules with higher HTP.[14] The patterns are, however, not permanent as with the reformation of hydrogen bonds at lower temperatures, the polymer film recovered to its initial state.

Herein, a hydrogen bonded CLC polymer coating which is thermally writable by using a hot pen or laser beam to produce a permanent photonic pattern is presented. The polymer coating is based on a CLC mixture that contains a non polymerizable dopant that can be evaporated at elevated temperatures.

2.2 Results and Discussion

2.2.1 Fabrication of CLC polymer coating

The CLC mixture (**Scheme 2.1**) used to prepare the polymer coating is similar

to the mixture reported by Shibaev *et. al.*[15] It consists of a diacrylate RM 257 (23.5 wt. %) and a monoacrylate RM 105 (30.5 wt. %) mesogen. Non-polymerizable dicarboxylic acid (R)-(+)-3-methyladipic acid or MAA (13.5 wt. %) was used as the chiral dopant to induce chiral nematic phase. Benzoic acid group functionalized polymerizable molecules 6OBA (16 wt. %) and 6OBAM (16 wt. %) were used to non-covalently bind to the chiral dopant by forming hydrogen bonds. Irgacure 369 (0.5 wt. %) was used as photoinitiator to induce photopolymerization and freeze the CLC phase.
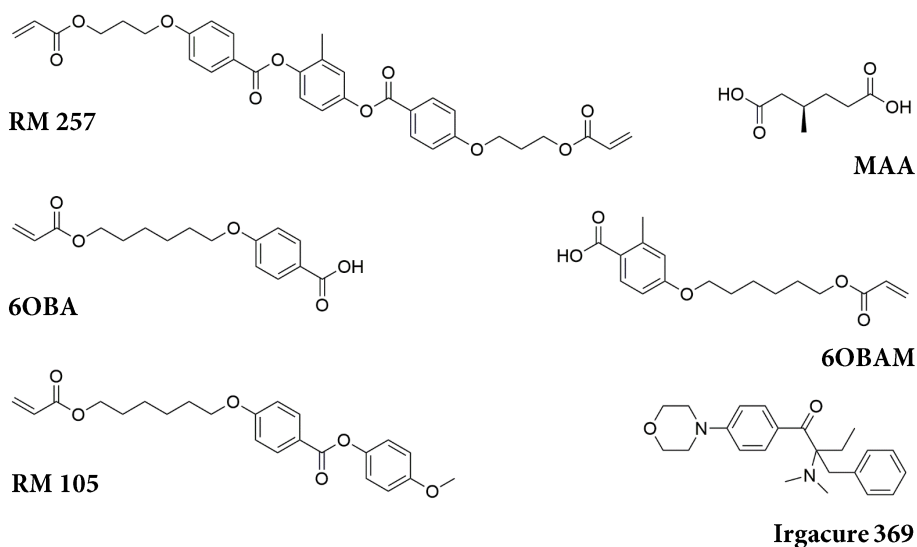
Scheme 2.1. Composition of the CLC mixture used for the preparation of the thermally writable polymer coating.

Shearing the CLC mixture along one direction between two glass plates –the bottom one was functionalized with methacrylate moieties while the top one was functionalized with fluorinated alkylsilane,[16] led to formation of planarly aligned CLC phase. Photopolymerization at room temperature by shining UV light resulted in an orange reflecting CLC polymer covalently bonded to the bottom glass substrate

with a selective reflection band (SRB) centered at λ = 615 nm (**Figure 2.1**). The top glass plate could be easily removed due to its hydrophobic nature to reveal the CLC polymer coating, ready to be patterned.
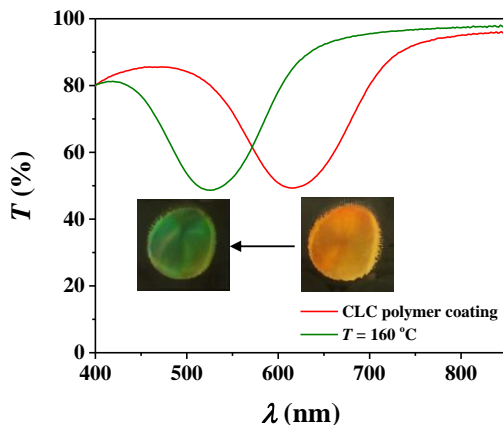
Figure 2.1. UV-Vis spectrum of the as-prepared CLC polymer coating and the same coating after heating to 160 °C.

The FT-IR spectrum of the polymer coating showed a very strong, broad signal of carbonyl vibrations at 1695 cm^{-1} with a shoulder around 1728 cm^{-1} due to stretching of carbonyl of ester moieties (**Figure 2.2a**). The broad nature of this peak indicates the presence of more than one type of hydrogen bonded carbonyl moieties. Absence of vibration peaks at 809 and 985 cm^{-1} implies absence of (C=C) bonds or in other words, complete polymerization.

Thermogravimetric analysis (TGA) revealed that at temperatures above 120 °C, the polymer coating begins to lose weight with reduction in weight by 13.5 wt. % when temperature reaches 180 °C (**Figure 2.2b**). This observed loss in weight can be attributed to evaporation of the non-covalently bonded chiral dopant MAA. Above 180 °C, the polymer begins to degrade. This result inspired us to investigate the optical properties of the polymer coating after being heated at 160 °C.

(a)

(b)
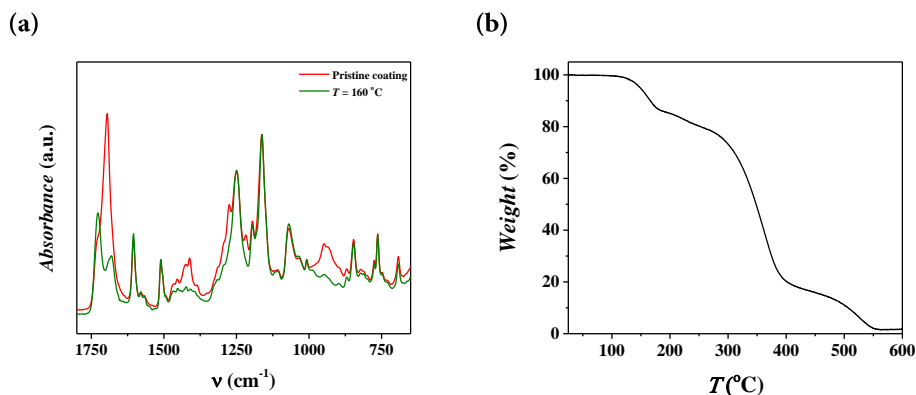
Figure 2.2. (a) FT-IR spectra of the CLC polymer coating before and after the heat treatment at temperature = 160 ºC. (b) Thermogravimetric analysis curve of the CLC polymer coating.

Heating the CLC polymer coating at 160 ºC for 30 min resulted in a change in color of the film from orange to green that could be detected by the naked eye (**Figure 2.1**). The UV-vis spectrum of the coating revealed that the reflection band undergoes a blue shift of 90 nm with the new reflection band centered at $\lambda \approx 525$ nm. As the number of helical pitches in the CLC is fixed, as imposed by the boundary conditions of the network formed during its polymerization, the blue shift suggests decrease in the pitch length. Interferometry shows that the thickness of the film has indeed reduced by 14.6 %, corresponding roughly to the weight % of MAA in the CLC composition. Interestingly the helical structure remains intact even after the removal of the chiral dopant.[16] FT-IR analysis (**Figure 2.2a**) showed that the intense peak at 1695 cm^{-1} has disappeared revealing two well-defined peaks – one at 1728 cm^{-1}, due to the C=O of ester groups and the other at 1680 cm^{-1} which indicates the presence of hydrogen bonded dimers of 6OBA and 6OBAM after the removal of MAA.[17] Intrigued by the results, we investigated the possibility of employing the CLC polymer coating as writable photonic paper.

2.2.2   Patterning in CLC polymer coating

For thermal patterning of the CLC polymer coating (~17 µm thickness), the abbreviation of our research group "SFD" was chosen. Writing with a hand-held hot pen led to change in color from orange to green at the path traced by pen, revealing a high contrast pattern "SFD" (**Figure 2.3a**). FT-IR spectrum of the patterned regions resembled that of the polymer coating heated to 160 ºC (**Figure 2.2a**) suggesting complete evaporation of MAA.

(a)   (b)
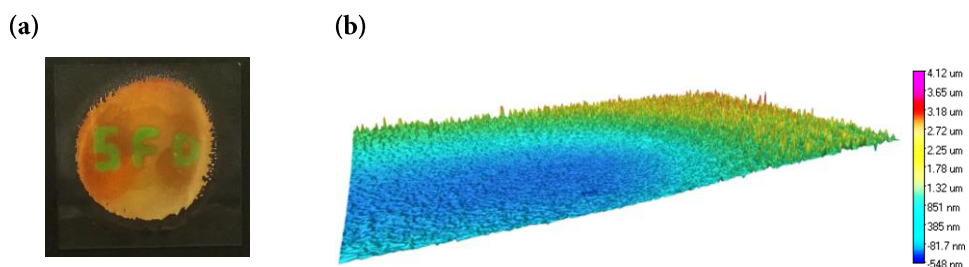
Figure 2.3. (a) Green colored SFD logo written in an orange colored CLC polymer coating by a hot pen. (b) Three-dimensional surface topography of the patterned polymer coating recorded at the interface of orange-green region. It shows a decrease in thickness by ~ 2.2 µm in the green color pattern (blue color coded area) with respect to orange background (green-red color coded area).

To investigate the influence of the removal of MAA on the thickness of the coating, height measurements were carried out at the orange-green interface. It was observed that the thickness reduces by ~ 2.2 µm, which translates to ~ 13 %, close to the weight fraction of the MAA (13.5 wt. %) removed (**Figure 2.3b**). This is in good agreement with 14.6 % decrease in the pitch length determined from the amount of blue shift observed for the reflection band. The polymer coating, after being thermally patterned, did not recover to its initial state and was stable at ambient conditions, even after 3 years.

In order to achieve greater precision on the patterns created, use of focused laser

beam as the tip of a pen was also investigated. Irradiating the CLC polymer coating with a laser beam (700 mW cm^{-2}, 25 sec) resulted in local heating, enough to rupture the intermolecular hydrogen bonds, thereby leading to evaporation of MAA from the laser exposed area. A decrease in thickness by 1 µm was observed in the laser exposed area as revealed by the surface topography analysis of the polymer film (**Figure 2.4a**). The logo of our university "TU/e" was patterned in green in an orange color polymer coating to demonstrate the possibilities of direct laser writing (**Figure 2.4b**).[18]
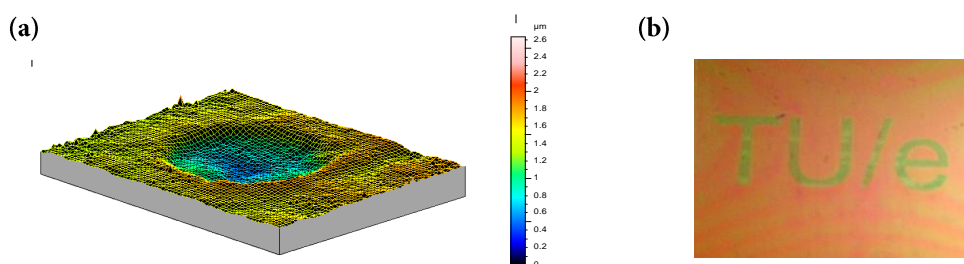
Figure 2.4. (a) Three-dimensional surface topography image of the CLC polymer coating obtained by local heating with laser beam. (b) Image of the laser patterned TU/e logo on the polymer coating.

2.3 Conclusion

We have fabricated a hydrogen-bonded supramolecular CLC polymer coating which can be used as a writable photonic paper. The photonic paper can be patterned easily and in a straightforward fashion by simply writing with a hot pen. The non-covalently bonded chiral dopant MAA undergoes evaporation on writing with the hot pen. This leads to a decrease in the helical pitch length in the patterned region resulting to a blue shift in the selective reflection band with respect to non-patterned region. This, in turn, creates a high contrast green color pattern on an orange background. Focused laser beam can also be used for photonic patterning and the

patterns created are more precise. These new, facile methods allow patterning of photonic polymer coatings in a controlled way with the color of the patterns easily tunable by the amount of MAA employed.

2.4 Experimental Details

2.4.1   Materials

RM257 and RM 105 were purchased from Merck. 6OBA and 6OBAM were obtained from Synthon. Irgacure 369 was from CIBA. Chiral dopant (R)-(+)-3-methyladipic acid, 1*H*, 1*H*, 2*H*, 2*H* – perfluorodecyltriethoxysilane and 3-(trimethoxysilyl)propyl methacrylate were from Sigma Aldrich. The solvents tetrahydrofuran, isopropanol and ethanol were bought from Biosolve.

2.4.2   Characterization

UV-Vis studies were carried out with a Shimadzu UV-3102 PC UV/Vis-near-IR scanning spectrophotometer. A Varian 670 FT-IR spectrometer with slide-on ATR (Ge) was used to record IR spectra. Thermogravimetric analyses were performed in TA TGA Q500. Photopolymerization was carried out with Omnicure series 2000 EXFO lamp. Height measurements were done using a Fogale Nanotech Zoomsurf 3D. Laser writing was carried out with an Argon Ion Laser (SpectraPhysics Beamlok 2050), operating at 351 nm.

2.4.3   Functionalization of glass substrates

Methacrylate and fluorinated alkylsilane coated functionalized glass substrates were prepared as reported previously by J. E. Stumpel *et al.*[19] Glass substrates were first cleaned by sonicating for 30 min in ethanol followed by treatment in a UV-ozone photoreactor (Ultra Violet Products, PR-100, 20 min) to activate the glass surfaces. The glass surfaces were then modified by spin coating (3000 rpm, 45 s) with

3-(trimethoxysilyl)propyl methacrylate solution (1 vol. % solution in a 1:1 water–isopropanol mixture) or 1 *H*, 1 *H*, 2 *H*, 2 *H* - perfluorodecyltriethoxysilane solution (1 vol. % solution in ethanol) followed by curing at 100 °C for 10 min to obtain methacrylate functionalized and fluorinated alkylsilane functionalized glass substrates respectively.

2.4.4   Preparation of CLC polymer coating

1 g of CLC mixture consisting of 23.5 wt % of RM 257, 30.5 wt. % of RM 105, 16 wt % of each of 6OBA and 6OBAM, 13.5 wt. % of (R)-(+)-3-methyladipic acid and 0.5 wt. % of Irgacure 369 was dissolved in 4 mL of tetrahydrofuran. Approximately 80 μL of this solution was dropped on methacrylate functionalized 5 cm ×5 cm glass slide. After evaporating the solvent by heating at 75ºC, it was cooled to room temperature and a 5 cm × 5 cm fluorinated alkylsilane functionalized glass substrate was placed directly on top and was sheared along one direction to obtain a planarly aligned orange color film. It was then photopolymerized by shining UV light (48 mW cm^{-2} intensity in the range 320-390 nm) for 5 min after which the upper glass substrate was removed to get the polymer coating.

2.5 References

[1]   J. X. Wang, L. B. Wang, Y. L. Song, L. Jiang, *J. Mater. Chem. C* **2013**, *1*, 6048.

[2]   H. Nam, K. Song, D. Ha, T. Kim, *Sci. Rep.* **2016**, *6*, 30885.

[3]   H. Hu, C. Chen, Q. Chen, *J. Mater. Chem. C* **2013**, *1*, 6013.

[4]   H. Hu, Q.-W. Chen, J. Tang, X.-Y. Hu, X.-H. Zhou, *J. Mater. Chem.* **2012**, *22*, 11048.

[5]   J. Ge, J. Goebl, L. He, Z. Lu, Y. Yin, *Adv. Mater.* **2009**, *21*, 4259.

[6]   T. Tian, N. Gao, C. Gu, J. Li, H. Wang, Y. Lan, X. Yin, G. Li, *ACS Appl. Mater. Interfaces* **2015**, *7*, 19516.

[7]   J. E. Stumpel, D. J. Broer, A. P. H. J. Schenning, *RSC Adv.* **2015**, *5*, 94650.

[8]   C. Liu, C. Yao, Y. Zhu, J. Ren, K. Lan, H. Peng, L. Ge, *Rsc Adv.* **2014**, *4*, 27281.

[9]   S. Ye, Q. Fu, J. Ge, *J. Mater. Chem.* **2012**, *22*, 367.

[10]   Z. Wang, J. Zhang, J. Xie, Z. Wang, Y. Yin, J. Li, Y. Li, S. Liang, L. Zhang, L. Cui, H. Zhang, B. Yang, *J. Mater. Chem.* **2012**, *22*, 7887.

[11]   S. Ye, Q. Fu, J. Ge, *Adv. Funct. Mater.* **2014**, *24*, 6430.

[12]   S. Ye, J. Ge, *J. Mater. Chem. C* **2015**, *3*, 8097.

[13]   H. Hu, H. Zhong, C. Chen, Q. Chen, *J. Mater. Chem. C* **2014**, *2*, 3695.

[14]   W. Hu, H. Cao, L. Song, H. Zhao, S. Li, Z. Yang, H. Yang, *J. Phys. Chem. B* **2009**, *113*, 13882.

[15]   P. V. Shibaev, D. Chiappetta, R. L. Sanford, P. Palffy-Muhoray, M. Moreira, W. Cao, M. M. Green, *Macromolecules* **2006**, *39*, 3986.

[16]   M. Moirangthem, R. Arts, M. Merkx, A. P. H. J. Schenning, *Adv. Funct. Mater.* **2016**, *26*, 1154.

[17]   J. E. Stumpel, C. Wouters, N. Herzer, J. Ziegler, D. J. Broer, C. W. M. Bastiaansen, A. P. H. J. Schenning, *Adv. Opt. Mater.* **2014**, *2*, 459.

[18]   D. J. Versteeg, C. W. M. Bastiaansen, D. J. Broer, *J. Appl. Phys.* **2002**, *91*, 4191.

[19]   J. E. Stumpel, E. R. Gil, A. B. Spoelstra, C. W. M. Bastiaansen, D. J. Broer, A. P. H. J. Schenning, *Adv. Funct. Mater.* **2015**, *25*, 3314.

Chapter 3

Rewritable Full Color Photonic Polymer using a Liquid Crystal Ink

Abstract: A printable and rewritable photonic polymer coating has been fabricated from a cholesteric liquid crystal. Full color images can be patterned in the polymer coatings by using a liquid crystal ink. The printed patterns can be erased and rewritten multiple times, making these coatings interesting as rewritable papers.

3.1 Introduction

Beauty of nature is enriched by the abundance of colorful patterns that arise due to photonic structures which are arrangements of periodically alternating refractive indices.[1–5] The natural photonic structures have inspired scientists to fabricate artificial photonic materials for applications such as sensors, security labels, house decors, displays and rewritable papers, using block copolymers, colloidal crystals, or cholesteric liquid crystals (CLC).[6–9] For example, rewritable photonic materials have been developed from colloidal crystals; however, the stability of the color of the patterns remains an issue.[10–19] Moreover, these patterns were limited to only two colors. In addition, in most cases the patterns remain invisible under normal conditions and require the aid of solvents such as water, ethanol or vapors for visualization.[20–24] Fabrication of photonic materials with full color stable patterns in dry environment remains a challenge.

Herein, we report on a photonic coating based on CLC polymer that can be inkjet-printed to obtain a rewritable photonic paper with stable full-color patterns (Scheme 3.1a). A CLC polymer is a one-dimensional photonic material with helicoidal molecular organization, and the wavelength of light reflected is directly proportional to the length of the helical pitch, making them very interesting for fabrication of responsive photonic materials with ease.[25–28] The full color patterns were obtained by using a liquid crystal (LC) as ink.

3.2 Results and Discussion

3.2.1   Fabrication of photonic polymer coating

The photonic polymer coating was fabricated from a CLC mixture (Scheme 3.1b) comprising of diacrylate (RM257) and monoacrylate (RM105) mesogens. A chiral dopant that also acts as a cross-linker (LC756) was added to induce CLC phase

36

(a)

(b)

LC756

RM257

RM105

Irgacure 651

5CB
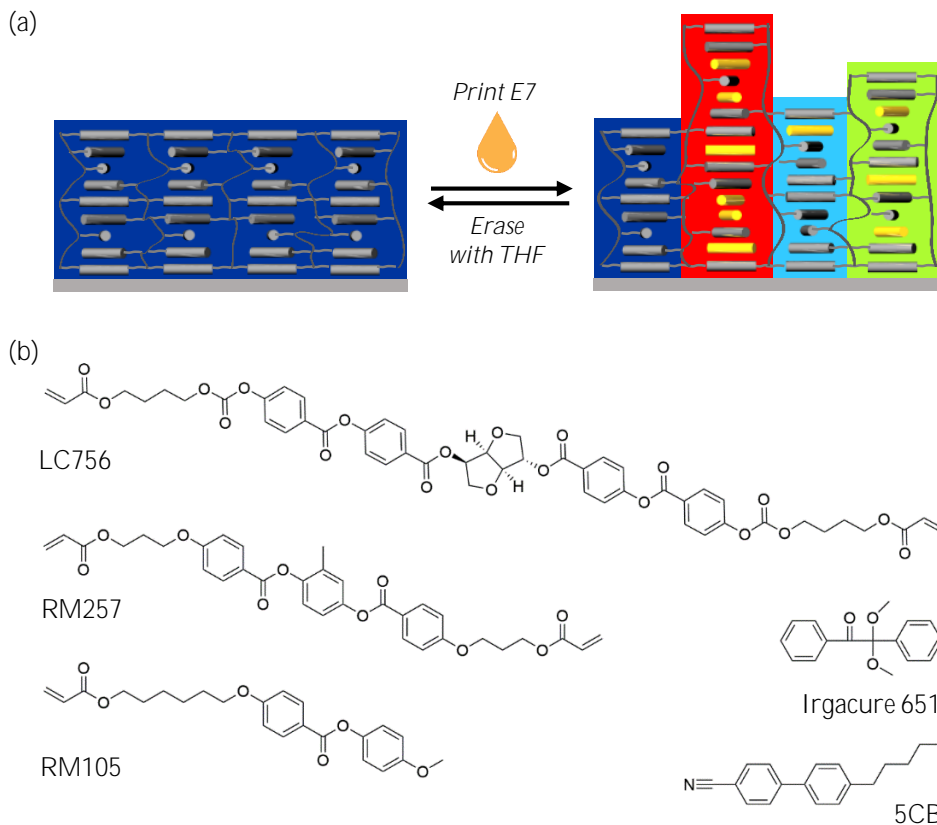
Scheme 3.1. (a) Schematic showing the working principle of patterning in the photonic polymer coating. (b) Structure of the chemical components used to fabricate the photonic polymer coating.

and a photoinitiator (Irgacure 651) was used to initiate the photopolymerization reaction and freeze the phase. Finally, to introduce patternability to the photonic polymer in a broad range of colors of the visible spectrum, a non-polymerizable cyanobiphenyl LC derivative (5CB, 30.0 wt %) which could be removed from the polymer network was used. Shearing the CLC mixture in between two glass plates – bottom one one functionalized with methacrylate and top one with fluorinated alkylsilane moieties – led to formation of a planarly aligned CLC film, which on polymerization by shining UV light and followed by removal of the top glass plate resulted in a red **colored CLC polymer coating** ($\lambda \approx 666$ nm) covalently attached to

the bottom glass plate (Figure 3.1a). Washing out the non-reactive 5CB mesogen with an organic solvent (tetrahydrofuran, THF) ultimately led to a violet colored polymer coating with reflection band centered at $\lambda \approx 384$ nm (Figure 3.1a). FT-IR spectrum (Figure 3.2b) of the coating revealed disappearance of the peak of the stretching vibration of (-C≡N) at 2225 cm^{-1}, revealing complete removal of 5CB.
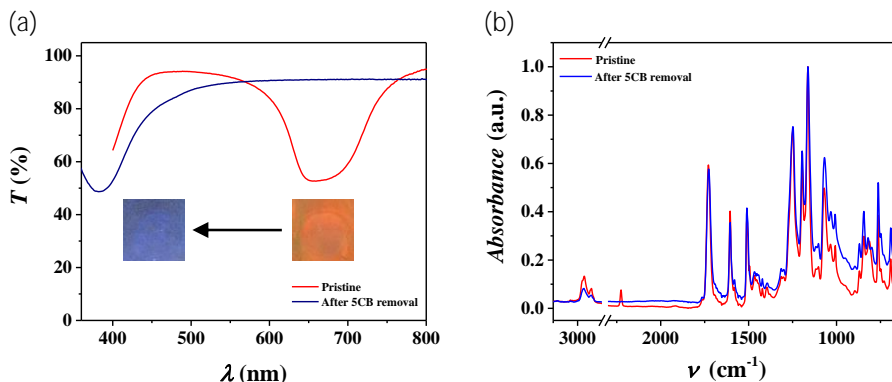
Figure 3.1. (a) UV-vis transmission spectra and (b) FT-IR spectra of the pristine CLC polymer coating and after removing 5CB. Inset of (a) shows the photographs of the polymer film before and after removing 5CB.

3.2.2 Inkjet printing of liquid crystal ink

Removal of the non-polymerizable 5CB led to collapse of the polymer network, reducing the helical pitch length to give the coating a violet color. This also rendered the network highly flexible with enhanced optical response to stimuli. This flexible network could be swollen with E7, which is an LC mixture of cyanobiphenyl and cyanoterphenyl derivatives exhibiting a nematic phase in the broad temperature range from -10 ^{o}C to 58 ^{o}C.[29] In order to achieve photonic patterns, local swelling of the polymer is essential. To do so, introducing E7 only at the desired areas becomes necessary and the most controlled method of doing this is employing the inkjet printing technique. Therefore, the printability of the polymer coating was first inves-

(a)

(b)
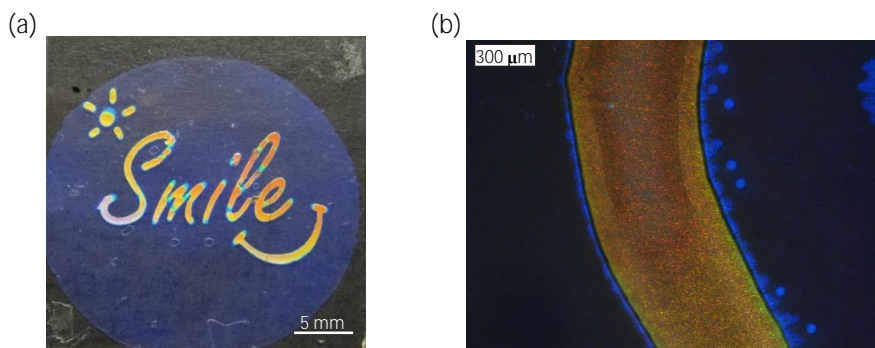
Figure 3.2. (a) Photograph of the CLC polymer coating patterned with letters saying "Smile", a smile icon, and a sun by inkjet-printing with E7 as the ink. (b) Polarized optical microscopy image of a part of "S" of the photonic pattern in (a). Both the images were captured at room temperature.

tigated with E7 as the ink.

As E7 is nematic at room temperature, it can be readily filled in an inkjet printer cartridge and printed in droplets of 10 pL in volume. For an ink to be jetted from the cartridge, a viscosity in the range of 10-12 cP is required. However, E7 at room temperature is highly viscous with viscosity $\approx$ 224 cP.[30] Therefore, the cartridge was heated above the isotropic phase transition temperature of E7 at 70 °C to lower its viscosity. In addition, the polymer coating was preheated to 60 °C to enhance the kinetics of swelling. The polymer coating was finally inkjet-printed with drop spacing maintained at 20 μm (1270 dpi) to make a pattern containing letters that say "Smile", a smile icon and a sun (Figure 3.2a). The areas where E7 was printed swelled immediately at 60 °C, causing an increase in the length of the helical pitch resulting in a color change from violet to orange. Cooling down the patterned polymer to room temperature had no effect on the color of the photonic patterns. The polarized optical microscopy (POM) image of the pattern created showed a sharp contrast between the printed area and the background, implying that there is negligible occurrence of lateral diffusion of E7 into the non-printed area (Figure 3.2b). A

plausible explanation could be the anisotropy of the CLC polymer network leading to a preferred transverse diffusion. Remarkably, other colors with wavelengths shorter than orange such as green and blue were also present at the edges. This signifies that spacing between the printed drops were too small and they were coalescing at a large scale leaving behind a non-uniform distribution of ink at the edges of the printed areas. However, this also shows that multiple structural colors are achievable with the CLC polymer coating and ink E7.
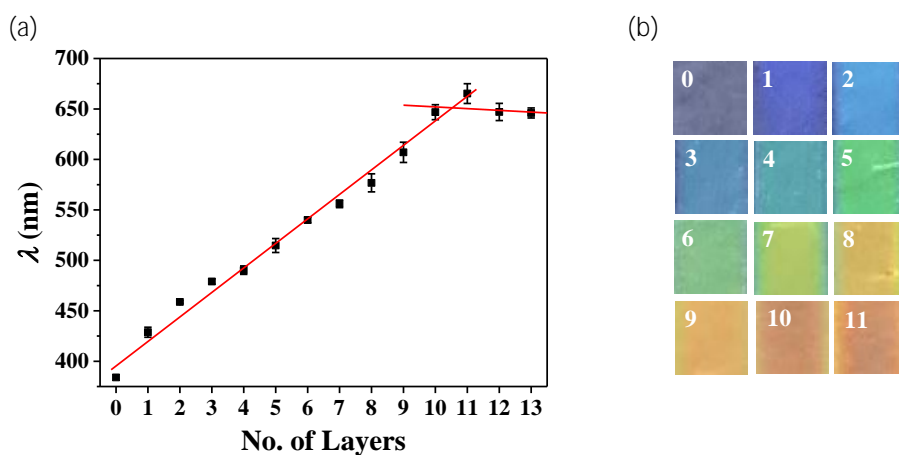
Figure 3.3. Wavelength of light reflected at room temperature by the photonic pattern with different number of layers of ink E7 printed. The red lines represent the linear fitted curves. Error bars indicate mean ± standard deviations for three measurements at different areas on the pattern. Inset shows the respective photographs of the pattern with the number representing the number of layers of ink printed.

3.2.3 Full color patterning using liquid crystal ink

To achieve multiple color patterns in the polymer coating, the amount of ink printed per print needs to be reduced. Therefore, the inkjet printer cartridge was replaced with another cartridge that prints droplets of 1 pL in volume. Moreover, the spacing between the drops was increased from 20 μm to 40 μm (635 dpi) and a rectangular pattern of dimension 1 mm × 5 mm was then printed with the cartridge heated at 70 °C and the polymer coating pre-heated at 60 °C. Printing the first layer

of E7 led to a slight swelling of the network and the much darker violet color ($\lambda \approx$ 384 nm) changed immediately into lighter violet ($\lambda \approx$ 429 nm) (Figure 3.3). Printing a second layer resulted in further swelling prompting the color to turn blue ($\lambda \approx$ 459 nm). A third layer of ink resulted in a further red shift of the wavelength of light reflected ($\lambda \approx$ 479 nm). A fourth layer made the pattern turn bluish-green ($\lambda \approx$ 490 nm) while a fifth layer led to a slight red shift to change the color into full green ($\lambda \approx$ 515 nm). Printing a sixth layer turned the pattern into lighter green ($\lambda \approx$ 540 nm) and a seventh layer made it greenish-yellow ($\lambda \approx$ 556 nm). Printing an eighth and ninth layers resulted in yellow ($\lambda \approx$ 577 nm) and orange ($\lambda \approx$ 607 nm) colors respectively. A tenth layer of ink led to further swelling of the polymer network resulting to red ($\lambda \approx$ 647 nm) color. Printing additional layers did not cause any significant changes and the color remained red. These results show that structural colors can be obtained having wavelength ranging from blue to red. On plotting the number of layers against the reflection wavelength, a linear relation is observed up to ten layers and after the tenth printing step, saturation takes place. This indicates that all the ink was absorbed after each printing step and maximum swelling of the polymer network was reached after the tenth step.

After having determined the number of layers required to achieve patterns in full structural colors ranging from violet to red in a dark violet background, an image with three flower plants, such that each has different color petals, pistils, and stem-leaf, was chosen to demonstrate the fabrication of full color patterns. Figure 3.4a shows the pattern with the amounts of E7 printed accordingly to obtain the different types of colors. UV-Vis measurement (Figure 3.4c) showed that the reflection band of the flower petals, labeled as F1, F2, F3 were centered at $\lambda \approx$ 641, 590, 461 nm while for the pistils, labeled as P1, P2, P3, it was centered at $\lambda \approx$ 438, 468, 568 nm. For the

leaves-stems, labeled as L1, L2, L3, the reflection band was centered at $\lambda \approx 488$, 530, 505 nm. Height profile measurement of the red color flower petals F1 showed 67.3 % increase in thickness, and is in good agreement with the observed 67.5 % increase in pitch length of the CLC polymer network (Figure 3.4d).
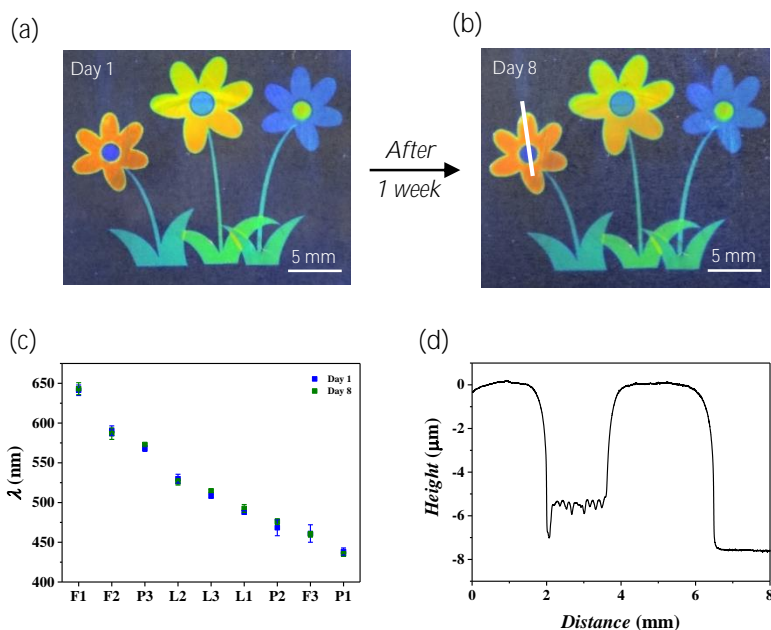
Figure 3.4. (a) Photograph of an inkjet-printed full color pattern on day 1 of printing. (b) Photograph of the same inkjet-printed pattern after 7 days. (c) Wavelength of light reflected by different color regions of the pattern on day 1 of printing and after 8 days. F1, F2, and F3 represents the red, orange, and blue flower petals. P1, P2, and P3 represents the violet, blue, and yellow pistils. Finally, L1, L2, and L3 represents the leaves-stems of the three flowers. Error bars indicate mean ± standard deviations for three measurements at different areas on the pattern. (d) Height profile measured along the white line in (b) passing through the red flower petals, violet pistils and much darker violet background.

3.2.4   Rewritability and durability of patterned photonic polymer coating

In order to investigate the effect of time on the color of the patterns, the printed pattern was stored at ambient conditions for a week. On the eighth day, UV-Vis spectra were measured and no significant change was found in the position of the reflection bands of the petals, pistils, or leaves-stems (Figure 3.4c), implying that the

photonic patterns are stable and remarkably durable. Figure 3.4b shows a photograph of the full color pattern after 7 days of being printed.

To demonstrate rewritability of the photonic polymer coatings, a coating that was patterned in three representative colors – orange, yellow, and bluish green, was erased by treating with THF which dissolved the E7 ink, leaving behind the violet coating with no photonic patterns (Figure 3.5a). The coating could then be re-printed and erased. Carrying out the print-erase cycle ten times showed similar optical properties of the printed patterns for each cycle (Figure 3.5b, c).
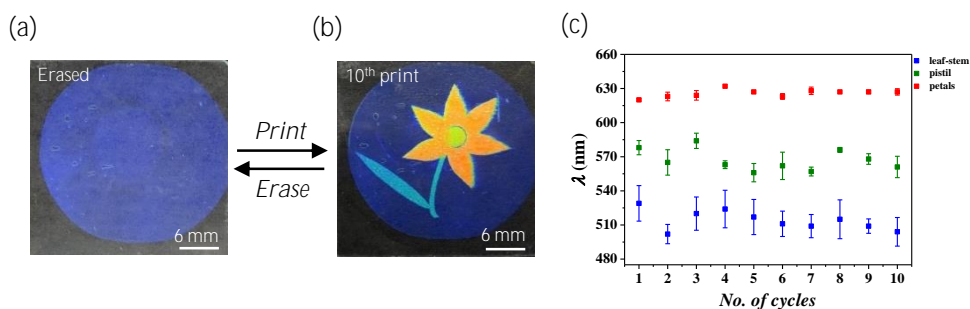
Figure 3.5. (a) Photograph of a polymer coating after erasing printed patterns with THF. (b) Photograph of the same polymer patterned with a flower image printed for the tenth time after 9 print-erase cycles. (c) Wavelength of light reflected by the different color parts of the flower patterns which had been printed successively after erasing the previous one. Error bars indicate mean ± standard deviations for three measurements at different areas on the pattern.

3.3 Conclusion

We have developed a fully rewritable and printable photonic coating from a CLC polymer network. The coating could be inkjet-printed with E7 mixture as LC ink to locally swell the network and create patterns of colors ranging from violet to red which are visible without the use of a solvent or vapor. The printed patterns were stable and durable in ambient conditions, and could be erased completely to print another new pattern. The range of colors can be further tuned by varying the amount of the non-polymerizable mesogen initially present in the network making these

photonic polymer coatings appealing as rewritable photonic papers. Furthermore, by using LC inks which are polymerizable, it will be possible to fabricate arbitrary polymer patterns which can, for example, change colors and topographies in response to a stimulus.[31,32]

3.4   Experimental Details

3.4.1   Materials

RM257, RM105, 5CB and E7 were bought from Merck. LC756 was bought from BASF. Irgacure 651 was obtained from CIBA. Tetrahydrofuran (THF) was obtained from Biosolve.

3.4.2   Characterization

Photopolymerization was carried out with Omnicure series 2000 EXFO lamp. UV-Visible spectra of the CLC polymer coatings were measured by a Perkin Elmer lambda 650 spectrophotometer. Ocean Optics UV-Visible spectrophotometer HR2000+ mounted on a DM2700 M microscope from Leica microsystems was used for recording the transmission spectra of the photonic patterns. The same microscope was used for capturing images with cross polarizers. FT-IR spectra were measured on a Varian 670 FT-IR spectrometer with slide-on ATR (Ge). Inkjet printing was done in Dimatix DMP 2800 (Dimatix-Fijifilm Inc., Santa Clara, USA) equipped with 10 pL cartridge (DMC-11610). Height profile measurement was carried out with Veeco Dektak 150 surface profiler. Images of the patterns were taken with a Sony Cyber-shot camera.

3.4.3   Functionalization of glass substrates

Methacrylate and fluorinated alkylsilane functionalized glass slides were prepared as reported in Chapter 2.

3.4.4   Preparation of photonic polymer coating

For making full color patterns, 1 g of CLC mixture consisting of 11.0 wt % of RM257, 44.0 wt % of RM105, 40.0 wt % of 5CB, 4.0 wt % of LC756, and 1.0 wt % of Irgacure 651 was dissolved in 2 mL THF. 40 µL of this solution was casted on a methacrylate functionalized 3×3 cm^2 glass substrate. After the evaporation of solvent at 75 °C, a fluorinated alkylsilane coated 3×3 cm^2 glass substrate was placed directly on top and on cooling down to room temperature, the glass substrates were sheared along one direction to obtain a red film. It was then followed by photopolymerization by shining UV light (48 mW cm^{-2} intensity in the range 320-390 nm) for 5 min after which the upper glass plate was removed to obtain the polymer coating. The polymer was then washed in THF to get the violet colored CLC polymer coating.

For the rewritability experiments, a CLC mixture with slightly modified compositions was used. 1g consisted of 15.5 wt % of RM257, 49.0 wt % of RM105, 30.0 wt % of 5CB, 4.5 wt % of LC756, and 1.0 wt % of Irgacure 651 and the pristine CLC polymer was yellow in color while after washing with THF, it turned violet.

3.4.5   Patterning by inkjet printing in polymer coating

10 pL cartridge consisting of 12 nozzles with diameter 21.5 µm was used for printing. E7 mixture was used as the ink. The cartridge temperature was set at 70 °C and the printing plate was maintained at 60 °C. Printing was carried out by using only 3 nozzles with a voltage of 13.0 and 8.0 V for 10 and 1 pL cartridges respectively and frequency 2.0 kHz using standard wave form.

3.5   References

[1]   J. Sun, B. Bhushan, J. Tong, *RSC Adv.* 2013, *3*, 14862.
[2]   J. Zi, X. Yu, Y. Li, X. Hu, C. Xu, X. Wang, X. Liu, R. Fu, *Proc. Natl. Acad. Sci.* 2003, *100*, 12576.

[3]   R. Hanlon, *Curr. Biol.* 2007, *17*, 400.

[4]   L. P. Biró, J. P. Vigneron, *Laser Photonics Rev.* 2011, *5*, 27.

[5]   F. P., M. H., *Nanomater. Nanotechnol.* 2014, *4*, 1.

[6]   L. Phan, R. Kautz, E. M. Leung, K. L. Naughton, Y. Van Dyke, A. A. Gorodetsky, *Chem. Mater.* 2016, *28*, 6804.

[7]   J. Ge, Y. Yin, *Angew. Chem., Int. Ed.* 2011, *50*, 1492.

[8]   M. Moirangthem, R. Arts, M. Merkx, A. P. H. J. Schenning, *Adv. Funct. Mater.* 2016, *26*, 1154.

[9]   M. Moirangthem, T. A. P. Engels, J. Murphy, C. W. M. Bastiaansen, A. P. H. J. Schenning, *ACS Appl. Mater. Interfaces* 2017, *9*, 32161.

[10]   Y. Fang, S. Y. Leo, Y. Ni, J. Wang, B. Wang, L. Yu, Z. Dong, Y. Dai, V. Basile, C. Taylor, P. Jiang, *ACS Appl. Mater. Interfaces* 2017, *9*, 5457.

[11]   Y. Fang, Y. Ni, S.-Y. Leo, C. Taylor, V. Basile, P. Jiang, *Nat. Commun.* 2015, *6*, 7416.

[12]   M. Moirangthem, J. E. Stumpel, B. Alp, P. Teunissen, C. W. M. Bastiaansen, A. P. H. J. Schenning, *Proc. SPIE* 2016, *9769*, 97690Y.

[13]   J. Ge, J. Goebl, L. He, Z. Lu, Y. Yin, *Adv. Mater.* 2009, *21*, 4259.

[14]   H. Hu, Q.-W. Chen, H. Wang, R. Li, W. Zhong, *J. Mater. Chem.* 2011, *21*, 13062.

[15]   X. Du, T. Li, L. Li, Z. Zhang, T. Wu, *J. Mater. Chem. C* 2015, *3*, 3542.

[16]   H. Fudouzi, Y. Xia, *Langmuir* 2003, *19*, 9653.

[17]   L. Bai, Z. Xie, W. Wang, C. Yuan, Y. Zhao, Z. Mu, Q. Zhong, Z. Gu, *ACS Nano* 2014, *8*, 11094.

[18]   H. Fudouzi, Y. Xia, *Adv. Mater.* 2003, *15*, 892.

[19]   Z. Wang, J. Zhang, J. Xie, Z. Wang, Y. Yin, J. Li, Y. Li, S. Liang, L. Zhang, L. Cui, H. Zhang, B. Yang, *J. Mater. Chem.* 2012, *22*, 7887.

[20]   H. S. Kang, J. Lee, S. M. Cho, T. H. Park, M. J. Kim, C. Park, S. W. Lee, K. L. Kim, D. Y. Ryu, J. Huh, E. L. Thomas, C. Park, *Adv. Mater.* 2017, *29*, 1.

[21]   M. K. Khan, A. Bsoul, K. Walus, W. Y. Hamad, M. J. Maclachlan, *Angew. Chem., Int. Ed.* 2015, *54*, 4304.

[22]   S. Ye, J. Ge, *J. Mater. Chem. C* 2015, *3*, 8097.

[23]   R. Xuan, J. Ge, *J. Mater. Chem.* 2012, *22*, 367.

[24]   M. Moirangthem, A. P. H. J. Schenning, *ACS Appl. Mater. Interfaces* 2018,10, 4168

[25]   M. Moirangthem, A. P. H. J. Schenning, in *Liquid Crystal Sensors*; A. P. H. J. Schenning, G. P. Crawford, D. J. Broer, Eds.; Taylor & Francis Group: Boca Raton, 2017; pp. 83–102.

[26]   D.-J. Mulder, A. P. H. J. Schenning, C. W. M. Bastiaansen, *J. Mater. Chem. C* 2014, *2*, 6695.

[27]   T. J. White, M. E. McConney, T. J. Bunning, *J. Mater. Chem.* 2010, *20*, 9832.

[28]   Q. Li, *Intelligent Stimuli Responsive Materials: From Well-defined Nanostructures to Applications*; John Wiley & Sons: Hoboken, New Jersey, 2013.

[29]   M. T. Viciosa, A. M. Nunes, A. Fernandes, P. L. Almeida, M. H. Godinho, M. D. Dionisio, *Liq. Cryst.* 2002, *29*, 429.

[30]   J.-S. Kim, M. Jamil, J. E. Jung, J. E. Jang, J. W. Lee, F. Ahmad, M.-K. Woo, J. Y. Kwak, Y. J. Jeon, *J. Inf. Disp.* 2011, *12*, 135.

[31]   J. E. Stumpel, E. R. Gil, A. B. Spoelstra, C. W. M. Bastiaansen, D. J. Broer, A. P. H. J. Schenning, *Adv. Funct. Mater.* 2015, *25*, 3314.

[32]   J. E. Stumpel, D. J. Broer, A. P. H. J. Schenning, *RSC Adv.* 2015, *5*, 94650.

Chapter 4

An Optical Sensor to Detect Calcium

In Serum

Abstract: An optical calcium sensor was fabricated based on a cholesteric liquid crystalline (CLC) polymer containing benzoic acid metal binding sites. A chiral imprinted CLC polymer, on treatment with KOH, yielded a responsive green reflecting coating. Investigation of various metal ions revealed that the polymer coating showed a large optical response, and selectivity for calcium ions, which is related to the pre-organized binding sites in the ordered liquid crystalline phase, leading to a blue reflecting coating. The photonic polymer coating was sensitive to Ca^{2+} within the physiologically relevant concentration range of 10^{-4} to 10^{-2} M. Measurement of total calcium concentration in serum was also investigated. The optical responses of normal serum and samples mimicking hypocalcemia and hypercalcemia could be clearly distinguished, providing a cheap, battery–free, and easy-to-use alternative for calcium determination in clinical diagnostics.

4.1 Introduction

Detection and quantification of metal ions is important in many fields including medical diagnosis, clinical toxicology, environmental monitoring and waste water management.[1] Several techniques, such as atomic absorption spectroscopy, inductively coupled plasma mass spectroscopy, and inductively coupled plasma optical emission spectroscopy are employed for determination of the amount of metal ions with great precision. Besides requiring specialized equipment, these techniques require complex sample preparation and are typically expensive. Therefore, development of an affordable, quick, and easy-to-use technology that enables detection of metal ions even in areas where access to laboratory facilities is limited remains of continued interest. In this respect, a test strip with an optical readout discernable by the naked eye is appealing.

Photonic crystals[2–5] that are able to reflect light have emerged as an attractive material for the development of optical sensors. Hydrogel based photonic crystals have been used to design various metal sensors,[6–8] whereby selectivity was introduced by incorporating different molecular recognition groups such as crown ether,[9–12] and 8-hydroxyquinoline.[13] Due to their one dimensional photonic structure and ease of fabrication, cholesteric liquid crystals (CLC)[14–17] have also attracted much attention as optical sensors. [18–21] To date, a few metal sensors from CLC materials have been reported by incorporating crown ether moieties for the detection of metal cations in aqueous solution.[22,23] Fabrication of optical metal sensor that shows a high selectivity and sensitivity remains a challenge, however.

We now report on a metal sensor based on CLC polymer coating that demonstrates a remarkable selectivity and optical response towards calcium, which is related to the preorganized binding sites in the liquid crystalline network. Varying

the Ca^{2+} concentration between 10^{-4} to 10^{-2} M induced a robust optical response that was clearly visible to the naked eye. The sensor could also be used as a test strip for detection of calcium in human serum.

4.2 Results and Discussion

4.2.1   Fabrication of polymer optical sensor
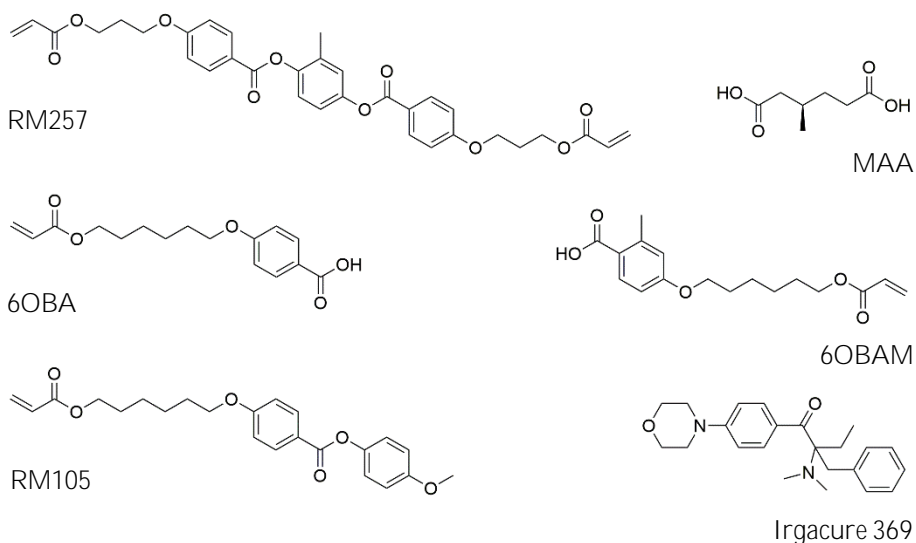
Scheme 4.1. CLC mixture used for fabrication of photonic polymer coatings.

The CLC mixture (Scheme 4.1) used in this study is similar to the one reported in Chapter 2. It consisted of a monoacrylate (RM105, 27.7 wt %) mesogen and a diacrylate (RM257, 22.5 wt %) mesogen. Benzoic acid group functionalized polymerizable molecules *viz.* 6OBA (16.4 wt %) and 6OBAM (16.4 wt %) were incorporated to bind metal ions. Two different benzoic acids were used to prevent crystallization of the CLC mixture at room temperature. Non-polymerizable dicarboxylic acid, R-(+)-3-methyladipic acid (MAA, 16.4 wt %) was added to act as the chiral dopant to induce formation of CLC phase. Irgacure 369 (0.6 wt %) was

used as the initiator for photopolymerization. The planar alignment of the CLC mixture was achieved by shearing between a methacrylate functionalized glass substrate (lower) and a fluorinated alkylsilane functionalized glass slide (upper). The CLC mixture was then photopolymerized at room temperature during which the polymer becomes covalently bonded to the methacrylate functionalized glass substrate. The upper glass slide was then removed to obtain a disc-shaped CLC polymer coating with a diameter ≈ 2 cm and a thickness ≈ 10 μm and the green selective reflection band (SRB) was centered at $\lambda \approx 512$ nm (Figure 4.1). The Fourier-Transform Infrared (FT-IR) spectrum of the polymer coating (Figure 4.2a) showed the absence of C=C double bond of the acrylate as no peaks are present at 809 or 985 cm^{-1}.[24] A highly intense peak centered at 1696 cm^{-1} was observed due to the stretching vibration of hydrogen bonded C=O. The broad nature of this peak suggests the presence of more than one type of H-bonded carboxylic acids[25] *i.e.*, H-bonded MAAs, H-bonded benzoic acids and mixed MAA-benzoic acid complexes. It should be noted that since the ratio of molar concentration of MAA to 6OBA and 6OBAM is 2:1:1, not all the carboxylic acid moieties of the MAA molecules are bound to the polymer network. Thermogravimetric analysis (TGA) showed a weight loss of 16.5 % in the temperature range of 120 to 200 °C (Figure 4.2b), which can be attributed to evaporation of MAA.

In order to enhance the optical response of the polymer coating, the chiral molecule MAA was removed by extracting using an organic solvent (tetrahydrofuran, THF).[26] The TGA profile (Figure 4.2b) of this more flexible polymer coating did not show any loss in weight below 300 °C, which is consistent with complete removal of MAA. The FT-IR spectrum showed a sharp vibration peak at 1680 cm^{-1} indicating the presence of H-bonded dimer of 6OBA and 6OBAM

(Figure 4.2a).[24] Upon removal of the chiral dopant the reflection band shifted to λ ≈ 380 nm indicating that the helical structure is still present and that a chiral-imprinted polymer network has been formed (Figure 4.1). The blue shift of $\Delta\lambda$ ≈ 130 nm of the SRB suggests a collapse of the polymer coating which resulted to a decrease in pitch length as the number of pitches is invariant after polymerization.[27] The remarkable wavelength shift of 25 % is higher than the weight fraction of the chiral dopant (16.4 wt %), suggesting that the shrinkage in the polymer coating, having covalent links to the glass substrate, mainly takes place in the vertical direction.
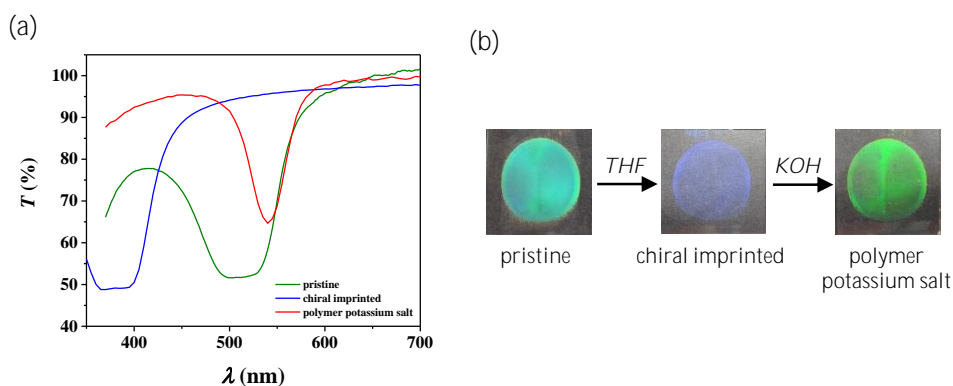
Figure 4.1. (a) UV-Vis transmission spectra and (b) photographs of the CLC polymer coating at different preparation steps.

In order to make the polymer coating responsive to metal ions, the chiral imprinted coating was treated with KOH to convert the benzoic acid units to potassium benzoate derivatives. FT-IR analysis of this KOH treated coating showed disappearance of a stretching vibration peak due to H-bonded C=O at 1680 cm^{-1} (Figure 4.2a). The peak at 1728 cm^{-1} due to the carbonyl of ester groups remained identical implying that KOH treatment does not affect the alkyl ester moieties. Two new peaks appeared at 1543 cm^{-1} and 1382 cm^{-1}, corresponding to the asymmetric

(a)

(b)
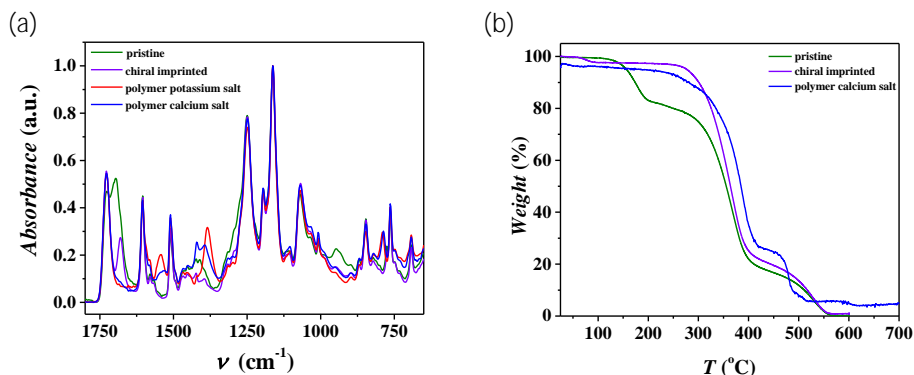
Figure 4.2. (a) FT-IR spectra of the pristine CLC polymer, chiral imprinted polymer, potassium polymer salt and calcium polymer salt coatings. (b) TGA of the pristine CLC polymer, chiral imprinted polymer and calcium polymer salt coatings.

and symmetric stretching of COO^-,[24] which is consistent with complete deprotonation of the benzoic acid groups to form a K^+-carboxylate salt. [24,28–30] This polymer potassium salt coating swelled by absorbing water from KOH solution leading to an increase in pitch and thus a change in color with the reflection band at $\lambda \approx 540$ nm (Figure 4.1) which was around the same wavelength as the pristine polymer. The bandwidth was narrower which might be due to the absorbed water lowering the birefringence in the coating.[31] This SRB was red shifted by 160 nm with respect to the chiral imprinted polymer showing the ability of the flexible polymer coating to reversibly change its optical properties over a large spectral range. When the polymer was placed in de-ionized water, a small blue shift ($\Delta\lambda \approx 17$ nm) of the green reflection band was observed.

4.2.2   Detection of metal ions in water

To investigate the binding efficacy of the potassium salt polymer towards metal cations, the coating was exposed to 0.75 mL of 0.1 M of monovalent and divalent cations such as Na^+, Mg^{2+}, Ca^{2+}, Zn^{2+}, Cd^{2+} and Pb^{2+} for 60 min and the optical resp-
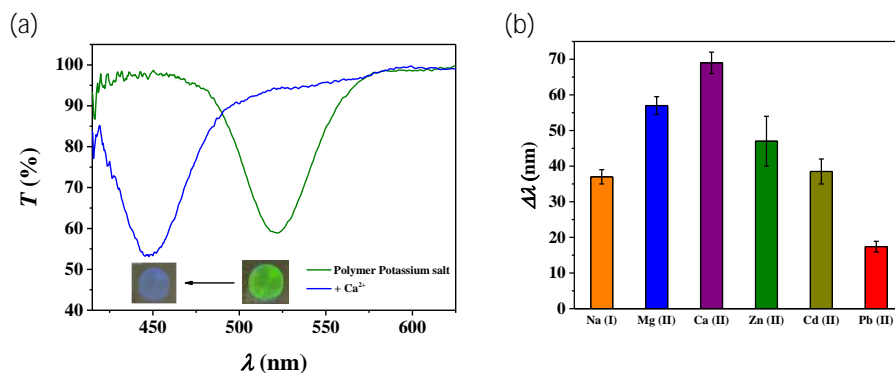
Figure 4.3. (a) UV-Vis transmission spectrum of the polymer potassium salt coating in water and after exposure to 0.1 M Ca^{2+} solution. Inset shows photographs of the coating before and after exposure to 0.1 M Ca^{2+} solution. (b) Blue shift observed for the reflection band of polymer potassium salt coating after exposure to 0.75 mL of 0.1 M $NaNO_3$, $Mg(NO_3)_2$, $Ca(NO_3)_2.4H_2O$, $Zn(NO_3)_2.6H_2O$, $Cd(NO_3)_2.4H_2O$ and $Pb(NO_3)_2$. Error bar indicates mean ±standard deviation for five measurements at different places on the coating. Duration of exposure to the metal ions solution was 60 min.

onse was monitored with UV-Vis spectroscopy. It was observed that in all cases the reflection band of the coatings blue shifted to different extents (Figure 4.3). Interestingly, a close examination of the blue shift, $\Delta\lambda$, of the SRB (Figure 4.3b), revealed that Ca^{2+} gave the highest $\Delta\lambda \approx 70$ nm yielding a blue reflecting polymer whose color change could be clearly seen by the naked eye (Figure 4.3b). To determine the selectivity of the polymer potassium salt coating, Na^+, Mg^{2+}, Ca^{2+}, Zn^{2+} and Cd^{2+} ions were dissolved together in water such that the concentration of each of the nitrate salt was 0.1 M. On exposing the polymer salt coating to this metal ions solution, the SRB blue shifted by nearly 65 nm which is very close to $\Delta\lambda$ (≈ 70 nm) observed for Ca^{2+} (Figure 4.4a). This suggests that Ca^{2+} ions has the highest binding affinity for the polymer coating relative to the other metal ions. To further test the Ca^{2+} selectivity, a Ca^{2+} polymer coating (*vide infra*) was exposed to Zn^{2+}, Mg^{2+}, Cd^{2+} and Na^+ solutions (each of 1 M concentration, 0.75 mL) consecutively. There was no change in the reflection band (Figure 4.4b), confirming that calcium is strongly

bound in the polymer coating (*vide infra*). From these studies it can be concluded that Ca^{2+} binds selectively and strongly to the polymer coating over all the other metal ions studied. The binding of Ca^{2+} apparently results in a large decrease in the length of helical pitch which may be due to dehydration of the coating leading to polymer shrinkage.[32] The bound Ca^{2+} ions can be washed away by treating the polymer with dilute HNO_3 and the resulting polymer, can be re-used. Moreover, the polymer potassium salt coatings can be stored at ambient conditions for days.
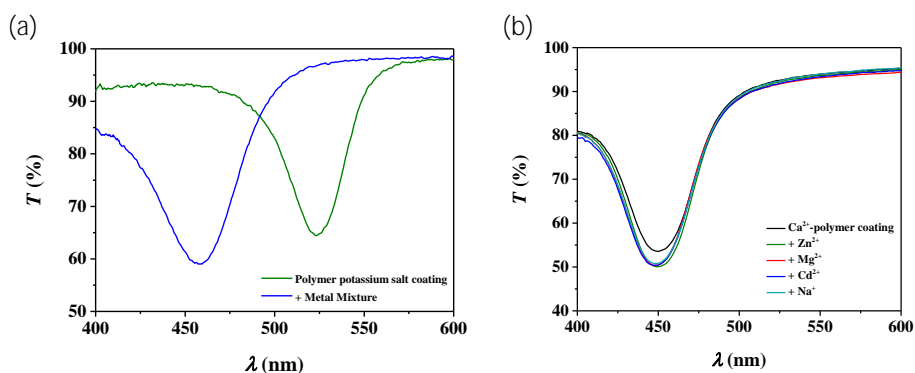
Figure 4.4. UV-Vis transmission spectrum of (a) polymer potassium salt coating before and after exposure to mixture of equimolar metal ions Na^+, Mg^{2+}, Ca^{2+}, Zn^{2+}, Cd^{2+}, Pb^{2+} (0.1 M each) (b) Calcium polymer salt coating on successive exposure to 1 M of Zn^{2+}, Mg^{2+}, Cd^{2+}, Na^+ solutions. Duration of exposure to the metal ions solution was 60 min.

4.2.3   Detection of calcium in water

To investigate the calcium selectivity and sensitivity in more detail, the kinetics of the exchange reaction of K^+ by Ca^{2+} was investigated. The polymer potassium salt coating was treated with Ca^{2+} (0.1 M) and the change of the reflection band was monitored by UV-Vis spectroscopy. Within a minute of exposure, the SRB of the wet polymer coating blue shifted by nearly 60 nm (Figure 4.5a). An additional blue shift of 10 nm was observed in the next 60 min, after which it did not change any further. This revealed that exchange between K^+ and Ca^{2+} is rapid and is

accompanied by release of absorbed water from the polymer and hence a blue shift of the SRB. FT-IR measurements showed an increase in the symmetric stretching frequency of COO^- from 1385 cm^{-1} to 1394 cm^{-1} and decrease in the asymmetric stretching frequency of COO^- from 1543 cm^{-1} to 1531 cm^{-1} (Figure 4.2a) indicating binding of COO^- to Ca^{2+}.[33,34]
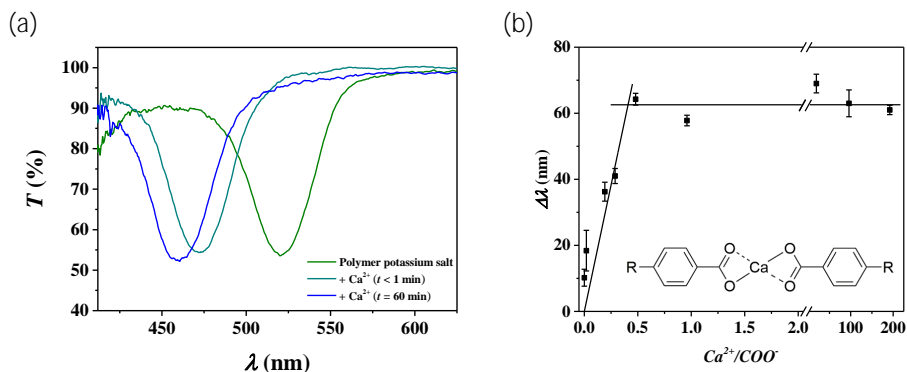
Figure 4.5. (a) UV-Vis transmission spectrum of the polymer potassium salt coating on exposure to 0.1 M Ca^{2+} solution taken at different time (b) blue shift of the reflection band of polymer potassium salt coating after exposure to different concentration of Ca^{2+} (inset – schematic of the expected stoichiometry of Ca-carboxylate complex). The X-axis represents the molar ratio of Ca^{2+} to COO^- binding sites. Error bar indicates mean±standard deviation for five measurements at different places on the coating. Duration of exposure to the Ca^{2+} solution was 60 min.

In order to determine the stoichiometry of calcium complexation, polymer potassium salt coatings were exposed to different concentration of Ca^{2+} ions. Figure 4.5b shows the blue shift of the SRB as a function of the ratio of Ca^{2+} ions to available benzoate binding sites (2.5×10^{18} per coating).[35] With an increased amount of Ca^{2+} ions, an increase in the blue shift was observed before saturation of the COO^- sites took place. A sharp inflection point was observed **when the amount of calcium ≈ 0.5** with respect to the binding sites indicating that two COO^- are binding one Ca^{2+} ion and that the binding is strong.[36] The TGA profile of fully saturated Ca^{2+}-polymer coating showed a content of 4 wt % at temperature above 600 °C (Figure 4.2b) which

corresponds to the amount of $CaCO_3$ that would be formed when Ca^{2+} binds to two COO^- binding sites and is heated up.[37]

The association constants of benzoic acid towards a variety of metal ions in solution do not show any preference for Ca^{2+}.[38] It is well known that divalent calcium prefers bidentate over monodentate binding of carboxylate.[39] In the CLC polymer coating, the benzoic acid groups are planarly aligned pointing towards each other by hydrogen bond interactions (*vide supra*). Most likely this preorganized planar like-geometry facilitated strong binding of calcium.[40] Calcium-carboxylate complexes have been shown to be less hydrated,[39,41] compared to other metal-carboxylate complexes, which is attributed to their low polarizing power of bound first shell water molecules.[42] This could explain the release of large amount of water leading to a large color change of the polymer coating upon binding to Ca^{2+}. Presumably, it is the preorganization that is causing the strong, fast and selective binding of Ca^{2+} with subsequent dehydration of the coating.

4.2.4 Detection of calcium in serum

To determine the effective range of calcium concentrations for which the polymer coating is most sensitive, the $\Delta\lambda$ of the SRB was plotted against different Ca^{2+} concentrations in logarithmic scale (Figure 4.6a). It can be seen that the increase in $\Delta\lambda$ occurs between 10^{-4} to 10^{-2} M concentrations of Ca^{2+}. It should be noted that this sensitivity, however, will depend on the number of binding sites and the thickness of the coating. Interestingly, for a healthy human the amount of total calcium in blood occurs in the range of 2.1×10^{-3} to 2.6×10^{-3} M[43] precisely in the range where the coating is most sensitive, indicating that perhaps our coating could be used as an alternative readout system for this important diagnostic parameter.[44–52] For a healthy human, total magnesium levels in blood are in the range of 0.7×10^{-3}

to 1×10^{-3} M.[53] In order to determine the sensitivity of our sensor towards calcium, a Mg^{2+}-polymer coating was treated with a 1 M Ca^{2+} solution (0.75 mL). A blue shift of 14 nm of the SRB (Figure 4.7) was observed indicating Ca^{2+} has replaced Mg^{2+} in the polymer coating.
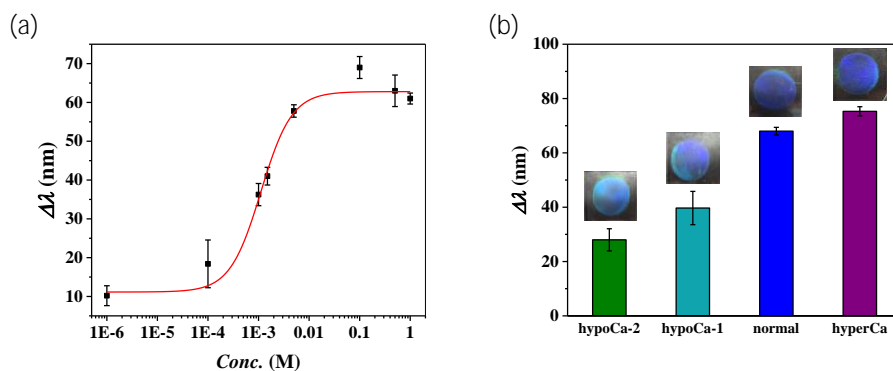
Figure 4.6. (a) Blue shift of the reflection band of polymer potassium salt coating after exposure to different molar concentration of Ca^{2+} ions [Ca^{2+}]. Error bar indicates mean±standard deviation for five measurements at different places on a coating. (b) Blue shift of the reflection band of polymer potassium salt coating after exposure to normal serum, hypocalcemia (hypoCa-1 and hypoCa-2) and hypercalcemia (hyperCa) samples. HypoCa-1 and HypoCa-2 were prepared by supplementing normal serum with 0.5 and 1 mM EDTA respectively. Error bar indicates mean±standard deviation for measurements of three different coatings. Inset shows photograph of the coatings after exposure to normal serum, hypocalcemia and hypercalcemia samples.

These results encouraged us to investigate the ability of the polymer potassium salt coating to detect calcium in serum. A blue-shift in the SRB by nearly 68 nm was observed when the polymer coating was treated with pooled normal human serum. In an attempt to explore the diagnostic potential of the coatings, we then conducted experiments treating the coatings with blood samples supplemented with 0.5 and 1 mM ethylenediaminetetraacetic acid (EDTA) (hypoCa-1 and hypoCa-2 respectively) or 1 mM $CaCl_2$ (hyperCa) in order to mimic hypo- and hypercalcemic blood samples, respectively (Figure 4.6b). As expected, coatings treated with blood
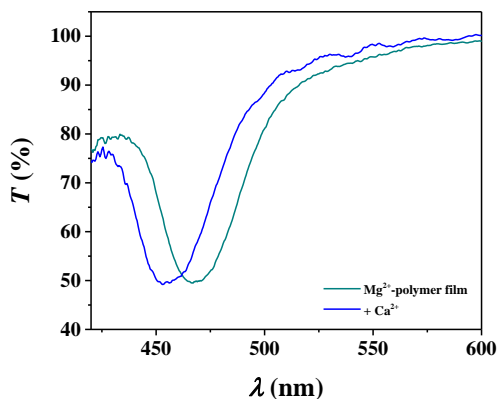
Figure 4.7. UV-Vis transmission spectrum of Mg^{2+}-CLC polymer coating before and after exposure to a 1M Ca^{2+} solution.

samples with a reduced Ca^{2+} concentration displayed a smaller blue-shift (around 40 nm for hypoCa-1 and around 28 nm for hypoCa-2), while coatings treated with blood samples with elevated Ca^{2+} levels displayed an increased blue-shift ($\approx$ 75 nm), slightly higher than the maximum blue shift ($\approx$ 69 nm) observed for aqueous Ca^{2+} which may be due to difference in osmotic pressure of blood serum compared to water. These results confirmed that the coating is sensitive to changes in Ca^{2+} levels in the physiologically relevant concentration range, and that the coating may eventually be used as an alternative, low-cost readout system for the detection and quantification of Ca^{2+} levels in blood serum. The difference in color of the coatings after exposure to serum simulating hypocalcemia and hypercalcemia cannot be easily observed unaided, however, this can probably be addressed by using a smartphone camera application.

4.3 Conclusion

An optical calcium sensor has been fabricated based on chiral imprinted cholesteric liquid crystalline polymer. The polymer photonic film shows a

remarkable selective response to calcium, with a color change from green to blue. This result is ascribed to liquid crystalline order in the material resulting in a pre-organized optimal binding geometry for calcium and the dehydration properties of the calcium complex. It suggests that CLC based sensors can be constructed that show a selective high optical response towards metal ions without using specific binding moieties. Most likely, the effective sensitivity of the sensor can be further optimized by varying the number of binding sites and the thickness of the polymer film. The calcium sensor could also be used as a test strip for qualitative detection of calcium in serum. Normal serum and samples mimicking hypocalcemia and hypercalcemia showed optical responses which could be distinguished spectroscopically. These optical materials hold promise in fabrication of cheap, easy-to-use, battery free metal ion sensors for clinical diagnostics.

4.4 Experimental Details

4.4.1   Materials

RM257 and RM105 were purchased from Merck. 6OBA and 6OBAM were obtained from Synthon. Irgacure 369 was from CIBA. Chiral dopant (R)-(+)-3-methyladipic acid, 3-(trimethoxysilyl)propyl methacrylate and 1*H*, 1*H*, 2*H*, 2*H* -perfluorodecyltriethoxysilane were from Sigma Aldrich. The solvents tetrahydrofuran, isopropanol and ethanol were bought from Biosolve.

4.4.2   Characterization

UV-Vis studies were carried out with a Shimadzu UV-3102 PC UV/Vis-near-IR scanning spectrophotometer. A Varian 670 FT-IR spectrometer with slide-on ATR (Ge) was used to record IR spectra. Thermogravimetric analyses were performed in TA TGA Q500. Photopolymerization was carried out with Omnicure series 2000

EXFO lamp. Height measurements were done using a Fogale Nanotech Zoomsurf 3D. Laser writing was carried out with a Argon Ion laser (SpectraPhysics Beamlok 2050), operating at 351 nm.

4.4.3   Functionalization of glass substrates

Methacrylate and fluorinated alkylsilane functionalized glass slides were prepared as reported in Chapter 2.

4.4.4   Preparation of CLC polymer coating

1 g of CLC mixture consisting of 23.5 wt % of RM 257, 30.5 wt % of RM 105, 16 wt % of each of 6OBA and 6OBAM, 13.5 wt % of (R)-(+)-3-methyladipic acid and 0.5 wt % of Irgacure 369 was dissolved in 4 mL of tetrahydrofuran. Approximately 80 µL of this solution was dropped on methacrylate functionalized 5 cm × 5 cm glass slide. After evaporating the solvent by heating at 75 °C, a fluorinated alkylsilane coated 5 cm × 5 cm glass slide was placed directly on top and cooled to room temperature simultaneously shearing along one direction to obtain a planarly aligned orange color coating. It was then followed by photopolymerization by shining UV light (48 mW cm^{-2} intensity in the range 320-390 nm) for 5 min after which the upper fluorinated alkylsilane coated glass was removed.

4.5 References

[1]   G. Aragay, J. Pons, A. Merkoçi, *Chem. Rev.* 2011, *111*, 3433.
[2]   H. Wang, K.-Q. Zhang, *Sensors* 2013, *13*, 4192.
[3]   C. Fenzl, T. Hirsch, O. S. Wolfbeis, *Angew. Chem., Int. Ed.* 2014, *53*, 3318.
[4]   J. Ge, Y. Yin, *Angew. Chem., Int. Ed.* 2011, *50*, 1492.
[5]   L. Wang, Q. Li, *Adv. Funct. Mater.* 2015, *26*, 10.
[6]   D. Arunbabu, A. Sannigrahi, T. Jana, *Soft Matter* 2011, *7*, 2592.
[7]   N. Gogoi, M. Barooah, G. Majumdar, D. Chowdhury, *ACS Appl. Mater. Interfaces* 2015, *7*, 3058.

[8]   B.-F. Ye, Y.-J. Zhao, Y. Cheng, T.-T. Li, Z.-Y. Xie, X.-W. Zhao, Z.-Z. Gu, *Nanoscale* 2012, *4*, 5998.

[9]   S. A. Asher, S. F. Peteu, C. E. Reese, M. X. Lin, D. Finegold, *Anal. Bioanal. Chem.* 2002, *373*, 632.

[10]   J. H. Holtz, S. A. Asher, *Nature* 1997, *389*, 829.

[11]   J. H. J. S. W. Holtz, C. H. Munro, S. A. Asher, *Anal. Chem.* 1998, *70*, 780.

[12]   C. E. Reese, S. A. Asher, *Anal. Chem.* 2003, *75*, 9534.

[13]   S. A. Asher, A. C. Sharma, A. V. Goponenko, M. M. Ward, *Anal. Chem.* 2003, *75*, 1676.

[14]   H. K. Bisoyi, Q. Li, *Acc. Chem. Res.* 2014, *47*, 3184.

[15]   Y. Wang, Q. Li, *Adv. Mater.* 2012, *24*, 1926.

[16]   Q. Li, Y. Li, J. Ma, D. K. Yang, T. J. White, T. J. Bunning, *Adv. Mater.* 2011, *23*, 5069.

[17]   J. Ma, Y. Li, T. White, A. Urbas, Q. Li, *Chem. Commun.* 2010, *46*, 3463.

[18]   R. J. Carlton, J. T. Hunter, D. S. Miller, R. Abbasi, P. C. Mushenheim, L. N. Tan, N. L. Abbott, *Liq. Cryst. Rev.* 2013, *1*, 29.

[19]   D. J. Broer, C. M. W. Bastiaansen, M. G. Debije, A. P. H. J. Schenning, *Angew. Chem., Int. Ed.* 2012, *51*, 7102.

[20]   T. J. White, M. E. McConney, T. J. Bunning, *J. Mater. Chem.* 2010, *20*, 9832.

[21]   M. Mitov, *Adv. Mater.* 2012, *24*, 6260.

[22]   S. Kado, Y. Takeshima, Y. Nakahara, K. Kimura, *J. Incl. Phenom. Macrocycl. Chem.* 2011, *72*, 227.

[23]   V. Stroganov, A. Ryabchun, A. Bobrovsky, V. Shibaev, *Macromol. Rapid Commun.* 2012, *33*, 1875.

[24]   J. E. Stumpel, C. Wouters, N. Herzer, J. Ziegler, D. J. Broer, C. W. M. Bastiaansen, A. P. H. J. Schenning, *Adv. Opt. Mater.* 2014, *2*, 459.

[25]   A. Martínez-Felipe, A. G. Cook, M. J. Wallage, C. T. Imrie, *Phase Transitions* 2014, *87*, 1191.

[26]   C. K. Chang, C. M. W. Bastiaansen, D. J. Broer, H. L. Kuo, *Adv. Funct. Mater.* 2012, *22*, 2855.

[27]   N. Herzer, H. Guneysu, D. J. D. Davies, D. Yildirim, A. R. Vaccaro, D. J. Broer, C. W. M. Bastiaansen, A. P. H. J. Schenning, *J. Am. Chem. Soc.* 2012, *134*, 7608.

[28]   P. V. Shibaev, R. L. Sanford, D. Chiappetta, P. Rivera, *Mol. Cryst. Liq. Cryst.* 2007, *479*, 161/[1199].

[29]   P. V. Shibaev, D. Chiappetta, R. L. Sanford, P. Palffy-Muhoray, M. Moreira, W. Cao, M. M. Green, *Macromolecules* 2006, *39*, 3986.

[30]   P. V. Shibaev, J. Madsen, A. Z. Genack, *Chem. Mater.* 2004, *16*, 1397.

[31]   D. Liu, C. W. M. Bastiaansen, J. M. J. den Toonder, D. J. Broer, *Angew. Chem., Int. Ed.* 2012, *51*, 892.

[32]   J. E. Stumpel, D. J. Broer, A. P. H. J. Schenning, *RSC Adv.* 2015, *5*, 94650.

[33]   T. Dudev, C. Lim, *J. Mol. Struct.* 2012, *1009*, 83.

[34]   M. Nara, H. Morii, M. Tanokura, *Biochim. Biophys. Acta - Biomembr.* 2013, *1828*, 2319.

[35]   H. P. C. van Kuringen, G. M. Eikelboom, I. K. Shishmanova, D. J. Broer, A. P. H. J. Schenning, *Adv. Funct. Mater.* 2014, *24*, 5045.

[36]   P. Thordarson, *Chem. Soc. Rev.* 2011, *40*, 1305.

[37]   M. Ghiasi, A. Malekzadeh, *Cryst. Res. Technol.* 2012, *47*, 471.

[38]   A. E. Martell, R. M. Smith, *Other Organic Ligands*; Springer Science+Business Media: New York, 1977.

[39]   T. Dudev, T. Dudev, C. Lim, C. Lim, *J. Phys. Chem. B* 2004, *108*, 4546.

[40]   J.-M. Lehn, *Chem. Soc. Rev.* 2007, *36*, 151.

[41]   T. Dudev, C. Lim, *Chem. Phys.* 2003, *103*, 773.

[42]   T. Dudev, C. Lim, *J. Am. Chem. Soc.* 2013, *135*, 17200.

[43]   S. Kim, J. W. Park, D. Kim, D. Kim, I. H. Lee, S. Jon, *Angew. Chem., Int. Ed.* 2009, *48*, 4138.

[44]   F. M. LaFerla, *Nat. Rev. Neurosci.* 2002, *3*, 862.

[45]   J. M. Lappe, D. Travers-gustafson, K. M. Davies, R. R. Recker, R. P. Heaney, *Am. J. Clin. Nutr.* 2007, *85*, 1586.

[46]   W. D. Fraser, *Lancet* 2015, *374*, 145.

[47]   K. D. Burman, J. M. Monchik, J. M. Earll, L. Wartofsky, *Ann. Intern. Med.* 1976, *84*, 668.

[48]   B. E. C. Nordin, *Nutrition* 1997, *13*, 664.

[49]   S. Kim, J. Kim, N. H. Lee, H. H. Jang, M. S. Han, *Chem. Commun.* 2011, *47*, 10299.

[50]   M. S. Eom, W. Jang, Y. S. Lee, G. Choi, Y.-U. Kwon, M. S. Han, *Chem. Commun.* 2012, *48*, 5566.

[51]   P. Caglar, S. A. Tuncel, N. Malcik, J. P. Landers, J. P. Ferrance, *Anal. Bioanal. Chem.* 2006, *386*, 1303.

[52]   Y. Guo, X. Tong, L. Ji, Z. Wang, H. Wang, J. Hu, R. Pei, *Chem. Commun.* 2015, *51*, 596.

[53]   H. Frankel, R. Haskell, S. Y. Lee, D. Miller, M. Rotondo, C. W. Schwab, *World J. Surg.* 1999, *23*, 966.

Chapter 5

Full Color Camouflage in a Printable

Blue-Colored Polymer

Abstract: A blue reflective photonic polymer coating which can be patterned in full color, from blue to red, by printing with an aqueous calcium nitrate solution has been fabricated. Color change in the cholesteric liquid crystalline polymer network over the entire visible spectrum is obtained by the use of a non-reactive mesogen. The pattern in the coating is hidden in the blue color dry state and appears upon exposure to water or by exhaling breath onto it due to different degrees of swelling of the polymer network. The degree of swelling depends on the printed amount of calcium which acts as a cross-linker. The printed full color pattern can also be hidden simply by using a circular polarizer. The responsive full color camouflage polymers are interesting for various applications ranging from responsive house and automobile decors to anticounterfeit labels and data encryption.

5.1 Introduction

Adaptive structural colors that arise due to the presence of periodic alteration of refractive indices are abundantly found in nature[1] and perform various functions such as thermoregulation to control body temperature, signaling to communicate to other members of the same species, mimicry to warn predators and camouflaging to hide from predators.[2–4] Over the years, researchers have been working to generate adaptive full structural colors and camouflage in polymers. Such responsive photonic materials could be interesting in adaptive and camouflage textiles, smart coatings for house decors and automobiles, and anticounterfeiting, for example.[5] These full colored photonic materials[6] generally consist of block copolymers, cholesteric liquid crystals or colloidal crystals and they can be patterned by locally chemically modifying their responsive properties.[7–16] Pattern fabrication using masks, however, severely limits production of diverse patterns, besides yielding patterns with only two colors. Although inkjet printing technology provides a viable solution for creating complex and diverse patterns, achieving full color camouflage in photonic-colored polymers remains a challenge.[17,18]

Cholesteric liquid crystalline (CLC) or chiral nematic polymers, [19–23] which are one-dimensional photonic materials, have captivated much attention because of the ease by which they can be fabricated into responsive materials. CLC polymers exhibit selective reflection of only one-handed circularly polarized light due to the presence of helical molecular organization with the wavelength of light reflected being directly proportional to length of the helical pitch. CLC polymers, with responsive full color, have not been explored. Until now, only chiral nematic mesoporous films with two colors have been reported.[17] Previously, we have reported an optical calcium sensor based on a CLC polymer showing reflective colors ranging from green to blue (see

also chapter 4).[24] We now report on a printable blue colored CLC polymer coating which can be patterned in full colors covering the visible spectrum from ~480 to ~640 nm with a single aqueous $Ca(NO_3)_2$ solution as the ink. The latent pattern reveals itself on exposure to water or by simply exhaling breath onto it (Scheme 5.1). Arbitrary full color camouflage patterns can be printed in the photonic polymer which can be, in principle, reprogrammed by acid-base treatment.
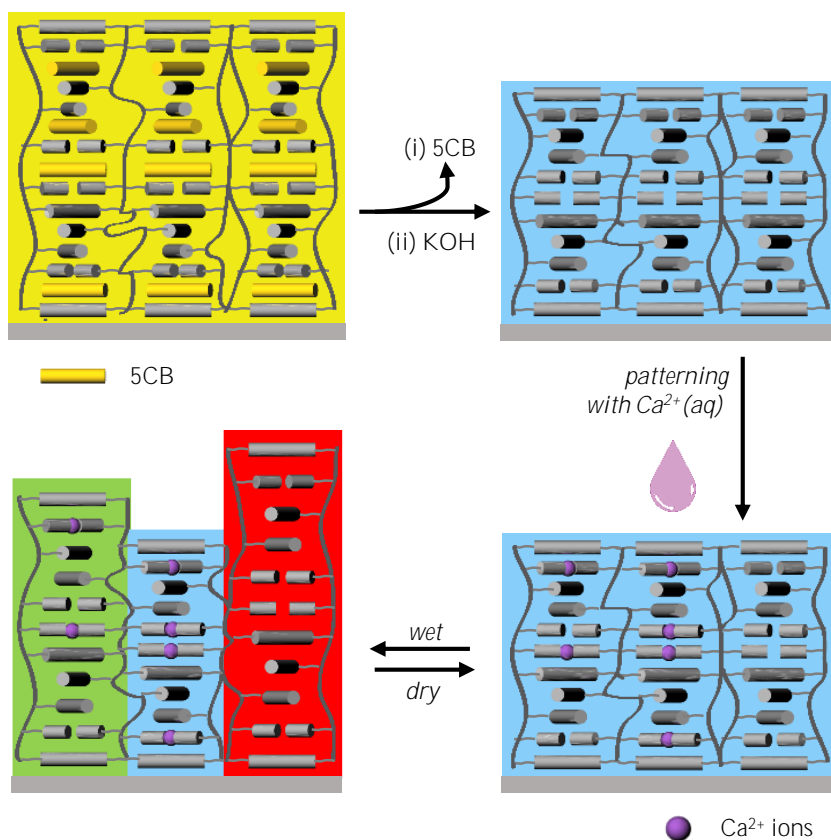
Scheme 5.1. Schematic showing the working principle of the full color camouflage in the CLC polymer coating. First, the non-reactive mesogen 5CB was removed leading to pitch shrinkage. After obtaining potassium salt polymer coating by treating with KOH, an aqueous solution of Ca^{2+} ions was used as ink for patterning. In the wet state, areas with different amount of Ca^{2+} ions swelled differently giving rise to a full color pattern while staying indistinguishable in the dry blue colored state.

5.2 Results and Discussion

5.2.1 Fabrication of CLC polymer coating
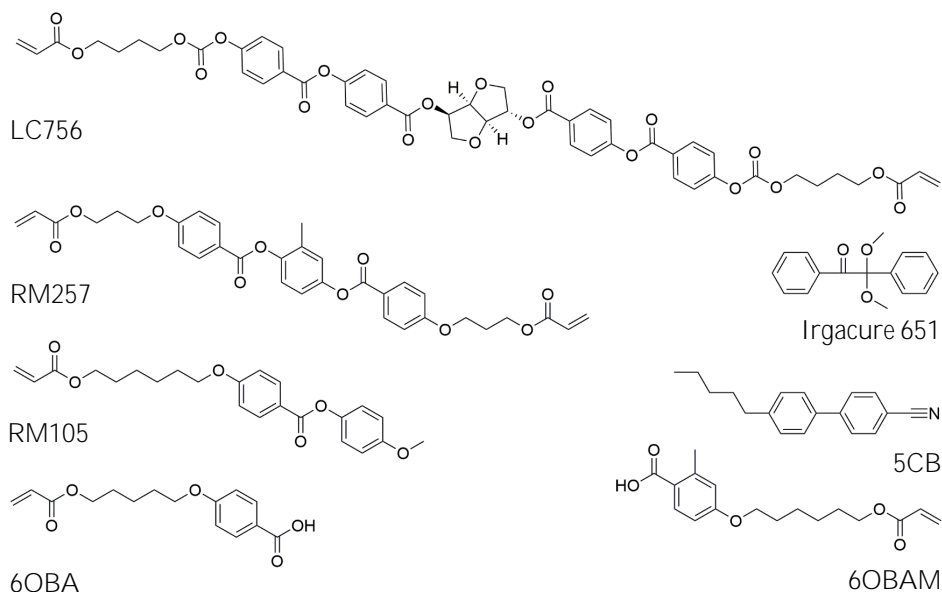
Scheme 5.2. CLC mixture used for fabrication of photonic polymer coatings.

The printable CLC polymer coating was fabricated from a monomer mixture (Scheme 5.2) consisting of diacrylate (RM257) and monoacrylate (RM105) mesogens. Hydrogen bonded benzoic acid functionalized polymerizable reactive mesogens (6OBA and 6OBAM) were used as ligands to bind to calcium ions. To induce a CLC phase, a right handed chiral dopant (LC756),[25] which also acts as a cross-linker, was added. Lastly, to enhance the response of the polymer coating to obtain a wide range of structural colors from blue to red, a removable, non-reactive mesogen (5CB) was used. The mixture also contained a photoinitiator (Irgacure 651, 0.6 wt %) to initiate the photopolymerization reaction. Shearing the CLC monomer mixture between methacrylate-functionalized and fluorinated alkylsilane-functionalized substrates resulted in planar alignment of the molecules which was

frozen by photopolymerization using UV light. Removal of the top glass plate followed by washing away the non-reactive mesogen 5CB with THF revealed a blue colored CLC polymer coating (λ = 450 nm) covalently bonded to the bottom plate (Figure 5.1a, b, c).[24] Treating the film with KOH solution resulted in rupture of **hydrogen bonds and formation of potassium salt polymer. On drying, a 15 μm thick** (Figure 5.1d) blue reflective (λ = 450 nm) hygroscopic polymer coating was obtained, which swelled and became red (λ = 630 nm) upon exposure to water due to an increase in the helical pitch. Drying led to pitch shrinkage and the coating returned to a blue color (λ = 450 nm), demonstrating a reversible color change covering almost the entire visible light spectrum.
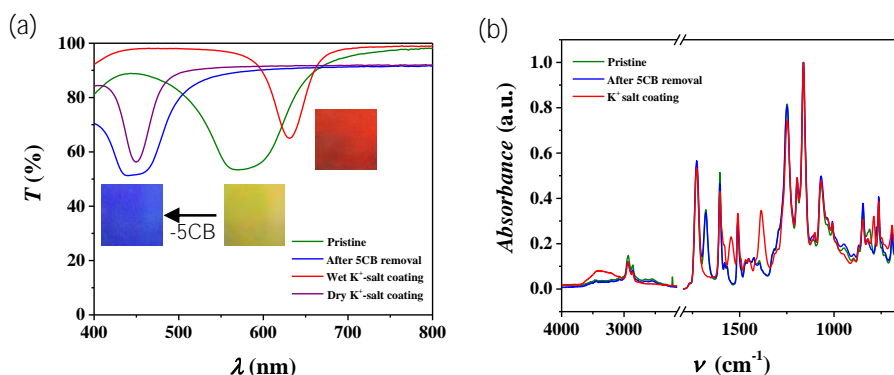
Figure 5.1. (a) UV-Vis transmission spectra, and (b) FT-IR spectra of the CLC polymer coating at different steps of fabrication. Inset shows the photographs of the pristine yellow, 5CB-removed blue, and wet potassium salt red coatings.

5.2.2 Full color pattern using Ca^{2+} as cross-linking agent

The color of the wet CLC polymer coating can be modified by Ca^{2+} ions which replaces K^+ ions and bind to the benzoate moieties.[24] Hence, photonic patterns can be created by locally introducing Ca^{2+} ions as cross-linkers. To determine the appropriate concentration of $Ca(NO_3)_2$ solutions required to achieve different colors in the visible spectrum, sponges were used in the form of stamps.[26] Sponges of 10 ×

2×1 mm^3 were simply cut out from a kitchen sponge and soaked in different concentrations of Ca(NO$_3$)$_2$ solution ranging from 0.01 to 100 mM. The sponges were then placed carefully on top of the potassium salt photonic coating. A color change took place in less than a minute, indicating a rapid K$^+$/Ca^{2+} ion exchange. UV-Vis spectroscopy of the wet polymer coating showed only one reflection band for any concentration employed, suggesting that K$^+$ and Ca^{2+} ions are uniformly distributed throughout the thickness of the film (Figure 5.2a). With concentrations 0.01 and 0.1 mM, the coating was found to reflect around 605 nm, *i.e.* $\Delta\lambda \approx 33$ nm blue shifted with respect to wet potassium salt coating, resulting in an orange color (Figure 5.2b). With increasing concentration, the wavelength of light reflected blue-shifted further due to lower degree of swelling causing decrease in pitch length. A
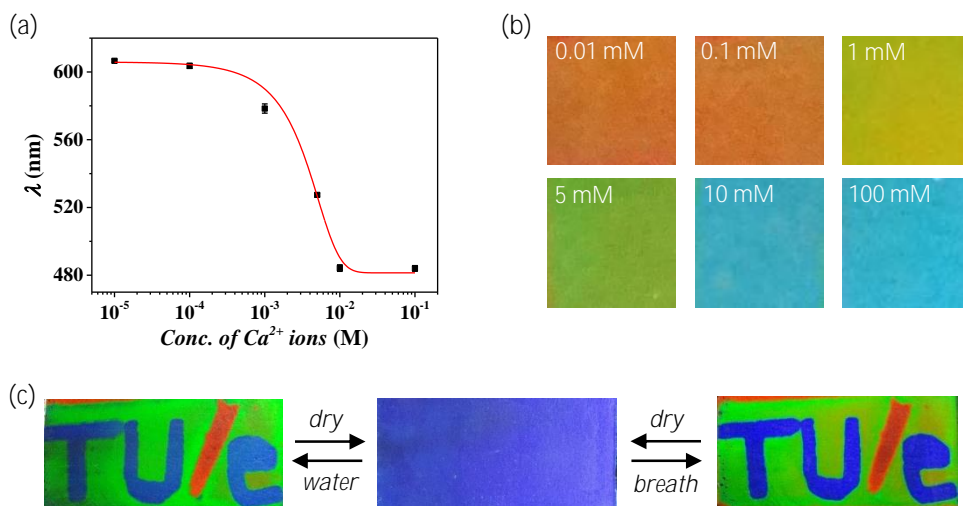
Figure 5.2. (a) Wavelength of light reflected by CLC potassium salt polymer coating treated with different concentrations of Ca(NO$_3$)$_2$ solution. The red line represents the fitted curve. Error bars indicate mean ± standard deviations for five measurements at different places on the pattern. (b) Images of the CLC coatings patterned with kitchen sponges soaked in different concentrations of Ca(NO$_3$)$_2$ solution. (c) Image of a sponge-written "TU/e" logo that appeared in wet state on exposure to water or exhaled breath but remained hidden in the dry state.

concentration of 1 mM gave rise to yellow color ($\lambda \approx 578$ nm; $\Delta\lambda \approx 60$ nm) and 5 mM resulted in a green reflection band ($\lambda \approx 527$ nm; $\Delta\lambda \approx 81$ nm). With a higher concentration of 10 mM, the film became blue ($\lambda \approx 484$ nm; $\Delta\lambda \approx 124$ nm). Increasing the concentration to 100 mM did not cause any further color shift and the film remained blue, suggesting all the K^+ ions have been replaced by Ca^{2+} ions leading to a fully crosslinked polymer network with drastically reduced degree of swelling. This showed that the color of the photonic polymer can be changed from red to blue (~480 to ~640 nm) by varying the calcium concentration between 0.1 and 10 mM.

The use of sponge as a stamp to write full color patterns was first investigated. The logo of the Eindhoven University of Technology "TU/e", which have the letters "T", "U", and "e" in blue and the slash "/" in red was chosen as the full color pattern. The background was selected to be green, and therefore a sponge (1 mm thick) soaked in 1 mM concentration of $Ca(NO_3)_2$ was used as a stamp to generate the green background. A small area was left untreated so that it would develop into a red slash upon swelling with water. The background consisted of both Ca^{2+} and K^+ ions homogeneously distributed while the slash consisted of K^+ ions only. Creating the letters with sponges of the same thickness (1 mm) soaked in 100 mM concentration of $Ca(NO_3)_2$ then led to local exchange of the remaining K^+ ions with Ca^{2+}. Wetting the patterned blue coating with water revealed the full color "TU/e" image (Figure 5.2c). As designed, the background was green ($\lambda \approx 570$ nm) and letters were blue ($\lambda \approx 483$ nm) while the slash was red ($\lambda \approx 636$ nm) (Figure 5.3a). Height profile measurement of the wet coating revealed a decrease in thickness in the region where the letters were written by 3.1 μm which translates to a 16.1 % reduction (Figure 5.3b). This corresponds well with the observed 15.3 % decrease in the pitch length. On the other hand, the thickness increased by 2.3 μm in the region where the slash
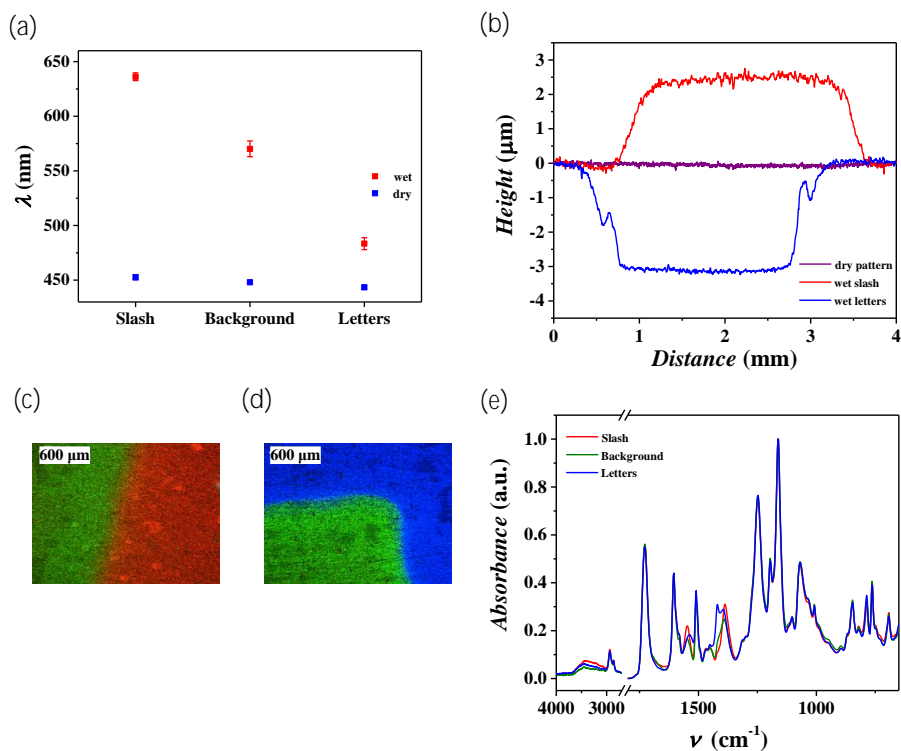
Figure 5.3. (a) Wavelength of light reflected by the "TU/e" logo in wet and dry state. Error bar indicates mean ± standard deviations for five measurements at different places on the pattern. (b) Height profile of the "TU/e" logo in wet state showed swelling for the slash and shrinkage for the letters with respect to the green background and nearly flat surface in the dry state. Polarized optical microscopy image (in incidence light mode) of (c) slash and (d) letter "T". (e) FT-IR spectra of the potassium salt CLC polymer coating patterned with different concentrations of $Ca(NO_3)_2$ solution. Slash consisted of only K^+ ions. Background consisted of both K^+ and Ca^{2+} ions. Letters consisted of only Ca^{2+} ions.

was written. This amounts to a 13 % increase, corresponding fairly well with the observed 11.6 % increase in pitch length on swelling. Polarized optical microscopy (POM) images showed a sharp border of the patterned area (Figure 5.3c, d), implying ions did not undergo lateral diffusion into the non-patterned area, probably due to the anisotropy of the CLC material. The FT-IR spectra showed shifting of symmetric stretching peak of benzoate salt to higher frequency, from 1387 cm^{-1} to 1394 cm^{-1}, while the asymmetric stretching peak shifted to lower frequency,

from 1547 cm^{-1} to 1537 cm^{-1}, confirming the formation of calcium benzoate dimers (Figure 5.2e) in the letter patterned areas.[24,27,28] Drying the film resulted in disappearance of the pattern and the coating was totally blue ($\lambda \approx 448$ nm) with a nearly flat surface profile (Figure 5.2b).

(a)

(b)

(c)

(d)
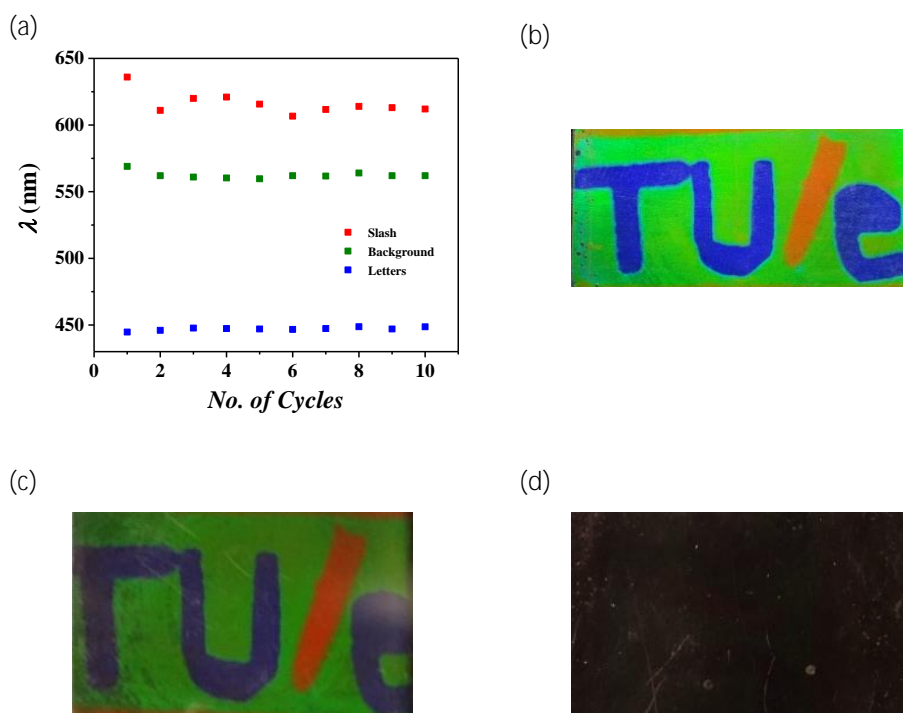
Figure 5.4. (a) Wavelength of light reflected by the "TU/e" pattern on repeated exposure to exhaled breath and drying. (b) Image of the pattern after tenth cycle of exposure to exhaled breath. Image of the "TU/e" pattern on wet coating as seen through (c) right-handed and (d) left-handed circular polarizer.

The trigger to reveal the hidden pattern is not limited to liquid water. Water vapor present in exhaled breath (relative humidity $\approx$ 95 %) was also enough to swell the coating within seconds to the same extent as that of water (Figure 5.2c). Response of the patterned coating was studied for ten cycles of exhaling breath (Figure 5.4a). It was found that repeated exposure to breath had negligible effect on

the optical response of the coating. After the first cycle, the red slash became more orange but in the later cycles, the reflection wavelength stayed nearly the same (Figure 5.4b). After the tenth cycle of exposure to exhaled breath, the color of the green background and blue letters remained nearly unchanged, implying that the response of the coating to breath is fully reversible.

It should be noted that the colored photonic patterns can also be hidden using a circular polarizer. The pattern in the right handed CLC polymer coating was visible through a right-handed circular polarizer while through a left-handed circular polarizer it was invisible and appeared completely dark (Figure 5.4c, d).

5.2.3   Arbitrary full color patterning by inkjet printing

To demonstrate that arbitrary full color high resolution patterns could be easily fabricated in the photonic polymer coatings, inkjet printing was explored with 100 mM $Ca(NO_3)_2$ aqueous solution as a single ink. With a cartridge that ejects drops of 10 pL volume and 27 μm diameter, a rectangular pattern of dimension 1×5 mm^2 was printed with spacing between the drops as 20 μm (1270 dpi). Swelling with water resulted in orange color pattern ($\lambda \approx 608$ nm), slightly blue shifted by $\Delta\lambda \approx 28$ nm with respect to the non-printed red area ($\lambda \approx 636$ nm) (Figure 5.5a). Printing a second layer on top of the first layer resulted in an increase in the amount of Ca^{2+} ions in the polymer network leading to less swelling and the pattern became yellowish green ($\lambda \approx 570$ nm; $\Delta\lambda \approx 66$ nm). On printing a third layer, the pattern became green ($\lambda \approx 532$ nm; $\Delta\lambda \approx 104$ nm) upon swelling. Printing additional layers led to further blue shifting of the reflection band until it became nearly constant around $\lambda \approx 489$ nm (blue color; $\Delta\lambda \approx 147$ nm) for 10 layers and more.

After having determined the number of layers required for obtaining a specific

color, a flower with blue petals, green leaf and stem, and red pistils and background was chosen as an image for inkjet printing. With use of the cartridge with 100 mM $Ca(NO_3)_2$ ink solution and the same drop spacing of 20 μm (1270 dpi), the flower pattern was printed by varying the number of layers accordingly. The flower pattern stayed hidden in dry state but in the wet state – either via exhaled breath or treatment with water- appeared in full color with high resolution (Figure 5.5b). The POM images showed that the patterns were of uniform color, implying the drop spacing was optimum for obtaining uniform layers of the ink. The border of the pattern was

Figure 5.5. (a) Wavelength of light reflected by pattern inkjet printed with different number of layers of the ink l00 and 10 mM $Ca(NO_3)_2$ aqueous solutions. The red line represents the fitted curve. Error bar indicates mean ± standard deviations for five measurements at different places on the pattern. (b) Image of an inkjet-printed full color flower pattern which appeared in the wet state but was hidden in the dry state. Polarized optical microscopy image (in incidence light mode) of (c) leaf and (d) petal patterns on the CLC polymer coating.

sharp for the green leaf-stem (Figure 5.5c). However, the blue petals were surrounded by a broad green border of width ≈ 170 nm (Figure 5.5d). As no lateral ion diffusion was observed in the case of sponge written patterns (*vide supra*), it is unlikely to occur in the inkjet-printed patterns. A possible explanation could be coalescence of printed ink drops at the border toward the bulk of the pattern causing a gradient of Ca^{2+} ions. The wavelength difference between the blue petals and the red background is large ($\Delta\lambda \approx 145$ nm) while that between the green leaf-stem and the red background is relatively small ($\Delta\lambda \approx 87$ nm), as a result, the gradient in Ca^{2+}
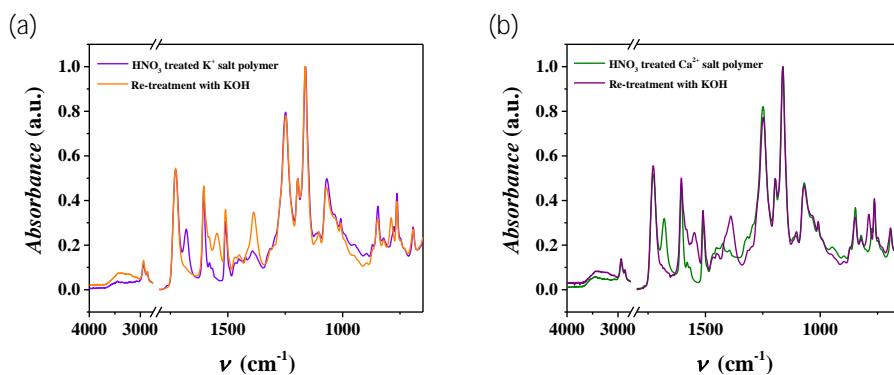
Figure 5.6. FT-IR spectra of (a) potassium salt CLC polymer coating and (b) calcium salt CLC polymer coating on treatment with acid (HNO_3) showing formation of hydrogen bonds and re-treatment with base (KOH) showing re-formation of benzoate salt moieties.

concentration causing a gradient in color is more pronounced in the blue petals. Interestingly, the printed patterns could be erased by re-protonating the benzoate moieties by treating with an acid such as HNO_3 (Figure 5.6) revealing the possibility to erase and reprogram the camouflage patterns.[24]

For the making of green, yellow, and orange colors with more precise wavelengths, a different concentration of calcium nitrate could be used. For example, with use of a lower concentration 10 mM $Ca(NO_3)_2$ solution as the ink, patterns that reflect light of wavelength in between 608 and 570 nm, and 570 and 532 nm could

also be obtained (Figure 5.7a), signifying the versatility of $Ca(NO_3)_2$ solution in producing full color, covering almost the entire visible spectra from red to blue by simply varying the number of layers of the ink – 100 or 10 mM concentrations. The photonic patterning by inkjet printing can be easily extended to printing any color pattern on any color background. For example, the "TU/e" logo could be printed with a green background and red slash and blue letters (Figure 5.7b) to obtain a high-resolution pattern with sharp borders in the wet state.

(a)   (b)
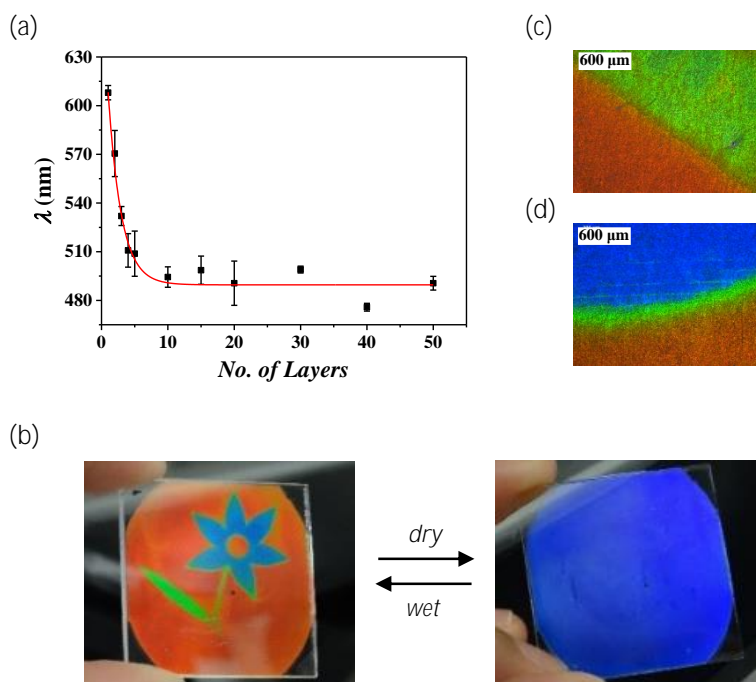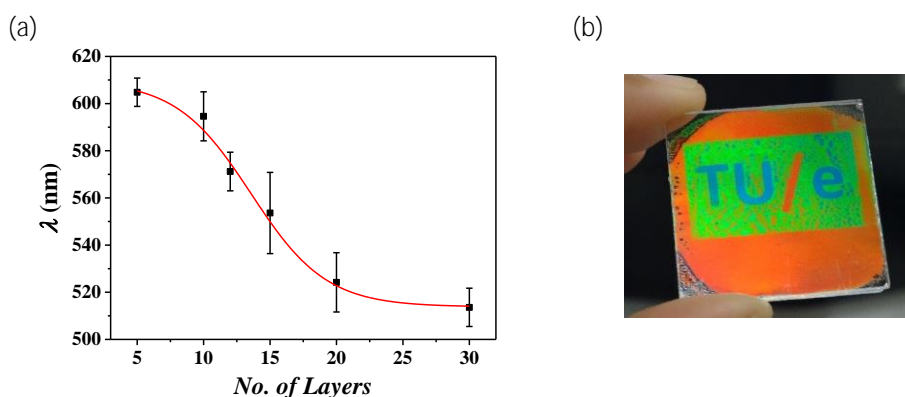

Figure 5.7. (a) Wavelength of light reflected by pattern inkjet printed with different number of layers of the ink 10 mM $Ca(NO_3)_2$ aqueous solution. The red line represents the fitted curve. Error bar indicates mean ± standard deviations for five measurements at different places on the pattern. (b) Image of an inkjet-printed "TU/e" pattern which appears in the wet state of polymer film.

5.3 Conclusion

We have fabricated a printable blue-colored CLC polymer coating that could be patterned with a single ink – calcium nitrate solution, in full colors covering the visible spectra from blue to red (~480 to ~640 nm). The patterns on the polymer functioned similarly to the naturally observed camouflage behavior by remaining hidden in dry environment and revealing itself in the presence of water or exhaled breath. The range of colors achievable could be tuned by simply changing the composition of the non-reactive mesogen. The responsive full color patterned

photonic polymers open up many interesting applications of photonic materials in the direction of adaptive camouflage textiles, anticounterfeit labels, data encryptions as well as for aesthetic purposes including home decorations and automobile coatings.

5.4 Experimental Details

5.4.1   Materials

RM257, RM105 and 5CB were bought from Merck. 6OBA and 6OBAM were obtained from Synthon Chemicals. LC756 was bought from BASF. Irgacure 651 was obatined from CIBA. KOH pellets and $Ca(NO_3)_2.4H_2O$ were bought from Sigma Aldrich. Tetrahydrofuran (THF) was obtained from Biosolve.

5.4.2   Characterization

Photopolymerization was done with Omnicure series 2000 EXFO lamp. UV-Visible spectra of the CLC polymer films were recorded in Perkin Elmer lambda 650 spectrophotometer. Ocean Optics UV-Visible spectrophotometer HR2000+ mounted on a DM6000 M microscope from Leica microsystems was used for measuring the transmission spectra of the photonic patterns. Height profile was determined with a Veeco Dektak 150 Surface profiler. FT-IR spectra were measured on a Varian 670 FT-IR spectrometer with slide-on ATR (Ge). Inkjet printing was carried out in Dimatix DMP 2800 (Dimatix-Fijifilm Inc., Santa Clara, USA) equipped with 10 pL cartridge (DMC-11610). Images of the film were captured with a Sony Cyber-shot camera.

5.4.3   Functionalization of glass substrates

Methacrylate functionalized and fluorinated alkylsilane functionalized glass substrates were fabricated as reported in Chapter 2.

5.4.4   Preparation of responsive CLC polymer coating

1 g of CLC mixture consisting of 17.9 wt % of RM257, 22.9 wt % of RM105, 18.0 wt % of each of 6OBA, 6OBAM and 5CB, 4.6 wt % of LC756, and 0.6 wt % of Irgacure 651 was dissolved in 2 mL THF. 40 μL of this solution was cast on a methacrylate functionalized 3×3 cm^2 glass substrate. After the solvent was evaporated by heating at 75 ^{o}C, a fluorinated alkylsilane coated 3×3 cm^2 glass substrate was placed directly on top and cooled to room temperature with simultaneous shearing along one direction to obtain a greenish yellow film. It was then followed by photopolymerization by shining UV light (48 mW cm^{-2} intensity in the range 320-390 nm) for 5 min after which the upper glass plate was removed to obtain the polymer coating. The polymer was first washed in THF and then treated with 1 M KOH to obtain the responsive potassium salt CLC polymer coating.

5.4.5   Patterning with sponge in polymer coating

Features of dimension $10 \times 2 \times 1$ mm^3 were cut out from a kitchen sponge and were soaked each in different concentrations of $Ca(NO_3)_2$ solution, *viz.* 0.01, 0.1, 1, 5, 10 and 100 mM. The fully soaked sponges were then placed carefully on top of a potassium salt CLC polymer coating. After an hour, the sponges were removed. Some $Ca(NO_3)_2$ solution droplets which were left behind on the surface of the film were absorbed with dry tissue paper and then washed with running distilled water. A clean glass plate was placed on top to trap the water and keep the coating in wet condition for UV-Vis measurements.

5.4.6   Patterning by inkjet printing in polymer coating

10 pL cartridge consisting of 12 nozzles with diameter 21.5 μm was used for printing. 100 mM $Ca(NO_3)_2$ solution was used as the ink. Printing was carried out by

using only 6 nozzles at room temperature with a voltage of 14.0 V and frequency 2.0 kHz using standard waveform. After the printing was over and a waiting period of an hour, the salts that had formed on the surface of the film were removed carefully with tissue paper and then washed with running distilled water. A clean glass plate was placed on top to trap the water and keep the coating in wet condition for UV-Vis measurements.

5.5 References

[1]   J. Sun, B. Bhushan, J. Tong, *RSC Adv.* 2013, *3*, 14862.

[2]   E. Kreit, L. M. Mathger, R. T. Hanlon, P. B. Dennis, R. R. Naik, E. Forsythe, J. Heikenfeld, *J. R. Soc. Interface* 2012, *10*, 1.

[3]   L. M. Mathger, E. J. Denton, N. J. Marshall, R. T. Hanlon, *J. R. Soc. Interface* 2009, *6*, S149.

[4]   J. Teyssier, S. V. Saenko, D. van der Marel, M. C. Milinkovitch, *Nat. Commun.* 2015, *6*, 6368.

[5]   L. Phan, W. G. Walkup IV, D. D. Ordinario, E. Karshalev, J. M. Jocson, A. M. Burke, A. A. Gorodetsky, *Adv. Mater.* 2013, *25*, 5621.

[6]   J. Ge, Y. Yin, *Angew. Chem., Int. Ed.* 2011, *50*, 1492.

[7]   R. Xuan, J. Ge, *J. Mater. Chem.* 2012, *22*, 367.

[8]   Z. Wang, J. Zhang, J. Xie, Z. Wang, Y. Yin, J. Li, Y. Li, S. Liang, L. Zhang, L. Cui, H. Zhang, B. Yang, *J. Mater. Chem.* 2012, *22*, 7887.

[9]   S. Ye, Q. Fu, J. Ge, *Adv. Funct. Mater.* 2014, *24*, 6430.

[10]   Q. Li, N. Qi, Y. Peng, Y. Zhang, L. Shi, X. Zhang, Y. Lai, K. Wei, I. S. Kim, K.-Q. Zhang, *RSC Adv.* 2017, *7*, 17889.

[11]   S. Ye, J. Ge, *J. Mater. Chem. C* 2015, *3*, 8097.

[12]   M. Chen, Y. Tian, J. Zhang, R. Hong, L. Chen, S. Chen, D. Y. Son, *J. Mater. Chem. C* 2016, *4*, 8765.

[13]   H. Hu, H. Zhong, C. Chen, Q. Chen, *J. Mater. Chem. C* 2014, *2*, 3695.

[14]   H. Hu, J. Tang, H. Zhong, Z. Xi, C. Chen, Q. Chen, *Sci. Rep.* 2013, *3*, 1484.

[15]   Y. Fang, S. Y. Leo, Y. Ni, J. Wang, B. Wang, L. Yu, Z. Dong, Y. Dai, V. Basile, C. Taylor, P. Jiang, *ACS Appl. Mater. Interfaces* 2017, *9*, 5457.

[16]   Y. Fang, Y. Ni, S.-Y. Leo, B. Wang, V. Basile, C. Taylor, P. Jiang, *ACS Appl. Mater. Interfaces* 2015, *7*, 23650.

[17]   M. K. Khan, A. Bsoul, K. Walus, W. Y. Hamad, M. J. Maclachlan, *Angew.*

Chem., Int. Ed. 2015, *54*, 4304.

[18]   H. S. Kang, J. Lee, S. M. Cho, T. H. Park, M. J. Kim, C. Park, S. W. Lee, K. L. Kim, D. Y. Ryu, J. Huh, E. L. Thomas, C. Park, *Adv. Mater.* 2017, *29*, 1.

[19]   M. Moirangthem, A. P. H. J. Schenning, In *Liquid Crystal Sensors*; Schenning, A. P. H. J.; Crawford, G. P.; Broer, D. J., Eds.; Taylor & Francis Group: Boca Raton, 2017; pp. 83–102.

[20]   D.-J. Mulder, A. P. H. J. Schenning, C. W. M. Bastiaansen, *J. Mater. Chem. C* 2014, *2*, 6695.

[21]   T. J. White, M. E. McConney, T. J. Bunning, *J. Mater. Chem.* 2010, *20*, 9832.

[22]   Q. Li, *Intelligent Stimuli Responsive Materials: From Well-defined Nanostructures to Applications*; John Wiley & Sons: Hoboken, New Jersey, 2013.

[23]   J. Lu, W. Gu, J. Wei, W. Zhang, Z. Zhang, Y. Yu, N. Zhou, X. Zhu, *J. Mater. Chem. C* 2016, *4*, 9576.

[24]   M. Moirangthem, R. Arts, M. Merkx, A. P. H. J. Schenning, *Adv. Funct. Mater.* 2016, *26*, 1154.

[25]   Y. Galagan, M. G. Debije, P. W. M. Blom, *Appl. Phys. Lett.* 2011, *98*, 43302.

[26]   L. T. De Haan, J. M. N. Verjans, D. J. Broer, C. W. M. Bastiaansen, A. P. H. J. Schenning, *J. Am. Chem. Soc.* 2014, *136*, 10585.

[27]   T. Dudev, C. Lim, *J. Mol. Struct.* 2012, *1009*, 83.

[28]   E. Spinner, *J. Chem. Soc. B* 1967, *6*, 874.

Chapter 6

Photonic Shape Memory Polymer with

Stable Multiple Colors

Abstract: A photonic shape memory polymer film which shows large color response (~ 155 nm) in a wide temperature range has been fabricated from a semi-interpenetrating network of a cholesteric liquid crystalline polymer and poly(benzyl acrylate). The large color response is achieved by mechanical embossing of the photonic film above its broad glass transition temperature. The embossed film, as it recovers to its original shape on heating through the broad thermal transition, exhibits multiple structural colors ranging from blue to orange. The relaxation behavior of the embossed film can be fully described using a Kelvin-Voigt model and it reveals that the influence of temperature on generation of the colors is much stronger than time, thereby producing stable multiple colors.

6.1 Introduction

Shape memory polymers (SMPs) are a fascinating class of smart materials as they can be deformed and locked into a temporary shape which, only under the influence of a specific stimulus like heat, solvent, pressure, light, *etc.*, recovers back to its original shape.[1–5] Photonic SMPs with the ability to reflect light due to their photonic structure[6,7] are a special class of polymers which can change shape as well as color. Such polymers are of great interest for development of, for example, battery-free optical sensors,[8–10] reconfigurable and rewritable optical devices[10–14] and lasers.[15–18] So far, shape memory photonic materials are limited to only two colors.[8–11,19] Designing a photonic SMP that displays multiple colors which are stable over a long period of time still remains a challenge.

SMPs with stable multi-shapes have been previously reported and were obtained by incorporating two or more discrete thermal transitions, which could be glass transition (T_g) or melting (T_m) temperatures, into the polymer.[20–23] The number of temporary shapes achieved is usually equal to the number of transitions. However, designing multi-shape polymers with this approach poses huge synthetic challenges.[24] A more versatile approach is to introduce a broad thermal transition which can be considered as an infinite number of discrete transitions T_{trans} which are so closely spaced that they form a continuum.[24] A polymer with broad thermal transition can, therefore, be tailor-programmed in several ways as per demand by choosing desired temperatures (one or more) out of the infinite transition temperatures for step-wise deformation and thus, a greater degree of freedom in designing multiple temporary shapes can be achieved.[25] A well-known strategy to produce broad glass transition is to use an interpenetrating polymer network (IPN).[26] Additionally, an IPN also provides the unique opportunity to combine the

properties of two different polymers.[27]

Here, we report on a photonic semi-interpenetrating network (semi-IPN) comprising of a photonic cholesteric liquid crystalline (CLC) polymer[28–34] (see Chapter 1) and poly(benzyl acrylate). In CLC, due to helical twisting of the average orientation (director) of the molecules, selective reflection of light takes place with the pitch of the helix determining the wavelength of reflection.[28,29] The semi IPN photonic film exhibits a broad glass transition (T_g) from 10 to 54 °C and can be deformed mechanically to a temporary shape, accompanied by a large change in color from orange to blue ($\Delta\lambda \approx 155$ nm). In response to rise in temperature through the T_g, shape recovery takes place in multi-stages displaying varying structural colors covering almost the entire visible spectrum. The process of shape recovery can be fully described using a Kelvin-Voigt model and it is shown that the multiple colors generated are stable over very long periods of time.

6.2 Results and Discussion

6.2.1 Fabrication of photonic polymer film
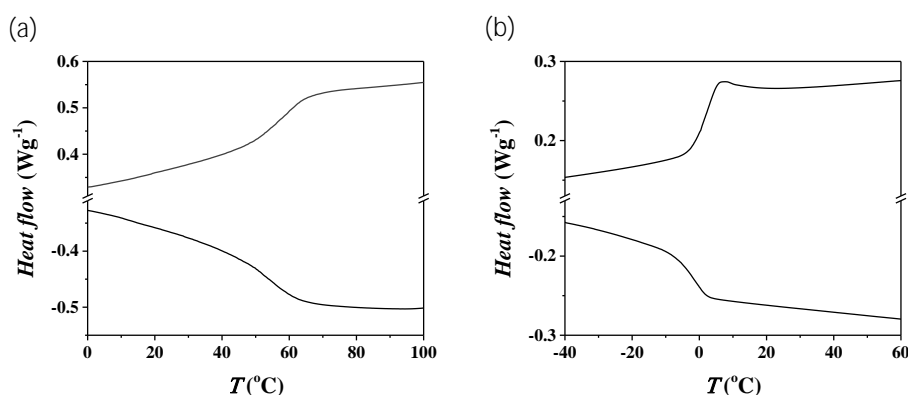
Figure 6.1. DSC curves for (a) CLC polymer without 5CB and (b) poly(benzyl acrylate). Rate of heating and cooling was maintained at 20 °C min-1.

In order to obtain a photonic polymer film with a broad T_g, a semi-interpenetrating network (semi-IPN) was fabricated from a CLC polymer film with a T_g of 60 °C (Figure 6.1a) and poly(benzyl acrylate) (abbreviated as poly(BA)) whose pure homopolymer has a T_g of ~6 °C (Figure 6.1b).[35] The benzyl acrylate (BA) monomer can readily penetrate into the CLC polymer due to π-π interactions between the benzene ring of the monomers and the polymer.[36]

The semi-IPN photonic film was fabricated from a monomer mixture consisting of a diacrylate (RM257, 29 wt %) and a monoacrylate (RM105, 35 wt %) mesogens (Scheme 6.1). It also contained a non-polymerizable mesogen (5CB, 30 wt %) to act as a porogen in order to facilitate incorporation of BA monomers.[27] A chiral molecule (LC756, 5 wt %) with polymerizable end groups was used to induce CLC phase. Irgacure 651 was added to initiate the photopolymerization reaction. The monomer mixture was filled in a polyimide coated cells with 70 μm spacer and was
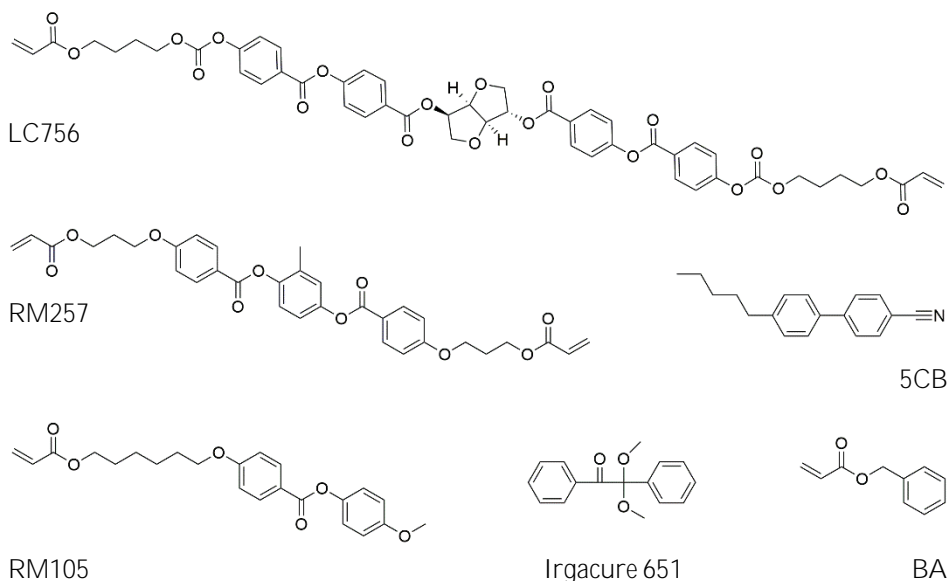
Scheme 6.1. Molecular structure of the components used for fabrication of the semi-interpenetrating network of CLC polymer and poly(benzyl acrylate).

(a)

(b)

(c)

(d)
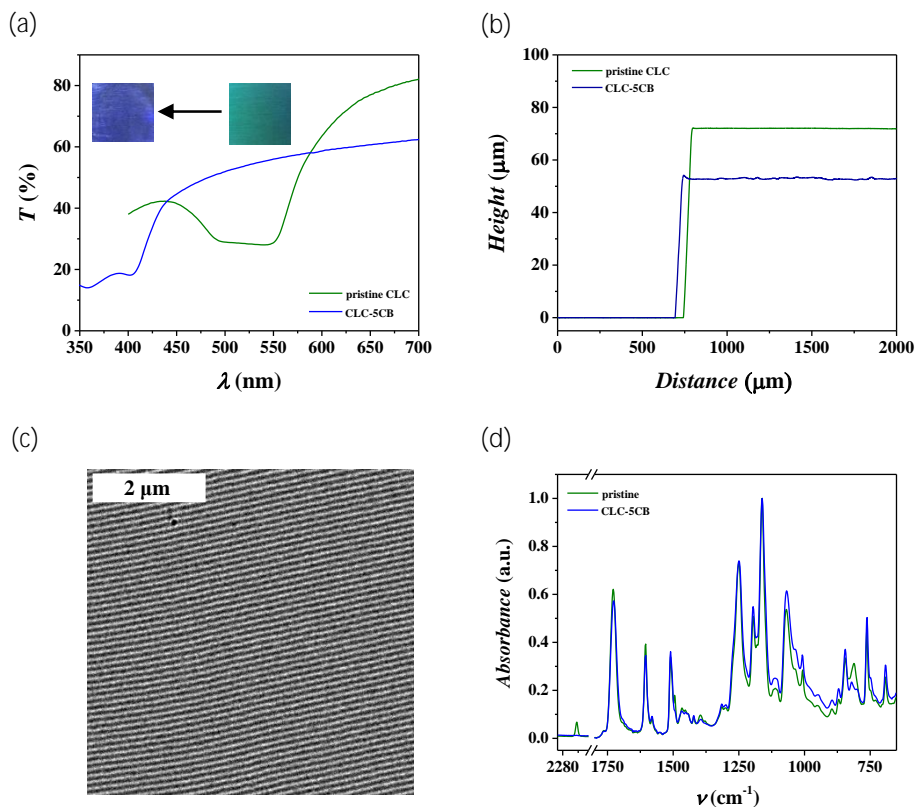
Figure 6.2. (a) UV-Vis spectrum of the pristine CLC polymer film and the film after removal of 5CB (CLC-5CB). Inset shows photographs of the polymer film before and after removing 5CB. (b) Height profile measurement of pristine CLC polymer film, film after removal of 5CB (CLC-5CB), and semi-interpenetrating network (semi-IPN) of the CLC polymer network and poly(benzyl acrylate). (c) TEM cross-section image of the CLC-5CB. The alternating bright and dark bands are due to the anisotropy arising from the cholesteric orientation. It has a periodicity of 115 nm.

photopolymerized at room temperature to obtain a free-standing green reflecting polymer film (~72 μm thick) with selective reflection band (SRB) centered at $\lambda \approx 515$ nm (Figure 6.2a, b). The porogen, 5CB, was removed by extracting with an organic solvent (tetrahydrofuran). This resulted to a large blue shift of the reflection band to $\lambda \approx 380$ nm implying shortening of helical pitch length by 26.2 % (Figure 6.2a, b), which is in good agreement with the 26.4 % decrease observed in the thickness of the

film (~53 μm). TEM image of the cross-section of the film revealed a periodic alternating bright and dark bands due to the helical orientation of the molecules (Figure 6.2c).[27] In the FT-IR spectrum, the peak at 2225 cm^{-1} originating from stretching vibration of (-C≡N) of 5CB had disappeared (Figure 6.2d) suggesting complete removal of 5CB.[27] DSC experiments showed that the polymer film undergoes a glass transition at 60 °C (Figure 6.1a). The blue CLC polymer film without 5CB (CLC-5CB) was then treated with BA monomer mixed with 1 wt % of photoinitiator (Irgacure 651) and this resulted to a change in color from blue to orange due to penetration of the monomers into the cholesteric polymer network causing an increase in pitch length. Photopolymerization of the swollen orange film led to formation of the photonic semi-IPN of the CLC polymer and poly(BA) (Figure 6.3a).

FT-IR spectroscopy of the semi-IPN photonic film showed a band centered at 748 cm^{-1} due to the rocking motion of the long (-CH$_2$) polymer backbone in poly(BA) (Figure 6.3b). The amount of poly(BA) incorporated was determined by subtracting the weight of the polymer film before treatment with BA, and was found to be 42.4 wt. %. The reflection band of the semi-IPN (~76 μm thick, Figure 6.3c) was centered at $\lambda \approx 590$ nm which translates to 40.8 % increase in pitch length ignoring the small refractive index changes (Figure 6.3a). This is in good agreement with the observed 43 % increase in film thickness. Moreover, TEM cross-section image of the semi-IPN also showed alternating bright and dark bands with a periodicity of 170 nm (Figure 6.3d); the periodicity corresponds to half a pitch length and correlates well with the observed reflection wavelength. The pitch length was found to be uniformly distributed throughout the semi-IPN film suggesting that the CLC polymer and poly(BA) are well mixed.

(a)

(b)

(c)

(d)
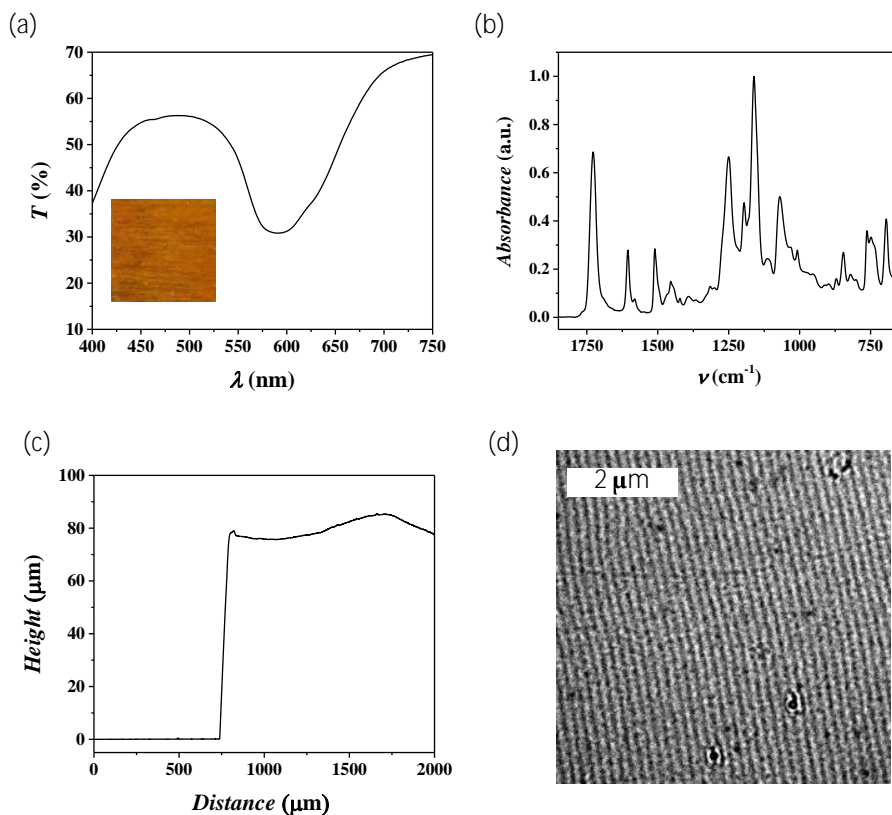
Figure 6.3. (a) UV-Vis spectrum of the semi-interpenetrating network (semi-IPN) of CLC polymer and poly(benzyl acrylate). Inset shows the photograph of the semi-IPN photonic film. (b) FT-IR curve and (c) height profile measurement of the semi-IPN. (d) TEM image of the cross-section of the semi-IPN film shows an alternating bright and dark bands with a periodicity of 170 nm.

The DSC curve of the semi-IPN is markedly different from that of the pure cholesteric polymer CLC-5CB and the pure homopolymer poly(BA). A broad glass transition that onsets at 10 °C (T_{low}) and ends at 54 °C (T_{high}) was observed instead of two distinct glass transitions (Figure 6.4). In the heating curve, however, the broad transition can be noticed to be consisting of two overlapping broad humps which are centered at 22 °C (T_{mid1}) and 45 °C (T_{mid2}) and can be assigned as T_g of the poly(BA)-dominant and the CLC polymer-dominant domains respectively. It can be said that physically, the semi-IPN behaves close to a single polymer with the thermal transit-

ion smeared out over a broad range of temperature.
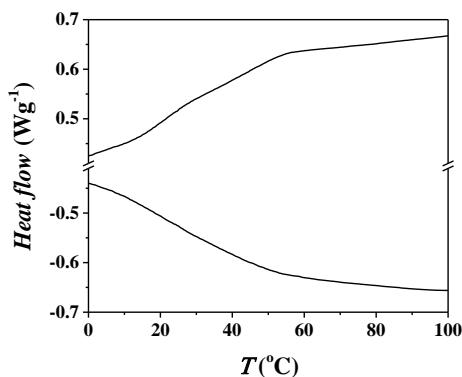
Figure 6.4. DSC curve of the semi-IPN film. Rate of heating and cooling was kept at 20 °C min^{-1}.

6.2.2   Mechanical embossing of photonic polymer film

The semi-IPN photonic film was mechanically embossed in two steps by using a spherical glass stamp (radius of curvature = 25.8 mm) – first, above the glass transition at T_1 = 75 °C (*i.e. T_{high}* + 21 °C) and second, in between T_{mid1} and T_{mid2} at T_2 = 40 °C (*i.e. T_{mid1}* + 18 °C) (Figure 6.5a). At T_1, a load of 0.7 Kg was used for embossing. Upon cooling to T_2, an extra load of 3.5 Kg was added. With a total load of 4.2 Kg, the film was then cooled down below the glass transition. At 0 °C, the load was finally removed and a spherical indentation with a diameter of 1.7 mm was obtained.

The central region of the indentation appeared blue in color and UV-Vis transmission spectrum showed that the reflection band has blue shifted by ~155 nm with the new position centered at $\lambda \approx 435$ nm (Figure 6.5b, c). The low transmittance value at 0 °C is due to condensation of water vapor on the surface of the film and this was not accounted for while making the baseline correction. On moving outward from the central blue embossed region, the degree of compression of the pitch length

(a)

(b)   (c)
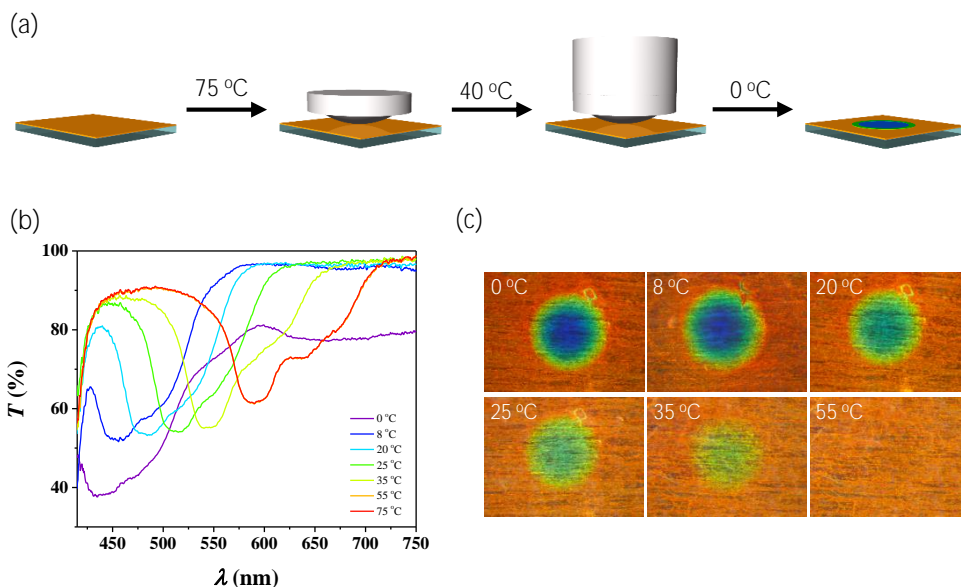
Figure 6.5. (a) Schematic representation of the steps followed in the mechanical embossing of the photonic polymer film. (b) UV-vis transmission spectra of the embossed area of the photonic polymer film shows red shift of the reflection band on increasing temperature from 0 °C to 75 °C. The film was kept at each temperature for 1 hour. (c) Images of the polymer film captured on increasing temperature shows change in color from blue to orange. The images of the film were captured after keeping each temperature for 7 hr.

decreases due to the spherical shape of the stamp used and the color shifted towards higher wavelength (Figure 6.5c). When the photonic semi-IPN was embossed in just one step at 75 °C with a load of 5.2 Kg and cooled directly to 0 °C, the color change was smaller ($\Delta\lambda \approx$112 nm) (Figure 6.6a). This implies that the method to emboss in two steps results in more efficient compression of helical pitch. Therefore, only the investigations carried out on the two-steps embossed film will be presented in the following sections. It should be noted here that mechanical embossing of the pure cholesteric polymer CLC-5CB resulted in a blue shift of the reflection band by only 7 nm (Figure 6.6b). This emphasizes the role of having a softer second polymer network, poly(BA) in our case, interpenetrated with the CLC polymer in obtaining

an enormous blue shift of reflection band.

(a)

(b)
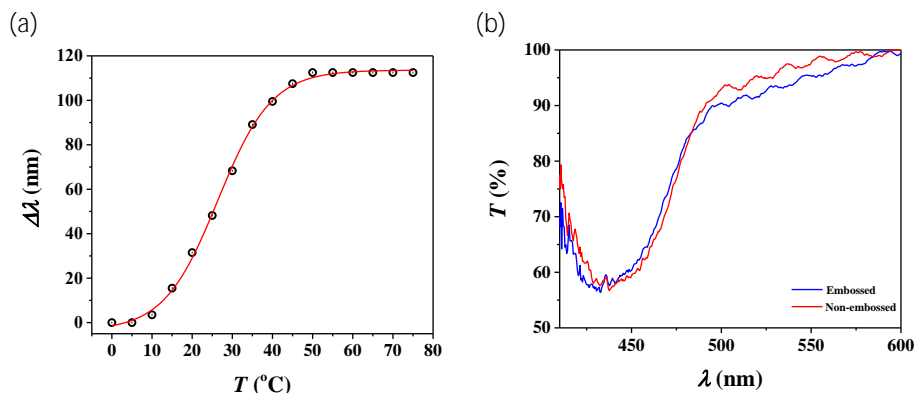
Figure 6.6. (a) Amount of red shift of the reflection band ($\Delta\lambda$) of the one step-embossed photonic polymer film observed at various temperatures after 1 hour. The red curve is the fitted curve to the data points. (b) UV-Vis transmission spectra of mechanically embossed and non-embossed CLC-5CB (with 4 wt. % chiral dopant LC756 but equal amount of crosslinker) polymer film showed a small difference of 7 nm. In both the cases, the mechanical embossing was done at 75 °C with a load of 5.2 Kg.

6.2.3   Shape recovery and optical response to temperature

The color response of the embossed polymer was investigated by heating step-wise through the T_g. The film was first heated to 8 °C. There was no visible color change even after keeping at 8 °C for 7 hr (Figure 6.5c). However, UV-Vis spectrum showed a small red shift of the reflection band ($\Delta\lambda$) of the central blue region by ~10 nm after an hour and keeping at 8 °C for longer than an hour hardly shifted the reflection band further (Figure 6.5b). The temperature was then increased to 20 °C and within an hour, the central region of the embossed area became bluish-green ($\Delta\lambda \approx 50$ nm, $t = 1$ hr) and the change in color was clearly visible to the naked eye (Figure 6.5b, c). UV-Vis transmission spectrum was also recorded for the embossed film after an hour for every 2 °C rise in temperature from 0 to 20 °C. As can be seen from Figure 6.7, the amount of red shift of the reflection band, $\Delta\lambda$, increases steadily with the increase in temperature. However, the change in color is too small (< 20 nm) at

92
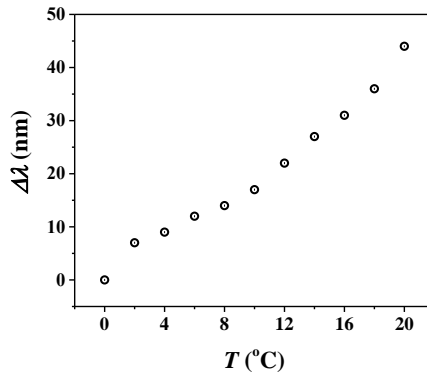
Figure 6.7. Observed red shifts of the reflection band ($\Delta\lambda$) of the central embossed area of the photonic polymer film after 1 hr at temperatures below room temperature.

very low temperatures (< 10 $^{\circ}$C) to be distinguishable to the naked eye. On increasing the temperature to 25 $^{\circ}$C, the embossed area turned green ($\Delta\lambda \approx 80$ nm, $t = 1$ hr). Heating the film to 35 $^{\circ}$C resulted to yellow reflective color ($\Delta\lambda \approx 110$ nm, $t = 1$ hr) and finally at 55 $^{\circ}$C, it returned to the original orange ($\Delta\lambda \approx 155$ nm, $t = 1$ hr), basically covering almost the entire visible color spectrum (Figure 6.5b, c). Lowering the temperature at any stage did not reverse the color of the indentation to what was
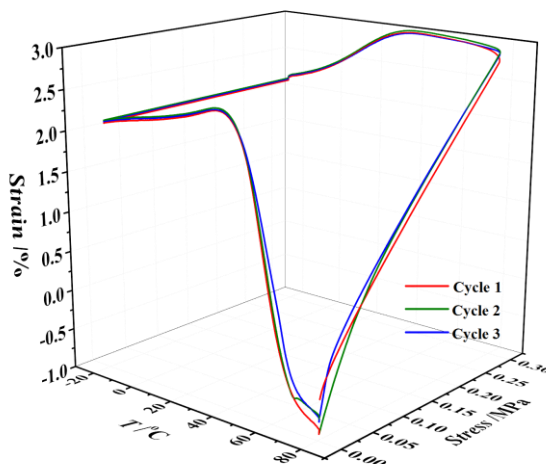
Figure 6.8. One-way shape memory cycles of the IPN photonic film showing reversible behavior.

observed prior to increase in temperature, demonstrating the characteristic behavior of one-way shape memory. The photonic film, however, can be mechanically embossed and recovered again. The recyclability was investigated for 3 shape memory cycles and it was found to be completely reversible (Figure 6.8).

The height profile measurement of the embossed area at room temperature (25 °C) showed that the indentation is spherical in shape and is 6 μm deep at the lowest point (Figure 6.9a). It translates to 6 % decrease in thickness at the center of the indentation, which means the pitch length is also shortened by 6 % with respect to that of the non-embossed film. However, the observed color of the central embossed area at 25 °C ($\lambda \approx 510$ nm) is blue shifted by ~45 nm from the expected color when the angle of incidence of light is 0°. This reveals that the optical response seen is, in fact, largely dependent on the angle of incidence, which is estimated to be ~23°, due to the curvature of the indentation.

To determine if the path followed to reach a temperature T in the regime of glass transition has an effect on the optical response of the embossed polymer film, two different heating routes were employed – (a) the sample was initially heated to (T-5) °C and later up to the desired temperature T, and (b) the sample was directly heated from 0 °C to T, and the amount of red shifts observed after 1 hr at T was examined (Figure 6.9b). The samples which were pre-heated to (T-5) °C were found to show slightly higher values of $\Delta\lambda$ as they have been stored for quite some time at temperatures just below the target temperature to recover to their initial (non-embossed) configuration. It can therefore be stated that when sufficient time has not been provided for complete recovery to take place (*vide infra*), they will always show a slightly higher optical response than those which are directly heated to the target temperature.

(a)

(b)
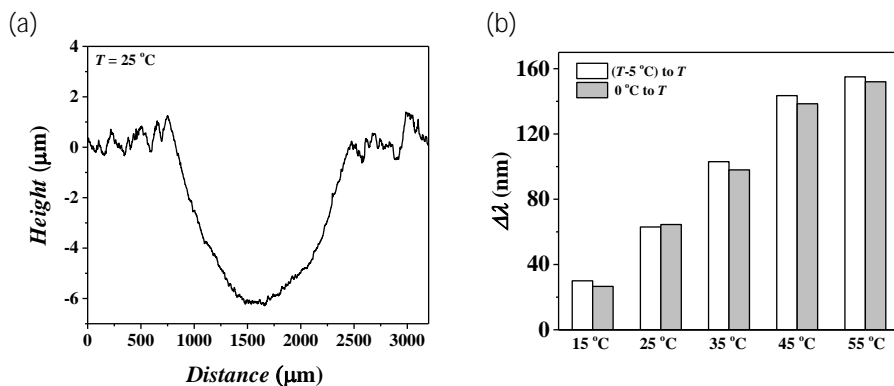
Figure 6.9. (a) Height profile of the embossed area at room temperature shows a spherical indentation as deep as ~ 6 μm at the lowest point. (b) Optical response, $\Delta\lambda$, of the embossed area of the photonic film at a temperature T after 1 hr for two different heating routes.

In order to determine the temperature dependent optical response in the entire glass transition region, different embossed films were heated directly from 0° C to different temperatures T = 8 to 75 $^{\circ}$C and after keeping at the desired temperatures for 7 hr, the red shifts ($\Delta\lambda$) of the reflection band were recorded (Figure 6.10). What is intriguing is that $\Delta\lambda$ follows a near-double sigmoidal trend - the first phase from 0 $^{\circ}$C to 30 $^{\circ}$C and the second phase from 30 $^{\circ}$C to 55 $^{\circ}$C – similar to the shape of the DSC heating curve (Figure 6.4). This may be attributed to the existence of a broad glass transition comprising of two overlapping transitions (T_{mid1} and T_{mid2}) corresponding to the poly(BA)-dominant and the CLC polymer-dominant domains. In the first phase, the chains of poly(BA) gain flexibility and begin to recover to their original configuration. The CLC polymer chains, due to their strong non-covalent interaction with poly(BA), are compelled to recover simultaneously to certain extent. This is supported by the red shift of the reflection band of the embossed area. On raising the temperature further to T_{mid2} and above, the CLC polymer network acquires full flexibility and consequently, complete shape recovery takes place at 55 $^{\circ}$C.
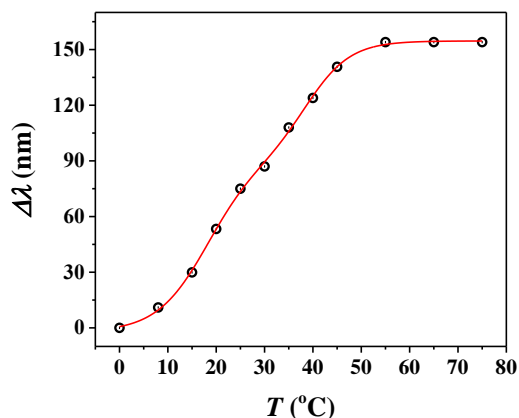
Figure 6.10. Observed red shifts of the reflection band ($\Delta\lambda$) of the central embossed area of different photonic films after 7 hr at various temperatures. The red curve is the fitted curve to the data points.

The kinetics of the recovery of original shape of the embossed photonic film was also studied in detail. Each embossed film was heated from 0 °C to a specific temperature T (8 °C $\leq T \leq$ 55 °C) and was kept at isothermal condition for 7 hr. Meanwhile, the reflection band of the films were monitored by UV-Vis spectroscopy. As the temperature was increased to and maintained at T, there was a steep increase in the amount of red shift of the reflection band ($\Delta\lambda_t$), with respect to the reflection band at 0 °C. In Figure 6.11a, the extent of shape recovery is plotted as a ratio of $\Delta\lambda_t$ to the maximum red shift observed ($\Delta\lambda_{max}$ = 155 nm), when complete recovery takes place at 75 °C, as a function of time. For any temperature (T), the rate of change of $\Delta\lambda_t / \Delta\lambda_{max}$ decreased continuously as time progressed and after an hour, the rate slowed down considerably. As a result, the difference in wavelengths of light reflected by the embossed film after 1 hr and 7 hrs is less than 12 nm. The data of Figure 6.11a have been replotted in Figure 6.11b on a semi-logarithmic plot to model the response of the photonic polymer film at a specific temperature. It becomes clear from this plot that the relaxation mechanism does not approach an equilibrium state

96
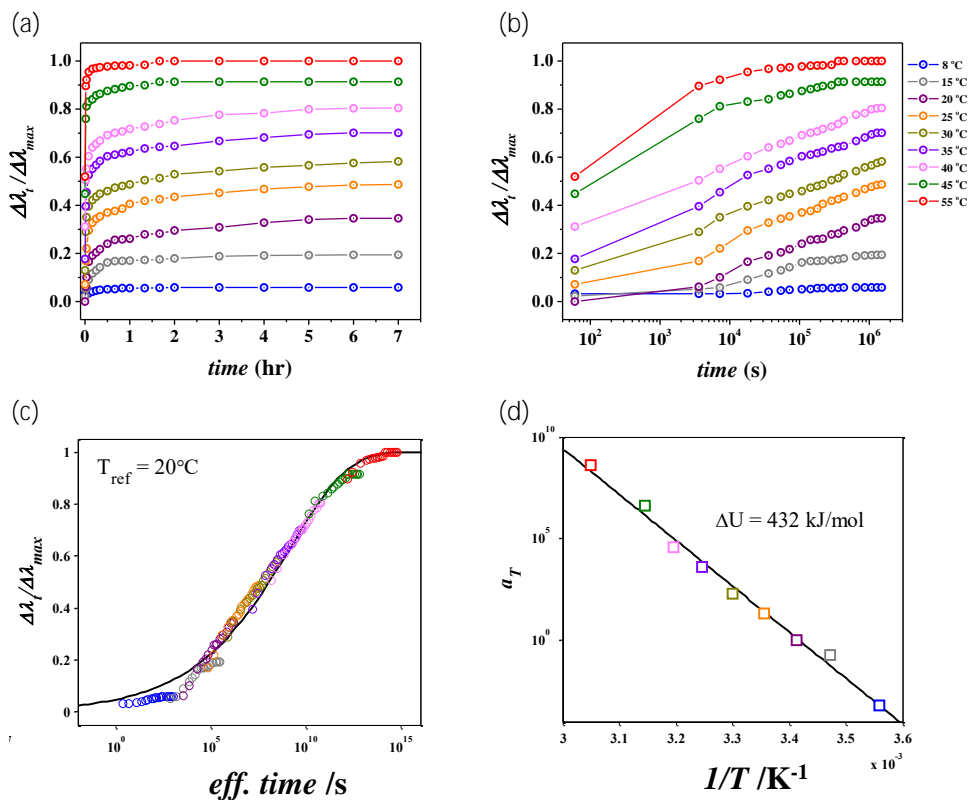
Figure 6.11. (a) Red shifts ($\Delta\lambda_t$) of the reflection band of the central embossed area measured at different temperatures over time with reference to the red shift observed at 75 °C ($\Delta\lambda_{max}$) on complete recovery. (b) Shape recovery data of (a) shown on a logarithmic time axis. (c) Master curve constructed from the data of subgraph (b) using Time-Temperature-Superposition (TTS); solid line is a fit according to Equation 1. (d) Shift factors used to construct the master curve; solid line is an Arrhenius fit.

at a given temperature, but rather continuously relaxes back to its original orange color.

By using horizontal shifting along the time axis, *i.e.* using Time-Temperature-Superposition (TTS), a master curve with respect to a reference temperature – here arbitrarily chosen as 20°C- was obtained (Figure 6.11c). The relaxation behavior of the photonic polymer film as displayed by the master curve can be described using a simple Kelvin-Voigt model, in which a spring and dashpot are modeled in parallel.[37]

The parallel spring here enforces the reversibility of the deformation and the dashpot governs the relevant time and temperature response. The non-exponentiallity of the response is accounted for by using the empirical Kohlrausch-Williams-Watts (KWW) equation[38–42] which is a stretched-exponential equation, often used to describe distributions of relaxation times in a continuous rather than discrete manner, consisting of two adjustable relaxation constants, *viz.* τ_{ref} and β:

$$\Delta\lambda_t/\Delta\lambda_{max}(t,T) = \left(1 - \exp\left(\frac{t_{eff}(t,T)}{\tau_{ref}}\right)^{\beta}\right) \tag{1}$$

Here, τ_{ref} is the average relaxation time with respect to a reference temperature and β is a parameter that describes the non-exponential behavior of the relaxation process or in other words, it is a measure of the width of the distribution of relaxation times. The best fit of the master curve was obtained when τ_{ref} has a value of 1.47×10^9 s at 20 °C, and β has a value of 0.14. As $\beta << 1$, the distribution of relaxation times is very broad and it correlates well with the experimentally observed very broad thermal transition that the photonic semi-IPN displayed. This shows that the model fully describes the relaxation behavior of the embossed film.

The TTS shift function a_T used to construct the master curve (Figure 6.11c) follows a standard Arrhenius type of temperature dependence (Figure 6.11d):

$$a_T(T) = \exp\left(\frac{\Delta U}{R}\left(\frac{1}{T} - \frac{1}{T_{ref}}\right)\right) \tag{2}$$

where ΔU is the activation energy, R the universal gas constant, T the temperature and τ_{ref} a reference temperature. The activation energy, ΔU, was found to be 432 kJ mol^{-1}; a rather large value indicating that the influence of temperature is (much) stronger compared to time. It must be noted that although the value might

appear large when considering a single molecular bond, it has to be interpreted in light of the cooperative motion of multiple chain segments.

The effective time, t_{eff}, required for the recovery of the embossed area to different temperatures can be calculated and is given by:

$$t_{eff}(t,T) = \int_0^t a_T^{-1}(T)dt' \qquad (3)$$

As can be seen from Figure 6.11c, at 20 °C, it will take ~10^{15} s for $\Delta\lambda_t/\Delta\lambda_{max}$ to reach the value 1. This implies that the embossed photonic film will take more than 30 million years to recover completely to the original orange color when stored at 20 °C. The recovery, therefore, basically takes place with formation of non-equilibrium configurations that display quasi-stable multiple colors ranging from blue to orange in the broad thermal transition regime.

6.3 Conclusion

A photonic shape memory polymer film which displays stable multiple colors covering almost the entire visible spectrum from blue to orange has been fabricated from a semi-interpenetrating network of a CLC polymer and poly(benzyl acrylate). The multiple structural colors are generated as the mechanically embossed photonic film recovers on heating through the broad thermal transition. The recovery process can be fully described using a Kelvin-Voigt model. It revealed that the recovery is dominated by temperature. In the first hour of recovery, the embossed photonic film displays time-temperature integrating behavior and as time progresses, its influence on the recovery continuously decreases, thereby generating stable colors. This makes such photonic shape memory polymers with stable multiple colors attractive for various applications ranging from optical sensors to reconfigurable optical materials

and devices. As the change in color can be fully described as function of temperature and time, these photonic materials can be easily programmed by changing the chemical composition of the semi-interpenetrating network in a modular approach.

6.4 Experimental Details

6.4.1   Materials

RM257, RM105 and 5CB were obtained from Merck. LC756 was bought from BASF. Benzyl acrylate was purchased from Sigma Aldrich. Irgacure 651 was from CIBA. Tetrahydrofuran was obtained from Biosolve.

6.4.2   Characterization

Photopolymerization was carried out with Omnicure series 2000 EXFO lamp. UV-Visible spectra of the photonic films were measured in Shimadzu UV-3102 PC spectrophotometer. Differential scanning calorimetry was performed in TA DSC Q1000. Thermogravimetric curve was measured in TA TGA Q500. FT-IR spectra were recorded using Varian 670 FT-IR spectrometer with slide-on ATR (Ge). Mechanical Embossing was carried out in a DACA Tribotrak with a spherical glass stamp of diameter 25.8 mm. Ocean Optics UV-Visible spectrophotometer HR2000+ mounted on a DM6000 M microscope from Leica microsystems was used for monitoring the shape recovery of embossed films. T95-PE from Linkam Scientific was used to study temperature dependent transmission spectra. Images of the embossed film were captured using Leica M80 stereomicroscope. Height profile was measured using Veeco Dektak 150 Surface profiler. Shape memory cycle measurement was carried out in DMA Q800. Transmission Electron Microscopy (TEM) was carried out by microtoming slices of the polymer films embedded in epoxy using a DiATOME diamond knife (Cryo 35°). The samples were trimmed

orthogonal to the plane of the film at room temperature and collected from the surface of a water reservoir using 200 mesh carbon-coated copper grids. The epoxy used consists of an epoxy resin (EpoFix Resin) and a hardener (EpoFix Hardener), manufactured by Struers, mixed in a 25:3 mass ratio. TEM imaging was performed using an FEI Tecnai 20 (type Sphera) TEM operating at 200 kV and mapped using a bottom mounted 1024 x 1024 Gatan MSC CCD camera (model 794).

6.4.3   Preparation of polyimide cells

Glass substrates were first cleaned by sonicating for 30 min in ethanol followed by treatment in a UV-ozone photoreactor (Ultra Violet Products, PR-100, 20 min) to activate the glass surfaces. The glass surfaces were then modified by spin coating (Karl Suss RC8 spincoater) AL 1051, first at 1000 rpm for 5 s and then at 5000 rpm for 40 s. It was followed by baking at 180 $^{\circ}$C for 90 minutes and rubbing unidirectionally on a velvet cloth. Finally, two of these substrates were glued together with a 70 μm spacer, such that the rubbing direction is anti-parellel to each other to obtain the polyimide cells.

6.4.4   Preparation of photonic polymer film

Mesogen mixture (1 g) consisting of 29 wt % RM257, 35 wt % RM105, 30 wt % 5CB, 5 wt % LC 756 and 1 wt % Irgacure 651 was dissolved in tetrahydrofuran (4 mL) to form a homogeneous solution. The solvent was later evaporated by heating at 75 $^{\circ}$C to obtain the cholesteric liquid crystalline (CLC) mixture. The CLC mixture was then filled in a polyimide cell with 70 μm spacer at 40 $^{\circ}$C followed by photopolymerization by irradiating UV light (48 mW cm^{-2} intensity in the range 320-390 nm) for 5 min. The cell was opened to obtain a free standing CLC polymer film. It was then treated with THF and dried, first at room temperature and then at 75 $^{\circ}$C,

after which the polymer film was exposed to benzyl acrylate mixed with 1 wt % of Irgacure 651 for 12 hr. After wiping out excess benzyl acrylate, it was photopolymerized in N_2 atmosphere by shining UV light (48 mW cm^{-2} intensity in the range 320-390 nm) for 15 min. The process was repeated again to incorporate higher amount of benzyl acrylate in the system.

6.5 References

[1]   G. J. Berg, M. K. McBride, C. Wang, C. N. Bowman, *Polymer* 2014, *55*, 5849.

[2]   J. Hu, Y. Zhu, H. Huang, J. Lu, *Prog. Polym. Sci.* 2012, *37*, 1720.

[3]   L. Sun, W. M. Huang, Z. Ding, Y. Zhao, C. C. Wang, H. Purnawali, C. Tang, *Mater. Des.* 2012, *33*, 577.

[4]   H. Meng, G. Li, *Polymer* 2013, *54*, 2199.

[5]   T. Xie, *Polymer* 2011, *52*, 4985.

[6]   J. Ge, Y. Yin, *Angew. Chem., Int. Ed.* 2011, *50*, 1492.

[7]   Q. Li, *Intelligent Stimuli Responsive Materials: From Well-defined Nanostructures to Applications*; John Wiley & Sons: Hoboken, New Jersey, 2013.

[8]   D. J. D. Davies, A. R. Vaccaro, S. M. Morris, N. Herzer, A. P. H. J. Schenning, C. W. M. Bastiaansen, *Adv. Funct. Mater.* 2013, *23*, 2723.

[9]   Y. Fang, Y. Ni, S.-Y. Leo, C. Taylor, V. Basile, P. Jiang, *Nat. Commun.* 2015, *6*, 7416.

[10]   Y. Fang, S. Y. Leo, Y. Ni, L. Yu, P. Qi, B. Wang, V. Basile, C. Taylor, P. Jiang, *Adv. Opt. Mater.* 2015, *3*, 1509.

[11]   Y. Fang, Y. Ni, S.-Y. Leo, B. Wang, V. Basile, C. Taylor, P. Jiang, *ACS Appl. Mater. Interfaces* 2015, *7*, 23650.

[12]   M. Behl, A. Lendlein, *J. Mater. Chem.* 2010, *20*, 3335.

[13]   H. Xu, C. Yu, S. Wang, V. Malyarchuk, T. Xie, J. A. Rogers, *Adv. Funct. Mater.* 2013, *23*, 3299.

[14]   Y. Fang, S. Y. Leo, Y. Ni, J. Wang, B. Wang, L. Yu, Z. Dong, Y. Dai, V. Basile, C. Taylor, P. Jiang, *ACS Appl. Mater. Interfaces* 2017, *9*, 5457.

[15]   H. Finkelmann, S. T. Kim, A. Muñoz, P. Palffy-Muhoray, B. Taheri, *Adv.*

Mater. 2001, *13*, 1069.

[16]   M. F. Moreira, I. C. S. Carvalho, W. Cao, C. Bailey, B. Taheri, P. Palffy-Muhoray, *Appl. Phys. Lett.* 2004, *85*, 2691.

[17]   H. Coles, S. Morris, *Nat. Photonics* 2010, *4*, 676.

[18]   P. V. Shibaev, V. Kopp, A. Genack, E. Hanelt, *Liq. Cryst.* 2003, *30*, 1391.

[19]   Y. Fang, Y. Ni, B. Choi, S. Y. Leo, J. Gao, B. Ge, C. Taylor, V. Basile, P. Jiang, *Adv. Mater.* 2015, *27*, 3696.

[20]   S. Ahn, P. Deshmukh, R. M. Kasi, *Macromolecules* 2010, *43*, 7330.

[21]   A. Espinha, G. Guidetti, M. C. Serrano, B. Frka-Petesic, A. G. Dumanli, W. Y. Hamad, Á. Blanco, C. López, S. Vignolini, *ACS Appl. Mater. Interfaces* 2016, *8*, 31935.

[22]   Z. Wen, T. Zhang, Y. Hui, W. Wang, K. Yang, Q. Zhou, Y. Wang, *J. Mater. Chem. A* 2015, *3*, 13435.

[23]   S. K. Ahn, R. M. Kasi, *Adv. Funct. Mater.* 2011, *21*, 4543.

[24]   T. Xie, *Nature* 2010, *464*, 267.

[25]   Q. Zhao, M. Behl, A. Lendlein, *Soft Matter* 2013, *9*, 1744.

[26]   J. Li, T. Liu, S. Xia, Y. Pan, Z. Zheng, X. Ding, Y. Peng, *J. Mater. Chem.* 2011, *21*, 12213.

[27]   J. E. Stumpel, E. R. Gil, A. B. Spoelstra, C. W. M. Bastiaansen, D. J. Broer, A. P. H. J. Schenning, *Adv. Funct. Mater.* 2015, *25*, 3314.

[28]   D.-J. Mulder, A. Schenning, C. Bastiaansen, *J. Mater. Chem. C* 2014, *2*, 6695.

[29]   T. J. White, M. E. McConney, T. J. Bunning, *J. Mater. Chem.* 2010, *20*, 9832.

[30]   R. J. Carlton, J. T. Hunter, D. S. Miller, R. Abbasi, P. C. Mushenheim, L. N. Tan, N. L. Abbott, *Liq. Cryst. Rev.* 2013, *1*, 29.

[31]   M. Mitov, *Adv. Mater.* 2012, *24*, 6260.

[32]   L. Wang, Q. Li, *Adv. Funct. Mater.* 2016, *26*, 10.

[33]   J. Lu, W. Gu, J. Wei, W. Zhang, Z. Zhang, Y. Yu, N. Zhou, X. Zhu, *J. Mater. Chem. C* 2016, *4*, 9576.

[34]   V. Shibaev, A. Bobrovsky, N. Boiko, *Prog. Polym. Sci.* 2003, *28*, 729.

[35]   P. Spahn, C. E. Finlayson, W. M. Etah, D. R. E. Snoswell, J. J. Baumberg, G. P. Hellmann, *J. Mater. Chem.* 2011, *21*, 8893.

[36]   C.-K. Chang, H.-L. Kuo, K.-T. Tang, S.-W. Chiu, *Appl. Phys. Lett.* 2011, *99*,

73504.

[37]   I. M. Ward, J. Sweeney, *An Introduction to the Mechanical Properties of Solid Polymers*; 2nd ed.; John Wiley and sons: Chichester, 2004.

[38]   F. Kohlrausch, *Ann. Phys.* 1866, *204*, 1.

[39]   F. Kohlrausch, *Ann. Phys.* 1866, *204*, 207.

[40]   F. Kohlrausch, *Ann. Phys.* 1866, *204*, 399.

[41]   G. Williams, D. C. Watts, *Trans. Faraday Soc.* 1970, *66*, 80.

[42]   S. Matsuoko, *Relaxation Phenomena in Polymers*; Hanser Publishers: Munich, 1992.

Chapter 7

Technology Assessment

Abstract: Potential applications of the photonic polymers which are described in this thesis are discussed. The challenges ahead in taking these polymers further to real life applications such as sensors, time temperature integrators and photonic papers are elaborated. Furthermore challenges such as dual responsiveness to both humidity and temperature, and fabrication of infrared reflective coatings are also discussed.

7.1 Introduction

The work described in this thesis has shown that by using polymerizable cholesteric liquid crystalline materials, responsive photonic polymers can be fabricated. The optical properties and mechanical strength of the polymer can be tuned by modifying the monomer composition. They can be systematically designed to show optical response in the presence of certain stimulus such as heat, humidity, water and upon exposure to chemical species like metal ions and other organic molecules. Such responsive photonic polymers are of interest for applications in the field of healthcare, food and pharmaceutical packaging, security, data encryptions, decors, displays among others. In this chapter, the potential applications of the photonic polymers as optical sensors, time temperature integrators, rewritable paper, and IR reflective coatings will be assessed.

7.2 Optical Sensors

Photonic coatings that can detect metal ions are appealing as optical sensors for testing drinkability of water.[1,2] They can also be interesting as diagnostic test strips for detection of mineral deficiencies. For instance, the optical sensor that can detect the presence of calcium in serum (Chapter 4) is a step-forward in the search for an affordable and easy-to use tool to diagnose hypocalcemia and hypercalcemia health conditions.[3] However, cross-sensitivity to other metal ions such as Mg^{2+}, Zn^{2+}, Cd^{2+}, Pb^{2+}, Na^+ remains an issue. When all the binding sites in the polymer coating are not fully saturated by Ca^{2+} ions and if any of the other ions are present, these ions will bind to the remaining sites, leading to a non-reliable color change. Furthermore, leaching out of potassium ions on subsequent treatment with water (Figure 7.1) is another problem that needs to be addressed. Although by re-treating the polymer

with KOH regenerates the polymer potassium salt, repeated treatment will lead to hydrolysis of the ester bonds present in the polymer. Such polymer coatings are therefore, more interesting as disposable optical sensors.
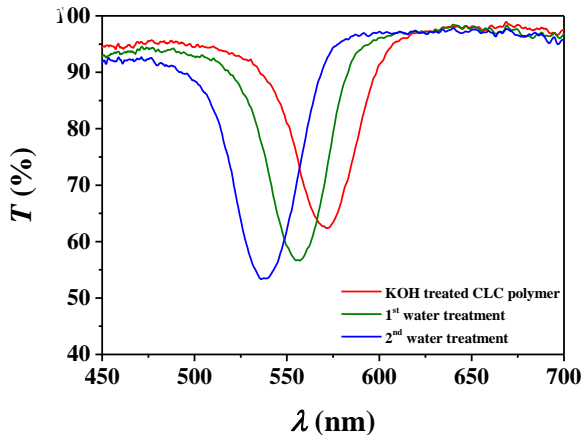

Figure 7.1. UV-Vis spectrum showing blue shift of the reflection band of potassium salt CLC polymer on subsequent treatment with water.

7.3 Time-temperature integrators

Food safety is a key attribute for defining food quality and is of paramount importance to avoid food-borne diseases.[4] Out of the various stages involved in ensuring food safety, proper storage during transportation plays a crucial role in deciding the shelf life of perishable food. For instance, storage temperature at or below 8 ^{o}C is required to prevent bacterial growth and formation of toxins.[5] A time-temperature (t-T) integrator device that exhibits an irreversible thermal transition resulting to structural change which manifests itself as a change in optical properties are interesting for recording the storage thermal history.

Shape memory photonic polymers described in Chapter 6 show time-temperature integrating behavior in a wide temperature range from 0 to 55 ^{o}C.[6–8] The optical response observed below room temperature makes such photonic

polymers very appealing as food packaging labels. Although the optical response is less than 20 nm below 10 °C, a change which is too small to be distinguishable by the naked eye, the approach presented in this thesis to make a semi-interpenetrating network with broad glass transition temperature can be further extended to design photonic polymers with desired temperature range and greater optical response for real life applications. It is important to consider that for practical applications, a coating that can be easily printed on the packaging material is most desirable. Embossing of polymer coatings (covalently bonded to a glass substrate) results in formation of cracks during shape recovery process (Figure 7.2). This problem can perhaps be solved by embossing micron size polymer drops. It may lead to a uniform color on embossing as well as eliminate the challenge of aligning the embossing stamp.
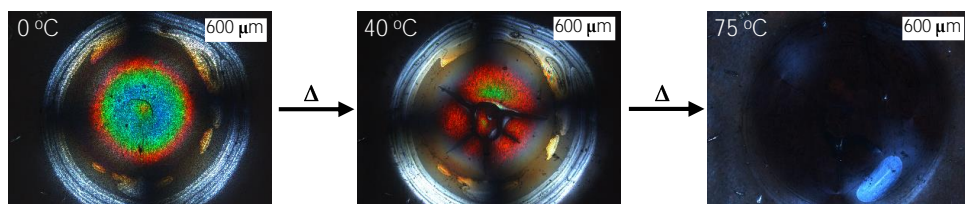
Figure 7.2. Polarized optical microscopy images of an embossed photonic polymer coating showed formation of cracks as shape recovery takes place on increasing temperature.

7.4 Photonic paper

One of the most interesting applications of the responsive photonic coatings is as photonic paper.[9] The color of the photonic polymer being purely structural, is stable and more durable than dyes and pigments which are prone to UV degradation. The photonic coatings can be used to create permanently colored patterns by writing with a hot pen (Chapter 2). Such coatings are attractive as photonic paper for important documents that need to be stored and preserved for over a long period of

time.[10] Resolution of the patterns can be further improved by using a pen with a tip of smaller diameter.

On the other hand, photonic polymers with patterns which can be readily erased and rewritten multiple times (Chapter 3) are appropriate for purposes where the information needs to be changed frequently, like in notice boards and signage. Such polymers could be an attractive alternative to cellulose-based paper and provide a solution to recycling of waste paper that produces shorter cellulose fibers with reduced ink absorption capacity.[11]

Photonic coatings in which the patterns can be hidden (Chapter 5) are appealing for use as security labels to authenticate consumer products, documents and banknotes.[12] Using exhaled breath as the trigger to see the hidden patterns is extremely convenient. However, it also brings forth certain drawbacks that accompany humidity responsive systems being sensitive to atmospheric conditions. Keeping the polymer coating in a highly humid or very cold environment will lead to unintended appearance of the hidden patterns.[13]

7.5 IR reflective coatings

Potassium salt cholesteric liquid crystalline (CLC) polymers, described in this thesis, which are responsive to both temperature and humidity can be interesting as infra-red (IR) light reflective coatings for maintaining indoor temperatures.[14] Broad reflection in the IR region of the solar spectrum is desirable for rejecting the maximum energy. This can be achieved by generating a concentration gradient of the chiral dopant while polymerizing the CLC mixture.[15]

As a proof of principle, a CLC polymer coating that reflects light of wavelength from ~770 nm to ~980 nm, *i.e.* 210 nm broad reflection band, at ambient conditions
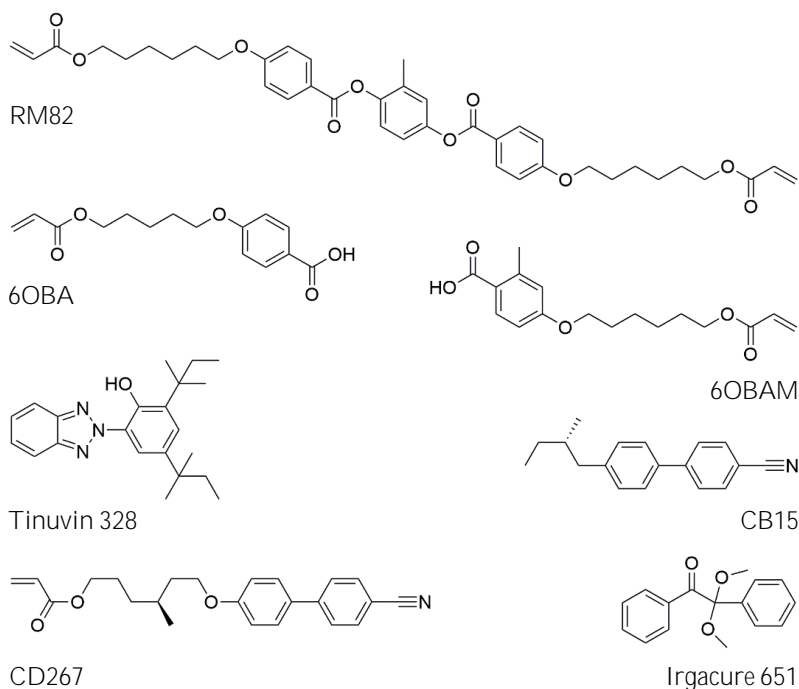
Scheme 7.1. Structure of the chemical components used in the fabrication of humidity and temperature responsive IR reflective coating.

was fabricated. The CLC mixture (Scheme 7.1) that was used consisted of a diacrylate (RM 82, 22.5 wt %, from Merck) to provide mechanical strength to the coating and monoacrylates with benzoic acid moieties (6OBA and 6OBAM, 9.65 wt % each, from Synthon) to make the coating hydrophilic. Two chiral molecules, one polymerizable with an acrylate end group (CD267, 6.5 wt %, from Philips Research Lab) and the other non-polymerizable (CB15, 5.7 wt %, from Merck) were used to induce the CLC phase.[15] A photoinotiator (Irgacure 651, 1.2 wt %, from CIBA) was added to initiate the photopolymerization reaction. At the same time, to create gradient of UV light intensity through the thickness of the film, a UV absorber (Tinuvin 328, 0.5 wt %, from CIBA) was used. Lastly, in order to facilitate the photo-induced diffusion, a nematic mixture (E7, 44.3 wt. %, from Merck) was added.

To make polymer coating, a cell containing one methacrylate functionalized and one rubbed polyimide coated glass plates was used with 30 μm spacers. Shining a low intensity UV lamp on the cell filled with the CLC mixture at 50 °C, such that the methacrylate functionalized plate faced the light, led to diffusion of reactive components including chiral molecule CD267 from bottom to top resulting to pitch gradient in the CLC polymer network. After fully polymerizing the sample with UV flood exposure followed by opening of the cell and washing away the non-reactive components, treatment with KOH gave the responsive potassium salt CLC polymer coating with ~210 nm broad reflection band.

At a relative humidity of ~90 %, the reflection band of the polymer coating was found to undergo a red shift of ~123 nm on cooling from 30 °C to -5 °C (Figure 7.3). There was no significant change in the broadness of the reflection band. This implies that as temperature decreases, more IR light will be transmitted. Hence, it can be very interesting in maintaining indoor temperatures in different seasons, for example in greenhouses where humidity is generally high.
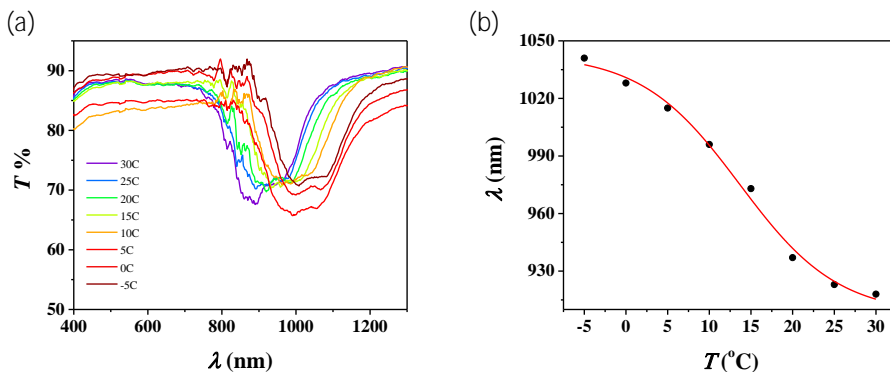

Figure 7.3. (a) UV-Vis spectrum of the IR reflective coating showed red shift of the reflection band on decreasing temperature at 90 % RH. (b) A plot showing the position of the reflection band as a function of temperature.

7.6 Conclusion

The research findings described in this thesis have demonstrated the versatility of cholesteric liquid crystalline based polymer in developing stimuli-responsive photonic materials. Such photonic materials have several potential applications as optical sensors, time-temperature integrators, photonic papers and IR reflective coatings and can provide alternative solutions to many of our pressing needs. Therefore, it is foreseen that photonic coatings will play an important role in meeting our societal challenges.

7.7 References

[1]   M. Moirangthem, A. P. H. J. Schenning, In *Liquid Crystal Sensors*; Schenning, A. P. H. J.; Crawford, G. P.; Broer, D. J., Eds.; Taylor & Francis Group: Boca Raton, 2017; pp. 83–102.

[2]   D.-J. Mulder, A. P. H. J. Schenning, C. W. M. Bastiaansen, *J. Mater. Chem. C* 2014, *2*, 6695.

[3]   M. Moirangthem, R. Arts, M. Merkx, A. P. H. J. Schenning, *Adv. Funct. Mater.* 2016, *26*, 1154.

[4]   A. Röhr, K. Lüddecke, S. Drusch, M. J. Müller, R. v. Alvensleben, *Food Control* 2005, *16*, 649.

[5]   *Food Standards Agency* 2016.

[6]   D. J. D. Davies, A. R. Vaccaro, S. M. Morris, N. Herzer, A. P. H. J. Schenning, C. W. M. Bastiaansen, *Adv. Funct. Mater.* 2013, *23*, 2723.

[7]   M. Moirangthem, T. A. P. Engels, J. Murphy, C. W. M. Bastiaansen, A. P. H. J. Schenning, *ACS Appl. Mater. Interfaces* 2017, *9*, 32161.

[8]   M. Cavallini, M. Melucci, *ACS Appl. Mater. Interfaces* 2015, *7*, 16897.

[9]   J. Ge, Y. Yin, *Angew. Chem., Int. Ed.* 2011, *50*, 1492.

[10]   M. Moirangthem, J. E. Stumpel, B. Alp, P. Teunissen, C. W. M. Bastiaansen, A. P. H. J. Schenning, *Proc. of SPIE* 2016, *9769*, 97690Y.

[11]   Y. Virtanen, S. Nilsson, *Environmental Impacts of Waste Paper Recycling*; 1st ed.; Taylor & Francis Group: London, 1993.

[12]   M. Moirangthem, A. P. H. J. Schenning, *ACS Appl. Mater. Interfaces* 2018, acsami.7b17892.

[13]   N. Herzer, H. Guneysu, D. J. D. Davies, D. Yildirim, A. R. Vaccaro, D. J. Broer, C. W. M. Bastiaansen, A. P. H. J. Schenning, *J. Am. Chem. Soc.* 2012, *134*, 7608.

[14]   H. Khandelwal, A. P. H. J. Schenning, M. G. Debije, *Adv. Energy Mater.* 2017, *7*, 1602209.

[15]   H. Khandelwal, R. C. G. M. Loonen, J. L. M. Hensen, M. G. Debije, A. P. H. J. Schenning, *Sci. Rep.* 2015, *5*, 2.

Acknowledgements

"It is good to have an end to journey toward, but it is the journey that matters in the end." — Ernest Hemingway

First and foremost, a very big thank you to Albert for giving me the opportunity to do my PhD at SFD. The project on responsive photonic polymers gave me four excellent years to play with "smart colors". It has been a great learning experience to work under your supervision. I have thoroughly enjoyed our interactions. Thank you for your constant support and encouragement.

Thank you, Dick for your intellectual insights on my projects – they have helped in improving my work continuously. Thank you, Cees for your advice on the importance of practicalities of the possible applications of the photonic polymers – it has broadened my perspectives. Thank you, Michael for all your valuable inputs which have greatly improved the quality of my research articles and my thesis.

I would like to thank prof. dr. Peng Jiang, prof. dr. Nathalie Katsonis and prof. dr. Rint Sijbesma for participating in my doctoral committee and for your comments and suggestions to improve my thesis further.

Thank you, Tom (Engels) for your help with the numerical calculations on the shape memory photonic polymers. I truly enjoyed working with you. Also thank you for being part of my doctoral committee.

Thank you, Jelle for passing on your knowledge about cholesteric liquid crystalline materials and guiding me during my initial days – it means a lot. Thank you, Remco and prof. dr. Merkx Maarten for your help with the study of calcium sensor in serum. It was a great experience working with you. Thank you, Eduardo for sharing your knowledge and experience of working with cholesteric liquid crystalline droplets. I would also like to thank dr. Hans Wyss for helping with fabrication of microfluidic device to make liquid crystalline droplets.

Thank you, Imma, Jeroen (Sol), Anouk. It was a good learning experience for me to work with you all. All the best with your career!

Thank you, Marjolijn for all your help throughout my stay in SFD. Thank you, Tom for making my PhD so smooth – I could disturb you any time any day whenever I had faced problems with instruments or measurement set-ups.

Last four years have been very memorable. Special thanks to Jelle, Jeroen and Wei for a lively office! Jelle, I will always remember the pink phone, the insect, and the capybara which decorated our office. Jeroen, you keep our office happening and your energy spreads positivity. I really appreciate your help/advice in trying to solve any problem, work-related or non-related. All the best for Lusoco! I am proud to have shared office with a CTO! ☺ Wei, I will miss listening to ring tones of many instant messages! ☺ On a more serious note, thank you for being reachable whenever I needed any help in the university. All the best with your PhD!

Thank you, the former and present members of SFD – Alberto (Belmonte Parra), Alberto (Concellón), Anne-Hélène, Anping, Berry, Danqing, Davey, Dirk Jan, Ellen, Fabian, Gilles, Huub, Jeffrey, Jurica, Kamlesh, Koen, Lihua, Laurens, Matthew, Marc, Marina, My, Rob, Sander, Sarah, Shaji, Simon, Stijn, Tim, Ting, Wanshu, Wilson, Xiaohong, Xinglong, Yuanyuan – for making life at SFD so enjoyable. Also, thank you for all your help in the past four years.

In no time of coming to Eindhoven, it became my home – thank you to all of you! Anne-Hélène, you are an inspiration! I admire your energy. Thank you for introducing me to whole new activities – climbing, skating, kayaking in ocean, "swimming" in ocean. Dirk Jan, I really appreciate your help in many ways – thank you for coming with me to orthodontist, I could not have done it all by myself. And I had the best holiday with both of you – in India and France. Thank you for all the wonderful evenings! Xiao – my Chinese sister and braces buddy! You're super cool! So sweet! And so caring! Seeing you always cheers me up – you're like a sunshine! Ting-Ting – my fearless Chinese sister! You're so considerate. And I will always remember the "forgot-to-eat" moment! Our girls' France trip was so much fun. Good luck with your upcoming "big" moments!

Hemelrijken was a perfect abode – thanks to you all! Deepak, you're one of a kind! The 25 km bike ride in perhaps my second week of learning to bike was one memorable afternoon! Walking nearly 10 km in search of a bus stop was another! I fondly remember many of such "interesting" moments. ☺ Sandip-Priyanka, our trip together to Ameland was wonderful. Sushil, you're one of the best cook whom I know. Thank you all of you for many amazing breakfasts, lunches, snacks, dinners, card nights and for always being available just a call away.

Thank you, Kamlesh-Swati – I had a great trip with you to London. Thank you, Nivedita-Yogesh – you are the most competent people for any advice any day. Thank you, Rohit, Sathish, Satish, Vinay – I enjoyed your company during lunch hours.

Thank you, Chidambar bhaiya-Gayatri di for many beautiful evenings and enlightening discussions and re-introducing me to cricket. Eindhoven still feels home because of you. Our trip to Dolomites and Venice was superb! Hoping for more such trips. Thank you, Rathna-Balu-Vihaan – having you (almost) next door was the best thing! It was always good to see you through the window "early" in the morning on Saturdays. I had always looked forward to visiting your place so that I could play with Vihaan "my youngest friend" and his toys. ☺ Thank you, Anindita for being a great host to me. I really enjoyed our time together.

Thank you, Int. PhD 2011 for keeping the 21-year-old Monali in me alive! Debopreeti, Krishnendu, Pallabi – I'm glad you could visit me, and Mohini, Neelima, Suseela – I'm waiting!

Thank you, Rana da for your kind words of encouragement. Thank you, Prof. C. N. R. Rao, Sebastian Sir, Subi Sir, Sridhar Sir for your support.

Thank you, Sneha – you have influenced me greatly. Thank you, Che Esther, Da Bidyanand for making me feel at home in Delhi.

I would also like to thank all my teachers who have trusted my capabilities and supported me in every possible ways.

Hitesh, we've seen each other grow, from being "carefree" and "all smiles" college going teenagers to much mature and responsible adults. Thank you for being by my side through the thick and thin.

Lastly, I am very fortunate to have an extremely supportive family – my parents, my sisters and brother, who believes in me, trusts my decisions wholeheartedly and gives me the liberty to grow and live my dreams.

Warm Regards,

Monali

Curriculum Vitae

Monali Moirangthem was born on March 15, 1991 in Thangmeiband, Manipur, India. After finishing secondary school in 2008 at Herbert School in Imphal, India, she studied Bachelor of Science (Honours) in **Chemistry at St. Stephen's College, University of Delhi** in Delhi, India. She was an INSPIRE fellow from 2008-2011. In 2011, she received a Diploma in Chemistry from Jawaharlal Nehru Centre for Advanced Scientific Research (JNCASR) in Bangalore, India. In the same year, she began her Master of Science studies as well in Chemical Science at JNCASR. In 2012, she became Babu Mathru Prasad Scholar for being the topper of the institute in Chemical Science. In May 2014, she **successfully defended her Master's thesis titled "Investigation of Few Layer MOFs and Anion Substituted Chromium (III) oxide" under the supervision of** Prof. C. N. R. Rao. She started her PhD project in June 2014 under the supervision of Prof. Albert Schenning and Prof. Dick Broer at Eindhoven University of Technology in Eindhoven, The Netherlands of which the results are presented in this thesis.

List of Publications

Research articles (related to this thesis)

M. Moirangthem, A. F. Scheers, A. P. H. J. Schenning, Rewritable Full Color Photonic Polymer using a Liquid Crystal Ink. *Chem. Commun.* 2018, Accepted Manuscript; DOI: 10.1039/C8CC02188K

M. Moirangthem, A. P. H. J. Schenning, Full Color Camouflage in a Printable Photonic Blue-Colored Polymer. *ACS Appl. Mater. Interfaces* 2018, 10, 4168

M. Moirangthem, T. A. P. Engels, J. Murphy, C. W. M. Bastiaansen, A. P. H. J. Schenning, Photonic Shape Memory Polymer with Stable Multiple Colors. *ACS Appl. Mater. Interfaces* 2017, 9, 32161

M. Moirangthem, J. E. Stumpel, B. Alp, P. Teunissen, C. W. M. Bastiaansen, A. P. H. J. Schenning, Hot pen and laser writable photonic polymer films. *SPIE Proceedings*, Vol. 9769, Emerging Liquid Crystal Technologies XI, 2016, 97690Y

M. Moirangthem, R. Arts, M. Merkx, A. P. H. J. Schenning, An Optical Sensor Based on a Photonic Polymer Film to Detect Calcium in Serum. *Adv. Funct. Mater.* 2016, 26, 1154

Research article (not related to this thesis)

M. B. Sreedhara, B. E. Prasad, M. Moirangthem, R. Murugavel, C. N. R. Rao, Isolation and characterization of nanosheets containing few layers of the Aurivillius family of oxides and metal-organic compounds. *J. Solid State Chem.* 2015, 224, 21

Book chapter

M. Moirangthem, A. P. H. J. Schenning, *Chapter 4 Cholesteric Liquid Crystalline Pol-*

ymer Networks as Optical Sensors in *Liquid Crystal sensors* (Editors: A. P. H. J. Schenning, G. P. Crawford, D. J. Broer), Taylor & Francis Group: Boca Raton, 2017, 83

Patent

C. W. M. Bastiaansen, K. Nickmans, A. J. J. Kragt, M. Moirangthem, A. P. H. J. Schenning, D. J. Broer, Photonic time-temperature indicators having an embossed interpenetrating network of cholesteric liquid crystalline polymers and a secondary polymer. *US 62/462180*; Filing date: 22nd February 2017